INFORMATION TO USERS

This manuscript has been reproduced from the microfilm master. UMI films the text directly from the original or copy submitted. Thus, some thesis and dissertation copies are in typewriter face, while others may be from any type of computer printer.

The quality of this reproduction is dependent upon the quality of the copy submitted. Broken or indistinct print, colored or poor quality illustrations and photographs, print bleedthrough, substandard margins, and improper alignment can adversely affect reproduction.

In the unlikely event that the author did not send UMI a complete manuscript and there are missing pages, these will be noted. Also, if unauthorized copyright material had to be removed, a note will indicate the deletion.

Oversize materials (e.g., maps, drawings, charts) are reproduced by sectioning the original, beginning at the upper left-hand corner and continuing from left to right in equal sections with small overlaps.

Photographs included in the original manuscript have been reproduced xerographically in this copy. Higher quality 6" x 9" black and white photographic prints are available for any photographs or illustrations appearing in this copy for an additional charge. Contact UMI directly to order.

ProQuest Information and Learning
300 North Zeeb Road, Ann Arbor, MI 48106-1346 USA
800-521-0600

Université d'Ottawa • University of Ottawa

AERODYNAMIC INSTABILITY OF INCLINED CABLES

by

Han Soo Kim

A thesis
Presented to the University of Ottawa in partial fulfillment of the requirements for
Master of Applied Science in Civil Engineering

Department of Civil Engineering
University of Ottawa
Ottawa, Canada
K1N 6N5

November 2001

The M. A. Sc. in Civil Engineering is a joint program
with Carlton University administered by the
Ottawa-Carlton Institute for Civil Engineering

This thesis is dedicated to my wife, Eun Ju Lee

사랑하는 나의 아내 은주에게....

ACKNOWLEDGEMENTS

The author would like to express his deepest appreciation to Dr. H. Tanaka, the research supervisor, for his tremendous support, guidance, and encouragement all through the period of this study.

Special thanks are addressed to Mr. M. G. Savage, Dr. G. L. Larose and other staff of the Applied Aerodynamic Laboratory, National Research Council, Canada, for their valuable and help during this study.

The author also extends his appreciation to engineers at RWDI of Guelph, Ontario. As a part of the joint research project, they designed and provided the spring system to support the cable model. In particular, Mr. J. Kottelenberg, Mechnaical Design Coordinator, provided useful for the model setup.

Special thanks are also expressed to Mr. C. Zurell and Dr. S. H. Cheng, the author's co-workers throughout the project. Dr. Cheng allowed the author to use her preliminary report of this project as a part of the thesis. Mr. Zurell was kind enough to proofread the draft of the thesis and correct English, which is not the author's first language.

Finally, the continuous efforts of my family and my wife Eun Ju Lee are greatly appreciated.

ABSTRACTS

A series of wind tunnel tests was conducted to investigate the existence of the galloping instability of inclined dry cables and also to identify the influence of some parameters on it. These parameters are the structural damping and cable surface roughness, which may have significant impact on the vibration characteristics.

The test results showed both the divergent type of galloping instability and the limited amplitude high wind speed vortex shedding excitation. Galloping instability was observed in only one case. Parametric study shows that the vortex shedding oscillation can be easily suppressed with an increase of the structural damping.

It was also shown that the instability criterion indicated by earlier research was too conservative compared to the results obtained from the present study.

TABLE OF CONTENTS

PAGE

PAGE

LIST OF TABLES

LIST OF FIGURES

GLOSSARY

C_D	Drag coefficient
C_L	Lift coefficient
D	Cable diameter
f	Cable frequency
f_v	Frequency of vortex shedding
L	Lift force
m	Mass per unit length
R_e	Reynolds number
S_c	Scruton number
S_t	Strouhal number
U	Mean wind speed
x	Horizontal separation between two cylinders
y	Vertical separation between two cylinders
α	Angle of rotation of the spring system
β	Wind attack angle
ρ	Air density

θ	**Cable inclination angle**
ζ	**Damping ratio**
ϕ	**Relative angle of wind against cable**

CHAPTER 1

INTRODUCTION

1.1 General

The mechanical principle of cable-stayed bridges has been long exhibited through human history. However, the prevalent use of cable-stayed bridges started only after the Second World War. About a half century ago, Dischinger built a bridge in Strömsund, Sweden, which is considered to be the first modern cable-stayed bridge.

Since then, cable-stayed bridges have been extensively developed in size and also in variation of structural arrangements. Cable-stayed bridges are not only sound and economical structures for medium-span crossings but they can also offer outstanding aesthetic qualities due to their small diameter cables and the wide variety of structural designs.

In order to satisfy both structural aesthetics and economic conditions, it is natural that more slender and lighter structures have been developed. As a result, a new problem related to structural dynamics has arisen. The characteristics of cables, with their light weight and large flexibility, together with their small structural damping, make the cables easily excited by the dynamic action of wind.

1.2 Scope of the present study

The topic of this thesis is to investigate the aerodynamic instability of inclined dry cables with a series of wind tunnel tests.

Chapter 2 of the thesis summarizes various types of cable vibration under aerodynamic excitations. Also, some of the vibration control methods, particularly for bridge stay-cables and power lines, are presented in this chapter.

Chapter 3 explains this experimental program of the study.
Chapter 4 is a summary of the test results, including the parametric changes of damping and cable surface roughness.
Discussions and conclusions are presented in Chapter 5.

This study took place as a part of the project carried out as a research contract with RWDI of Guelph, Ontario, in collaboration with the Institute of Aerospace Research, National Research Council Canada. There is, as a result, an overlap of its contents with the materials already reported to RWDI as a part of the contractual duties [45].

CHAPTER 2

AERODYNAMICS OF CABLES

2.1. Introduction

. Focus on the aerodynamic excitation of cables became important when electric power transmission lines and large scale cable supported structures emerged. One of the reasons why cable dynamics became a big engineering issue was because of their inherently low structural damping. The structural damping of cables is typically less than 0.1% of critical, which is at least an order of magnitude less in comparison to other types of structural members. This chapter gives a general description of the aerodynamic problems of cables by considering their dynamic characteristics, excitation mechanisms and possible ways to suppress their occurrence for practical purposes.

There are various types of cable vibration under aerodynamic excitations. They can be categorized as follows:

a) Vortex-induced vibration, or Aeolian oscillation;
b) Buffeting due to wind gust;
c) Classical galloping typically observed in iced cables;
d) Wake interference, or wake galloping and resonant buffeting;
e) Rain-wind vibration;
f) Reynolds number related drag instability;
g) Dry inclined cable galloping; and
h) High-wind speed vortex excitation.

Each of these is briefly explained in the following section.

2.2. Various types of wind-induced cable vibration

2.2.1. Aeolian oscillation

Aerodynamic excitation by vortex shedding is probably the most widely known of all wind-induced vibrations since ancient times. This phenomenon occurs at relatively low wind speed and often in high frequencies and small amplitudes.

The basic mechanism of excitation is a resonance to the frequency of vortex shedding, which is given by

$$f_V = \frac{U \cdot S_t}{D} \qquad (2\text{-}1)$$

where D = the outer diameter of the cable, U = the mean wind speed. S_t is the Strouhal number, which is approximately 0.19 ~ 0.20 for a circular cross-section when the Reynolds number is the order of 10^5 or less.

Once the vibration starts, it tends to control the frequency of vortex formation, which in turn gives the regular fluctuation of forces. In this way the vibration remains in a condition of resonance over a range of air speeds, or the cable vibration is " locked-in" on the structure-fluid coupling. Since the cable's fundamental frequency is often in the range of 0.2 ~ 2 Hz, the resonance is likely to occur with higher harmonic modes with vibration frequencies of 10 ~ 50 Hz, where the mechanical self-damping is likely to be quite high. The maximum vibration amplitude usually does not exceed one cable diameter, peak-to-peak. This peak amplitude is inversely proportional to both the mass per unit length and structural damping ratio. The same mechanism of wind excitation could cause much more serious engineering problems for towers, chimneys and bridge road decks.

However, aeolian vibration of cables is not a serious concern for engineers other than possible fatigue damage near cable clamps of power transmission lines.

2.2.2. Buffeting due to wind gust

Buffeting oscillation is induced by flow turbulence. Due to its random nature, it is usual to design structures based on the " equivalent static load " including the estimated gust loads rather than directly calculating the structural deflection. The estimation of such structural deflection is a complex process, and detailed information about the structure and the flow characteristics is required. The basic idea of the recommendation is to come up with a gust response factor, calculated by a conventional buffeting analysis in the frequency domain. The procedure involved in establishing this factor for civil engineering structures was originally presented by Davenport [1]. For bridge stay-cables, buffeting is less significant except the case of wake interference, where the existence of upstream objects is the cause of disturbance for downstream cables. Electric wires along the main cable of the Golden Gate Bridge exhibited this problem a few decades ago.

2.2.3. Classical galloping typically observed in iced cables

This aerodynamic instability has been studied extensively in connection with the problems of destructive power transmission line vibration since the early 1930's. The vibration is observed when the deposit of ice on the line surface changes the cross-sectional shape of the transmission line. The vibration has been observed mainly in the vertical direction but is often coupled with torsion, with a low frequency of less than 1Hz, and often with large amplitudes of 10 to 20m.

Galloping instability occurs when the negative slope of the lift curve is greater than the drag, which is well known as the Den Hartog criterion [2]:

$$\frac{dC_L}{d\alpha} + C_D < 0 \qquad (2-2)$$

where C_L, C_D, and α are the lift and drag coefficients, and the angle of attack, respectively.

In order to apply this criterion, the magnitude of C_L and C_D need to be experimentally determined. With the assumption that the structure vibrates in a simple harmonic mode in the transverse direction against the wind, Scruton (1960) presented a

procedure for obtaining the steady amplitude based on the quasi-steady assumption [3]. Further to this, Parkinson and Brooks (1961) obtained the nonlinear vibration amplitude of the response by assuming polynomial expressions for drag and lift coefficients. This amplitude is obtained using the value of non-dimensional structural damping and reduced velocity after giving the transverse force coefficients as a polynomial function of the angle of attack [4]. Novak (1969) introduced a concept of the universal response curve and gave detailed discussion on the non-linear characteristics of the response for various types of aerodynamic lift force and effects of wind turbulence [5].

For the case of circular cylinders, there should not be any galloping instability, according to these theories, since the transverse lift force does not exist. However, Irwin suggested that for vertically inclined cables the wind effectively sees an elliptical cross-section, which could cause across-wind force characteristics leading to galloping [6].

2.2.4. Wake interference, or wake galloping and resonant buffeting

The dynamic behaviour of structures excited by wind can be dramatically altered by their proximity to neighboring structures. These mechanisms that lead to aerodynamically induced motion do not even exist for a single isolated structure. Much research on this category of fluid-structure interaction has been motivated by problems encountered with the closely spaced tubes exposed to internal flow of heat exchangers and with bundled conductors used in high voltage electric power transmission lines.

Wake interference aerodynamic instabilities may arise when two horizontally strung cylinders are subjected to the wind in such a way that one cylinder lies in the wake of the other. In this case, if the wake vortex frequency coincides with a natural frequency of downstream structure, resonant buffeting can occur. This excitation is sometimes observed in tall slender chimneys, towers and stacks. Another aerodynamic phenomenon related to bundled conductors is wake galloping. This particular type of motion occurs often in the wind speed of 7m/s to 18m/s. In vertical galloping vibration of bundled conductors, the peak-to-peak amplitude has been observed to be more than one meter.

The aerodynamic mechanism of wake galloping has been studied extensively by many researchers including Cooper and Wardlaw [7] and Simpson and Flowers [8]. This

phenomenon can occur with either closely spaced or largely spaced cylinders. In the closely spaced cylinders in the range of $-2 \leq y/D \leq 2$ and $1 \leq x/D \leq 4$ (Fig. 2-1), the flow around both of two cylinders is significantly altered by aerodynamic interference between them. Vibration starts at the critical flow speed of 5 to 20m/s, and the observed amplitude of vibration is usually less than $3D$: D being the cable diameter. For largely spaced cylinders in the range of $8 \leq y/D \leq 20$, the interference only affects the downstream cylinder and the flow around the upstream cylinder is no longer affected by the downstream cylinder response. Similar problems are provoked in the stay-cables of cable-stayed bridges when two cables are closely positioned.

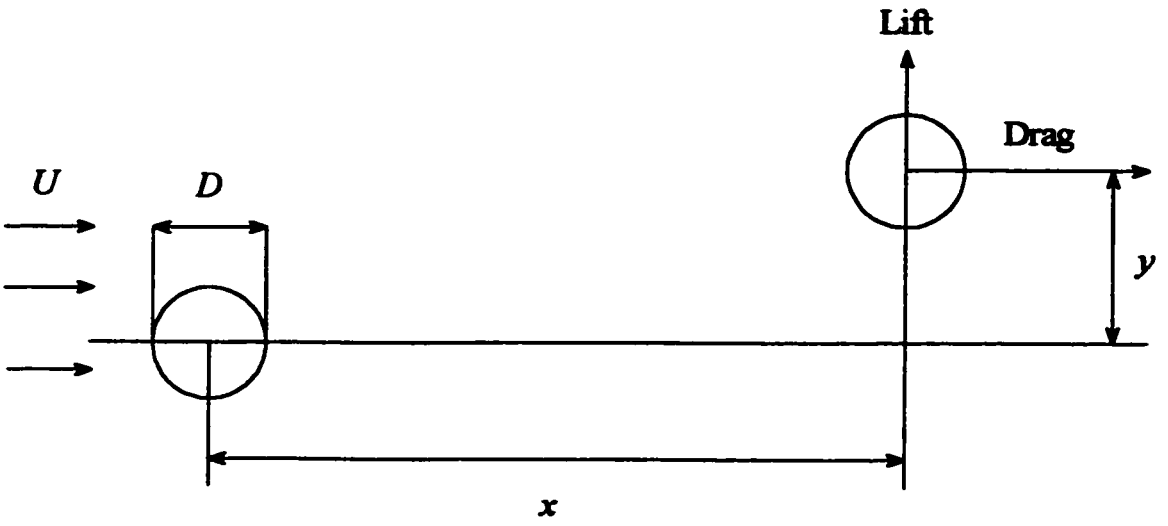

Figure 2-1. Wake interference between two circular cylinders

2.2.5. Rain-wind vibration

This vibration has been observed in the cables of many cable-stayed bridges. It is said to have been first observed at the Koehlbrand Bridge in Hamburg in 1974 [9]. At that time, researchers could not explain the mechanism of this excitation.

However, after a similar mechanism was observed in Japan in the 1980's [10], Hikami (1988) reproduced it with the wind-tunnel model test and found that this mechanism was neither vortex-induced vibration nor wake galloping, but a new kind of excitation. The observed frequency was 1 to 3 Hz, which was well below the critical frequency for the vortex-induced oscillation and the cables were too far apart in distance to cause any aerodynamic interference such as wake galloping. The observed vibration amplitude was up to approximately $2D$: D being the cable diameter. Vibrations usually occur at the mean wind speed of 8 to 15m/s, corresponding to the reduced wind speed range of 20 ~ 80, and the plane of the vertically inclined cable is horizontally skewed against the mean flow direction.

The most interesting aspect of this vibration is in the fact that it occurs when it is raining, but not too heavily. The mechanism of this excitation is not fully understood yet, but is considered to occur in two steps. First, the water rivulets are formed on the cable surface as a result of a sensitive balance between the gravity, capillary and aerodynamic forces. Once formed, they change the cross-sectional shape of the cable. The wind speed range of 8 to15m/s usually corresponds to the critical speed to maintain the upper rivulet on the surface, which becomes the flow separation point.

A wind speed lower than this range cannot maintain the upper rivulet on the cable's critical surface. These water rivulets give rise to the negative slope of lift curve against the change of the angle of attack, resulting in the Den Hartog type galloping instability [11]. Second, once the cable vibration starts, the water rivulet itself also vibrates along the cable surface in circumferential direction and this motion is said to make the modal aerodynamic damping negative [9]. Saito (1994) defined the zone of instability for rain-wind vibrations [12]. Irwin has suggested that the rain-wind vibration could be avoided if the mass-damping parameter defined on the Scruton number, $S_c = m\zeta/\rho D^2$, is more than 10 [6], where ρ = air density, m = the cable mass per unit length,

and ζ = structural damping as the ratio to critical. This criterion has been used to assess the required damping to avoid rain-wind vibration.

2.2.6. Reynolds number related drag instabilities

For circular cylindrical structures such as cables, the magnitude of the drag coefficient depends highly on the Reynolds number. In this respect, there are typically four ranges of the Reynolds number: the sub-critical range, critical range, supercritical range, and the transcritical range. In the critical Reynolds number range, the drag drastically decreases with increasing Reynolds number (Fig. 2-2). If the cable starts to swing back and forth in the along wind direction, the changes in the relative wind speed will in fact create negative aerodynamic damping.

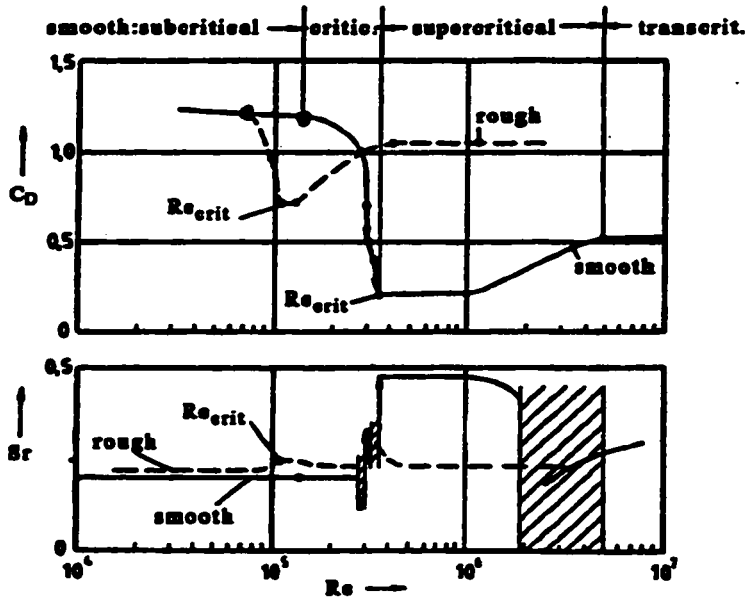

Figure 2-2. Reynolds number versus drag coefficients and Strouhal number relationship

A newly erected conductor line, crossing the River Severn, England, suffered a number of large amplitude horizontal swinging motions induced by wind in 1959-61 [13, 14]. The vibration was severe enough to cause a number of faults and hence it became a

serious engineering problem. There was apparently no vertical conductor motion associated with it. Vibration frequency was found in the range of 0.128 ~ 0.130 Hz, which approximately corresponds to the first asymmetric mode in lateral sway. The vibration was observed at the wind speed of 13 to 15m/s and most of the time the mean wind direction was 10° to 25° deviated from the normal to the span. It was interesting that the observed instability was in a relatively narrow range in terms of both wind speed and its direction. This case was found to be rather unusual example of instability caused by the change of drag force sensitive to the Reynolds number.

The problem was shown by the fact that a stranded wire gives different cross-sectional shapes for horizontally yawed wind. Considering the range of Reynolds number and possible cable diameters, similar instability is conceivable for bridge stay cables, too. However, so far no particular case has been attributed to this mechanism.

2.2.7. Dry inclined cable galloping

The circular sectional shape of a single cable does not induce galloping when it is subjected to the wind normal to the cable, since there are no aerodynamic force characteristics to initiate it.

However, Saito et al. (1994) have reported that the instability could occur when the cables are not normal to the air flow [12]. From their data, it can be concluded that the instability criterion would be given by the following equation:

$$\frac{U_{crit}}{fD} = 35\sqrt{\frac{m\zeta}{\rho D^2}} = 35\sqrt{S_c} \qquad (2\text{-}3)$$

where U = a mean wind speed, f = cable frequency, D = cable diameter, ρ = air density, m = the cable mass per unit length, and ζ = structural damping as the ratio to critical.

According to the above reference, their test results are applicable to the cases where the mean wind direction is nearly parallel to the plane of the cable ($\beta = 0°$) and the angle between cable axis and wind direction is 30° to 60°. It is a difficult condition to clear for bridge stay cables in particular with a typical diameter of 0.15 to 0.20m. If the

realistic range of the Scruton number, S_c, is between 3 and 10, for example, the equation suggests a critical reduced velocity of 60 to 110, which means a critical wind speed in the range of probably 10 to 25m/s. At the same time, it is not justifiable to disregard the possibility of this instability entirely just because it cannot be clarified.

Due to these reasons, there is a strong need to study on this criterion more extensively to see whether or not it has to be observed without exceptions. Possible questions to be studied are as follows:

a) Mechanism of instability

b) Effects of structural damping

c) Effects of cable mass

d) Effects of cable surface roughness

e) Any influence of wind conditions

This thesis reports a part of the study recently carried out on this issue.

2.2.8. High-wind speed vortex excitation

This mechanism has been recently proposed as an explanation for the vibration observed in the inclined cables.

Matsumoto (1992) showed that these vibrations are observed at reduced wind speeds of 20, 40, 60 and so on. These velocities are far higher than the resonant speed in ordinary vortex-excitation. From a series of wind tunnel tests, Matsumoto suggested that there should be a different type of excitation, which could be explained by the existence of an axial airflow behind the inclined cable combining with the conventional von Karman shedding. He explained that the axial flow and vortex-shedding wake flow interact with each other in the wake. The flow visualization using the liquid paraffin confirmed the existence of the axial flow and has also clearly showed the enhanced vortex shedding interaction (Fig. 2-3).

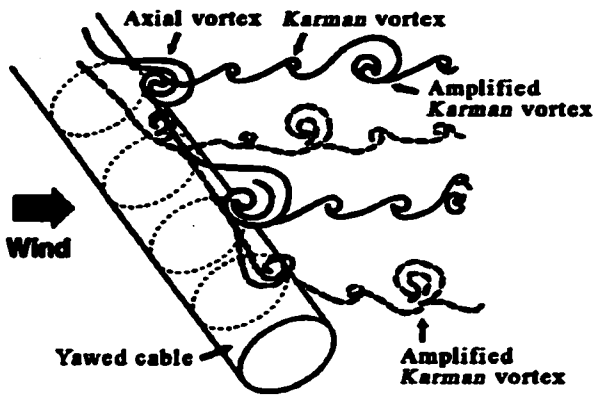

Figure 2-3. Axial and Karman vortex in the yawed cylinder [15]

The frequency of the enhanced vortices, according to Matsumoto, corresponds to the reduced wind speed of 20 [15,16,17,18]. However, the detailed mechanism of the axial flow vortex of an inclined cable need to be further investigated.

2.3. Control methods of wind-induced cable vibrations

Civil engineering structures including bridges, buildings and towers usually have an overall structural damping at the level of 1% of critical. Hence, if there is any possibility of serious dynamic excitations anticipated and yet damping is significantly lower than this level, there should be a warning flag. Cables, such as the ones used in cable-stayed bridges and other cable-supported structures, are prone to wind excitation because of their flexible characteristics and inherently low damping level, usually the order of 0.1% of critical or even less.

Due to these unavoidable characteristics, there have been various attempts to control the vibrations of stay cables of cable-stayed bridge and hanger ropes of suspension bridges. Introduction of artificial dampers is a possible consequence. There have been various dampers developed and applied to power transmission lines and bridge cables. Some of them are referred to here.

2.3.1. Dampers commonly used for power lines

Past experience in this field is important since there have been so many types of relatively inexpensive, simple dampers developed. Aeolian vibration dampers widely used are typically as follows [19]:

The Stockbridge type damper (Figure 2-4) is one of the earliest commercial damping devices, consisting of two pear-shaped masses supported on a length of steel strand. When the end-masses vibrate in their natural frequencies, the steel strand is bent and friction is caused by slipping between wires dissipates vibration energy. Two masses and the strands are sometimes made non-symmetric to make the damper more sensitive to different frequencies. A possible problem of this damper is fatigue failure of the steel strand, ironically, particularly when the damper is effectively working. This damper has been also used for bridge cables.

(a)

(b)

Figure 2-4. Original (a) and re-deigned Stockbridge damper (b)

However, recent study [20] shows that Hydro-Québec has developed a new damper using two elastromeric articulations instead of messengers. This articulation, according to the reference [20], is "based on elastomeric cylinders located in cavities in such a way that the arm rotation not only produces shear in the elastomer but also gives compression to minimize any risk of cracking. Such a technology allowed stoppers to be incorporated in the articulations to avoid damage to dampers under severe ice storm conditions". It has been further innovated to obtain multiple damper resonance frequencies.

Torsional damper (Figure 2-5), which was invented in Canada, consists of an arm and a mass joined through a polymer disc system. When twisting vibration occurs, the polymer is shear loaded due to the inertia of the damper mass. However, it was subsequently abandoned because of inefficiency at most frequencies.

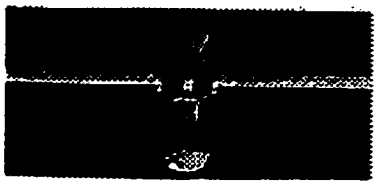

Figure 2-5. Torsional damper

Impact damper invented by a Swedish inventor Elgra consists of a vertical stem having three cast masses loosely fitted to a vertical shaft and each mass rests on a polymer washer. When the conductor acceleration exceeds 1g, these masses do not follow the conductor motion any more and start rattling, which results in vertical impacts and dissipates energy. Tests have shown that this type of damper works well for an acceleration of about 2*g*. However, it was discarded from service in Sweden and elsewhere because of excessive wear at the connecting rod joint.

There are a number of other types of Aeolian vibration dampers mentioned in the literature [19] together with the past experience and experimental observations. In comparison to the vortex shedding excitation case, wake-induced vibration of bundled conductors are often controlled by tilting the bundles, adjusting the cable separation, and staggering the subspan systems. Associated with the last methods, flexible spacer-dampers have been used but they are often structurally complicated and expensive. More

serious vibration problems for power-lines are galloping and vibrations related to wake interferences.

However, most damping mechanisms or protection measures used to prevent these vibrations and their damages are not directly applicable to cable vibrations in general.

2.3.2. Dampers used for stay cables of cable-stayed bridges

Various methods have been developed to suppress the vibration of stay cables and hanger ropes of suspension bridges. Several researchers have investigated the viscous damper attached transversely to damp the response of the cable structures, too.

Among the simplest ideas of artificial dampers are the use of viscous or visco-elastic materials particularly at the cable anchorage and the tie ropes in various ways. Tie ropes can be installed in horizontal, vertical, or diagonal ways depending on the case but the fundamental idea is much the same. The method has been applied to many bridges including Farø, Normandy, Meiko-Nishi, and others. The Normandy and Yokohama-Bay Bridges were equipped with spacer-dampers to provide the connectors or spacers with a simple damping mechanism. The use of the visco-elastic anchorage system, inserting the neoprene rubber washer into the anchorage socket, is installed in the stay cables, too. [21, 22, 23]

Complementary method of visco-elastic anchorage system is the use of the shock absorber or a dashpot, near the anchorage. Brotonne, Sunshine, Aratsu and some other bridges have these dampers and they seem to be quite effective. In order to make the installation of the damper most effective, the damper's damping can be properly designed by considering the overall modal damping. [21, 24]

However, cable connection using tie ropes and viscous damper have not proven to be well-balanced countermeasures from the structural aesthetics, installation and maintenance. Research on this problem has been extensively carried out all over the world, and led to solutions such as the passive magnetic damper and active control damper. The passive magnetic damper mechanism changes the vibration mode of cables. The active control damper uses the external force applied by an actuator to suppress the

dynamic response. These methods also have some disadvantages for their commercial application because of production costs, reliability, and maintenance costs.

Another suppression method involves the application of various surface treatments to the cables, particularly for controling rain-wind induced vibration. Actually, surface treatment methods have been used extensively to control other structures, too, such as chimney stacks, pipelines, towers etc. in prevention of vortex excitation and galloping instability. Examples of the stay cable vibration using surface treatment methods are the Higashi-Kobe Bridge cables with longitudinal fins, the Yuge Bridge cables fitted with parallel grooves, and the Tatara Bridge cables given surface indentations. [23, 24]

In this chapter, various wind-induced vibration mechanisms and vibration control methods were discussed but some mechanism such as inclined dry cable vibration and high-speed vortex excitation have not yet clearly been defined. The following chapters of the thesis deal mainly with these topics.

CHAPTER 3

EXPERIMENT

3.1 Objective

In 1994, Japanese researchers (Saito et al.) reported that galloping instability could occur without deposition of ice or rain when the cables were inclined against wind. According to this report [12], instability was possible when the angle between the cable axis and the wind direction was 30° to 60°. If this instability criterion is applied without any exceptions, many existing bridge stay-cables would be categorized as "prone to galloping". However, in reality most of the existing bridge stay-cables have been surviving without any problems related to this galloping instability. From this point, it is obvious that this criterion has to be examined carefully.

The objective of this study is to confirm the existence of the above-mentioned galloping instability of the inclined dry cables and also to identify the influence of some parameters such as structural damping and cable surface roughness, which may have significant impact on the vibration.

To this end, a series of wind tunnel tests was conducted at the "Propulsion" wind tunnel, using a two-dimension sectional model of an inclined dry cable. The wind tunnel belongs to the Institute of Aerospace Research (IAR), National Research Council of Canada (NRCC). The experimental program was a part of the collaborative research effort between the University of Ottawa, IAR/NRCC, and an industrial partner, RWDI of Guelph, Ontario, under the initiative of the university. The spring system supporting the cable model was designed and manufactured by RWDI and installed in the wind tunnel in May 2001.

3.2 Model cable and its setup

A section of cable was used as the model. The properties of the model are: 0.16m in outer diameter, 6.4m in length, and a mass of 60.8kg/m. Figures showing the cable model and spring systems are shown in Figure 3-1.

The cable model is a hollow steel pipe and there is a concentric internal cylinder fixed inside of it to adjust the weight and also to help in the model installation. The inner cylinder is also a steel pipe of 0.1m diameter (Figure. 3-2). The outer surface of the model is wrapped with a polyethylene sheet to make the surface smooth.

Each end of the cable is connected to four springs to allow movement in two perpendicular directions. For this study, the lateral direction of the spring system is defined as the cross-wind direction corresponding to the direction of the spring angle α in the wind tunnel and the vertical direction of the spring system is the along-wind direction. The up-wind end of the cable was located above the ceiling of the tunnel and is connected to an axial wire to partially support the cable weight. The lower end of the cable is also supported by a four-spring rig, which is identical to the one at the upper-end, except the lower end rig is placed on two beams which were installed across the wind tunnel section. The same setup of the springs was used through the whole test series. These springs have a total mass of 60kg, and have vertical and lateral spring constants of 4.99kN/m and 4.78kN/m, respectively.

The vertical test setup angle ϕ and the rotation angle of the spring system α are related to a combination of the vertical inclination angle θ and the horizontal yaw angle β on the bridge stay-cables. The definition and the relationship between these angles are given in Table 3-1 and Appendix A. Elevations of the setup are given in Figs. 3-3 to 3- 5.

Table 3-1. The model setup angle

	Cable inclination angle (θ)	Wind attack angle (β)	Cable-wind relative angle (ϕ)	Setup of rotation angle of spring system (α)
Setup 1B	45	0	45	0
Setup 1C	30	35.30	45	54.74
Setup 2A	60	0	60	0
Setup 2C	45	45	60	54.74
Setup 3A	35	0	35	0
Setup 3B	20	29.35	35	58.70

3.3 Facilities used

3.3.1 Wind tunnel

The wind tunnel is of the open circuit type and its test section is 3.05m (width), by 6.10m (height), and 12.19m long (Figs. 3-6 and 3-7). The non-uniformities of mean speed in the test section are less than 0.5% and the deviation of flow direction is less than 1 degree from the longitudinal axis. The floor of the working section can be elevated by about 0.5m. The flow enters the test section through a contraction cone which accelerates the flow and improves the uniformity of the flow velocity. The maximum available mean wind speed in the test section is about 39m/s. The wind speed at the test section tends to be less stable when the mean wind speed is less than 5m/s, depending on the outside weather condition.

3.3.2 Experimental Apparatus

The following apparatus were used for the measurements:

1) Pitot-tubes
2) Non-contact type displacement sensors and controllers (Matsushita, ANR1226 and ANR5141)
3) Measuring device of the angle of inclination (Lucas Angle Star's digital protractor)
4) Low-pass filter (Frequency Devices, Model 901)
5) Mechanical dampers (Airpot dampers and elastic rubber bands)

For wind speed measurement, two standard Pitot-tubes were installed at both sides of the test section, at 2.07m from the inlet, 0.37m inside from the wall surface, and 3.61m above the tunnel floor. For the wind tunnel operation, the wind speed was set from a pressure differential obtained from static taps on the contraction and working section of the wind tunnel. The pressure was read with a very sensitive Druck LPM 9381 high differential pressure transducer, 20.32cm water maximum and 0.1% accuracy at maximum 20.32cm water.

In order to obtain the amplitude of cable motion in both lateral and vertical directions, two displacement sensors, Intelligent Laser Sensors Model ANR1226 and Controllers Model ANR5141, were installed at each end of the cable. The laser sensing heads were placed 0.25m away from the targets. These laser devices can measure the displacement in the range of ±150mm with the linearity error of less than 0.4%.

To measure the inclination of the cable in relation to the wind direction and the direction of the spring support, Lucas Angle Star's digital protractor was used.

It was found that there was mechanical noise throughout the tests at the frequency of approximately 40Hz. This was presumably caused by the vibration of the wind tunnel shell. A low-pass filter Model 901 was used with a cut-off frequency of 10Hz.

For the consideration of damping effects, additional damping was provided by either the Airpot dampers (Fig. 3-8) or by attaching rubber bands on the springs. Also, the

surface roughness of the model was modified slightly by spraying a kind of liquid glue. The characteristics of additional dampings and the surface roughness effects provided to the system are discussed in Chapter 4.

3.4 Experimental procedure

All test cases were conducted with mean wind speeds of 7 to 39m/s and with smooth flow condition. The experimental procedures are as follows:

1) Free vibration of the model in still air was initiated by manual excitation in order to measure the frequency given in Table 3-2 and structural damping of each case. The results are given in Appendix B. The free vibration record in both lateral and vertical modes were stored and analyzed by the data acquisition system and natural frequency and damping in each direction were calculated.

Table 3-2. The cable model natural frequency

The model setup (smooth surface, no additional damping)	Natural frequency (Hz)	
	Lateral	Vertical
Setup 1B	1.430	1.389
Setup 1C	1.424	1.401
Setup 2A	1.418	1.390
Setup 2C	1.421	1.404
Setup 3A	1.430	1.392
Setup 3B	1.422	1.422

2) According to Reference [12], galloping instability was observed at a reduced wind speed range of 60 ~ 110. This range corresponds to the critical wind speed of 13 ~ 25m/s with the present setup. The wind speed for the tests was first set at 7 ~ 8m/s in the present experimental procedures and was increased by approximately 1m/s increments up to the maximum wind speed available in the tunnel. The reason the initial wind speed was set at 7 ~ 8m/s is that the objective of the study is to find the onset wind speed of galloping instability rather than the vortex excitation. The vibration amplitude of the model was limited approximately to the cable diameter

(D = 160mm) because of the clearance of the wind tunnel ceiling for the model setup.

3) When the vibration did not occur at these wind speeds, excitation of cable by hand was done to observe whether or not the amplitude would increase.

4) The surface roughness was modified by spraying liquid glue to examine if it could make any difference in cable response. Structural damping of the system was also modified by using elastic rubber bands or the Airpot damper.

5) The procedure from (1) to (3) was repeated for each run.

6) Frequency ratio of two directions was also changed to examine its difference on the cable response.

3.5 Data acquisition

The experimental results were obtained through 7 channels of the data acquisition system, Analog-to-Digital DAQ. The channels from one to four are for the displacements or the amplitudes in both lateral and vertical directions. The other channels are for two readings of the wind speed and wind tunnel temperature.

The analogue outputs from the displacement transducers were sampled at a frequency of 100Hz. A spectral analysis of the cable motion signal is also performed to determine the natural frequency of each case. The results are given in Appendix B.

The dynamic pressure in the test section was measured with Pitot-tubes placed one on each side of the wind tunnel working section wall, and were connected to the Druck transducer (Model 103545 and 103551) before reaching the data acquisition.

The temperature of the flow in the test section (RTDs) and the barometric pressure (Ruska 6200) were also recorded for each run.

The flowchart of the outputs is shown at Figure 3-9 and the input of each channel is explained in Table 3-3.

Table 3-3. Data acquisition

Input Channels	
Channel 1	Lateral Direction at Upwind end (X direction)
Channel 2	Vertical Direction at Upwind end (Y direction)
Channel 3	Lateral Direction at Downwind end (X direction)
Channel 4	Vertical Direction at Downwind end (Y direction)
Channel 5	Pitot 1
Channel 6	Pitot 2
Channel 7	Temperature

Output plot (Computer screen)	
Plot 1	Lateral direction displacements versus time at each end
Plot 2	Vertical direction displacements versus time at each end
Plot 3	Resultant displacement versus time at each end
Plot 4	Angle versus time at each end

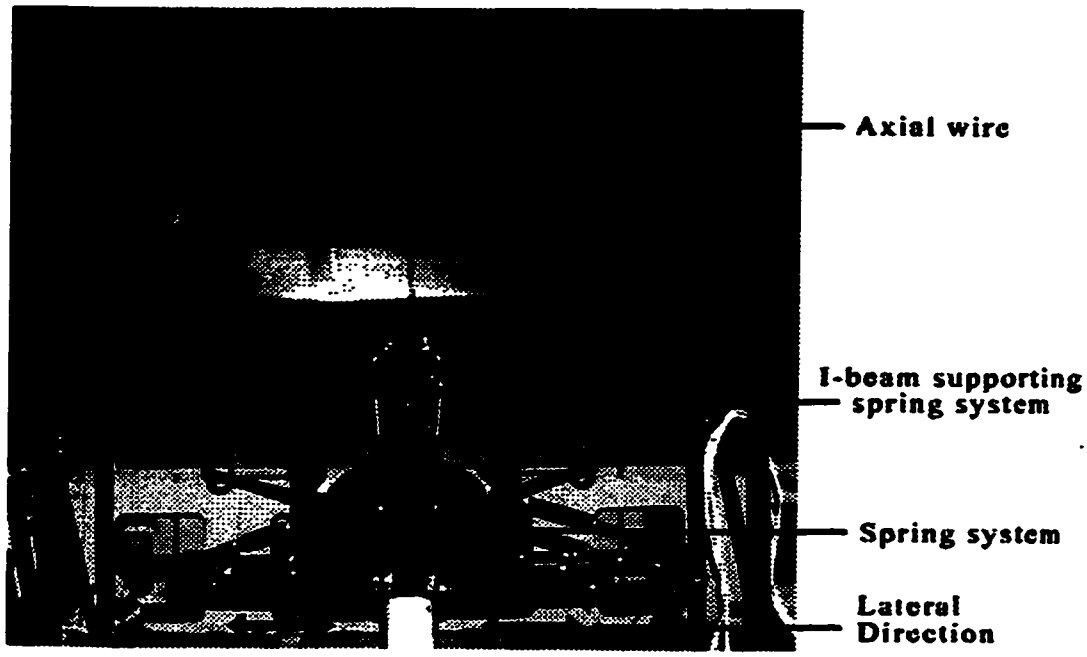

a) Up-wind end of the cable setup (rotation of spring system α=0°)

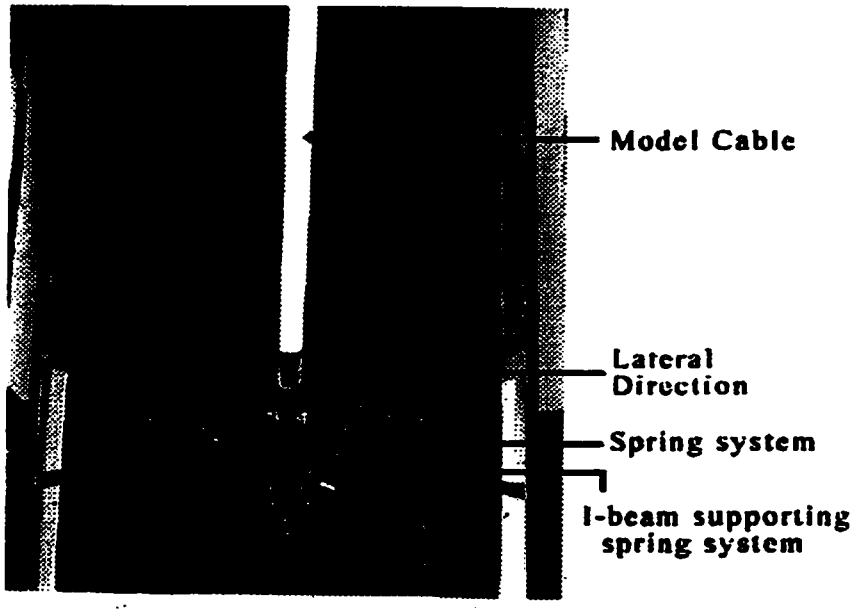

b) Lower-end of the cable setup (rotation of spring system α=0°)

Figure 3-1. Spring system and model setup

c) Up-wind end of the cable setup (rotation of spring system α=54.7°)

d) Lower-end of the cable setup (rotation of spring system α=54.7°)

Figure 3-1 (continued). Spring system and model setup

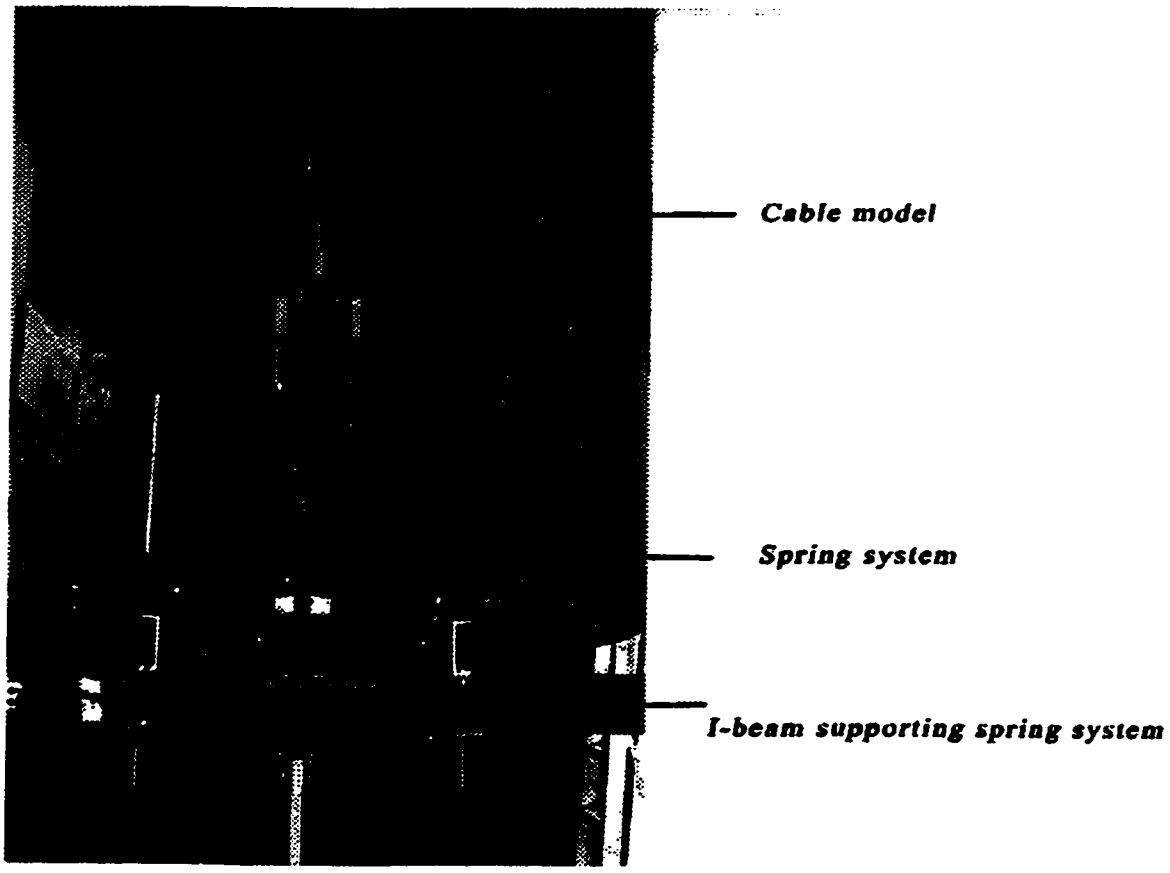

e)

Figure 3-1 (continued). Spring system and model setup

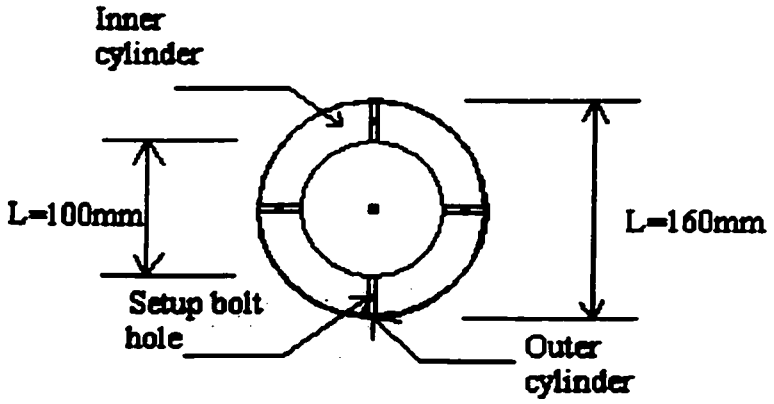

Figure 3-2. Model cable cross-section and dimension

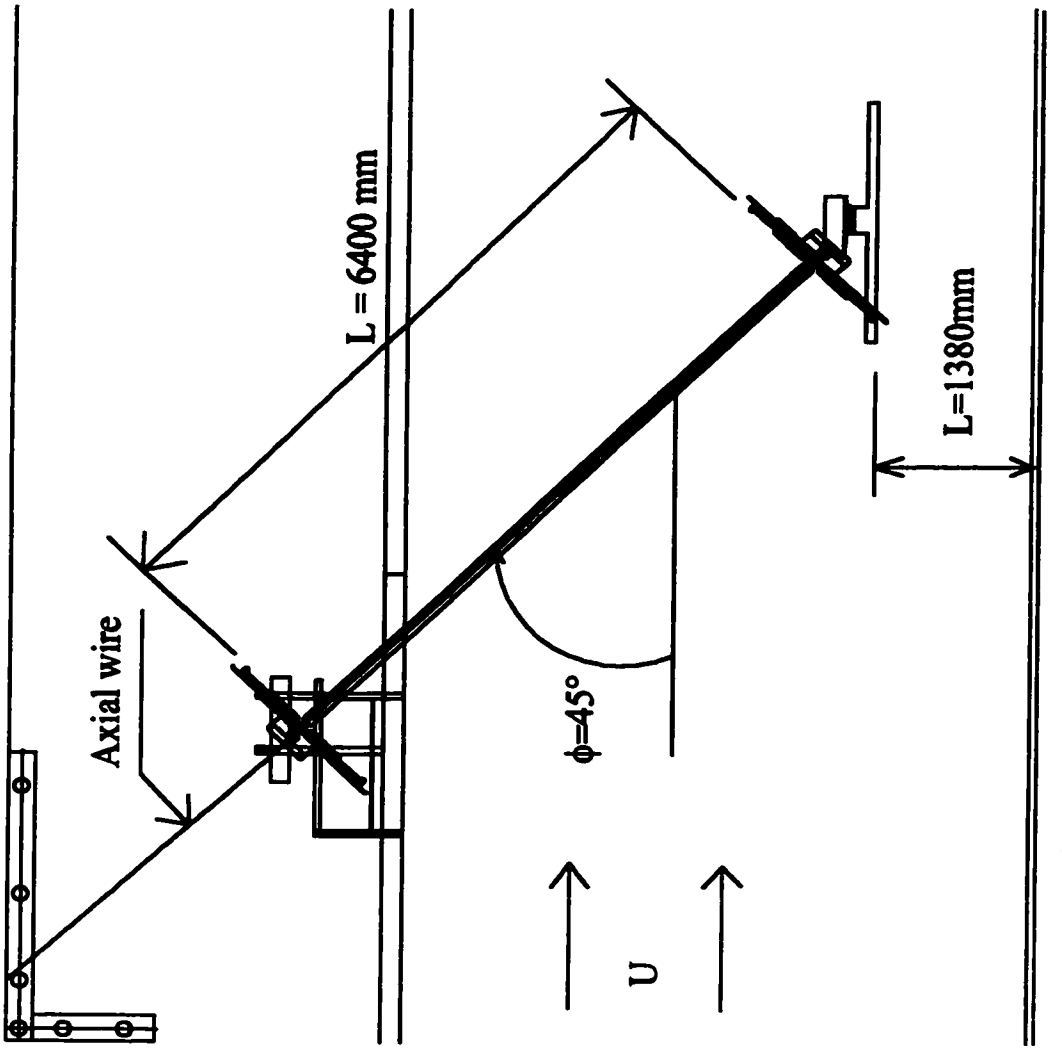

Figure 3-3. Side view of setup 1B and 1C

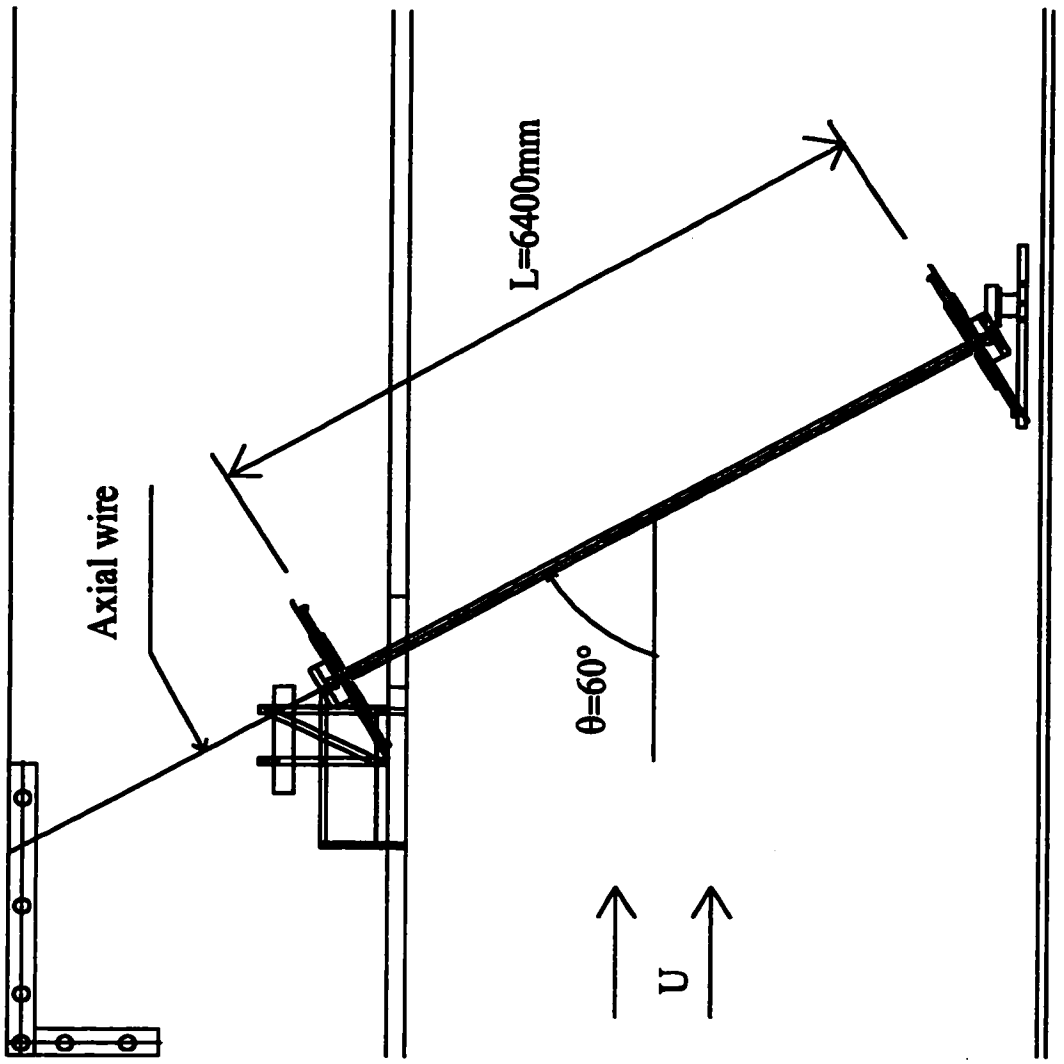

Figure 3-4. Side view of Setup 2A and 2C

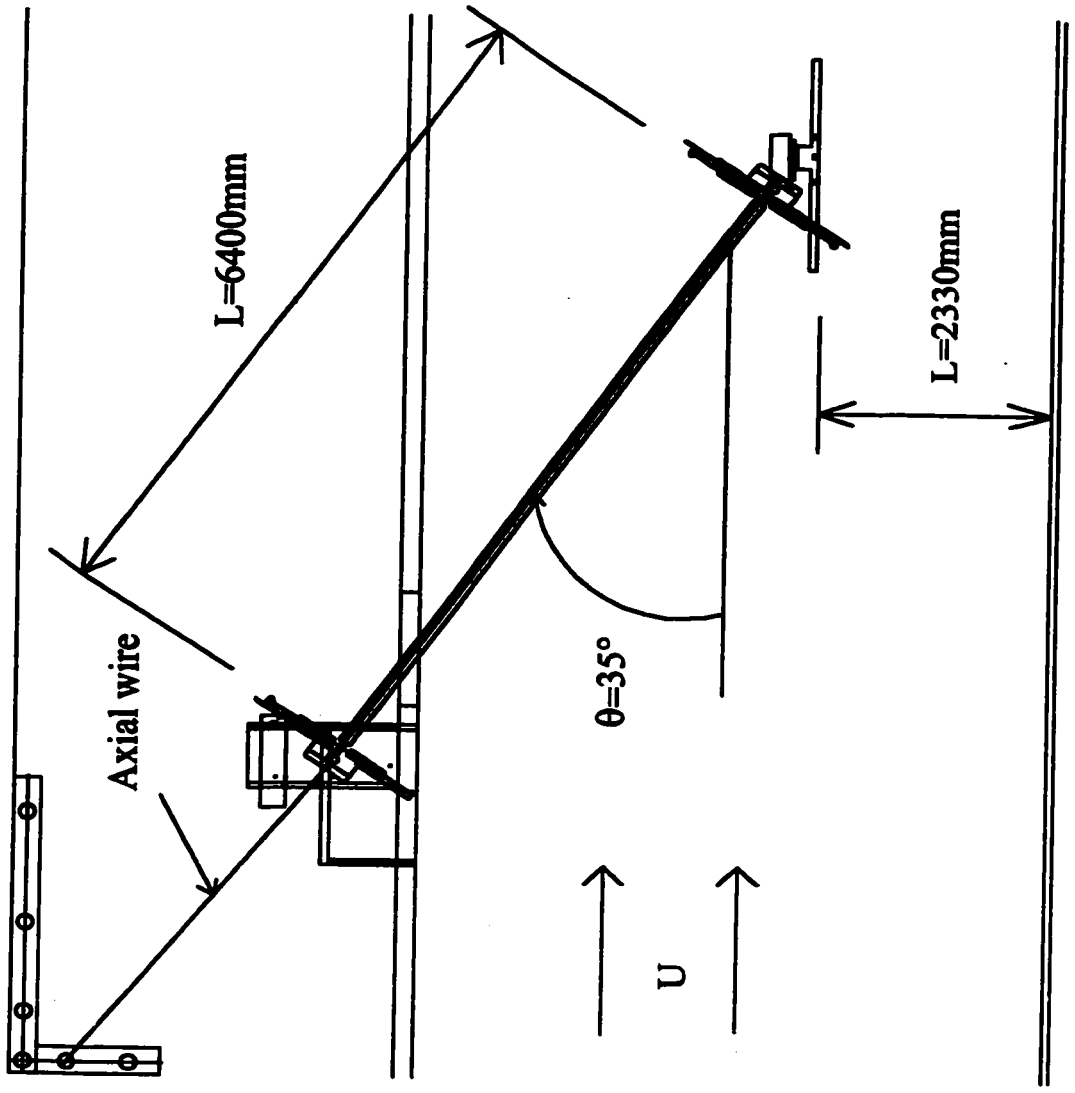

Figure 3-5. Side view of Setup 3A and 3C

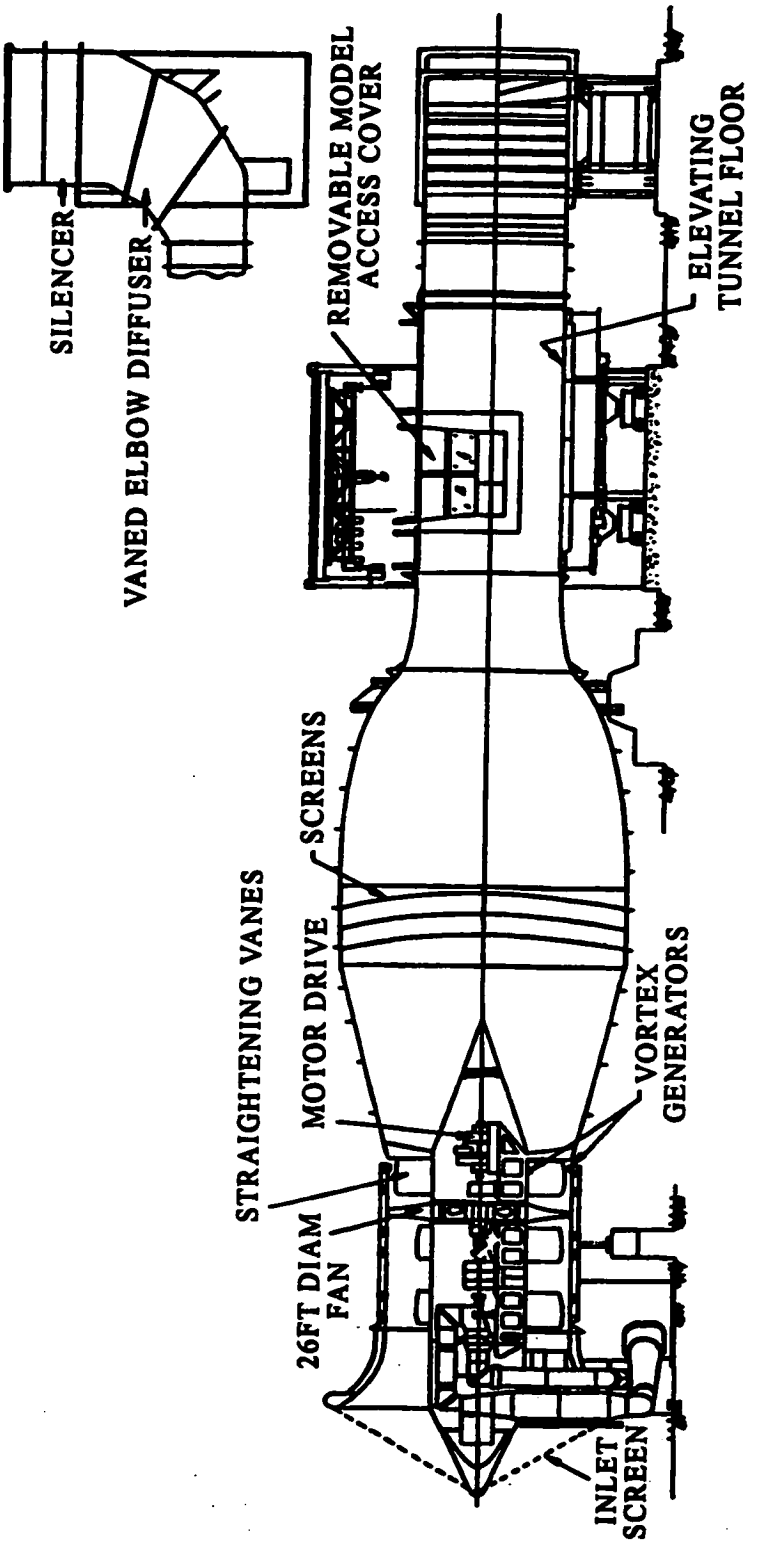

Figure 3-6. Wind tunnel (NRCC)

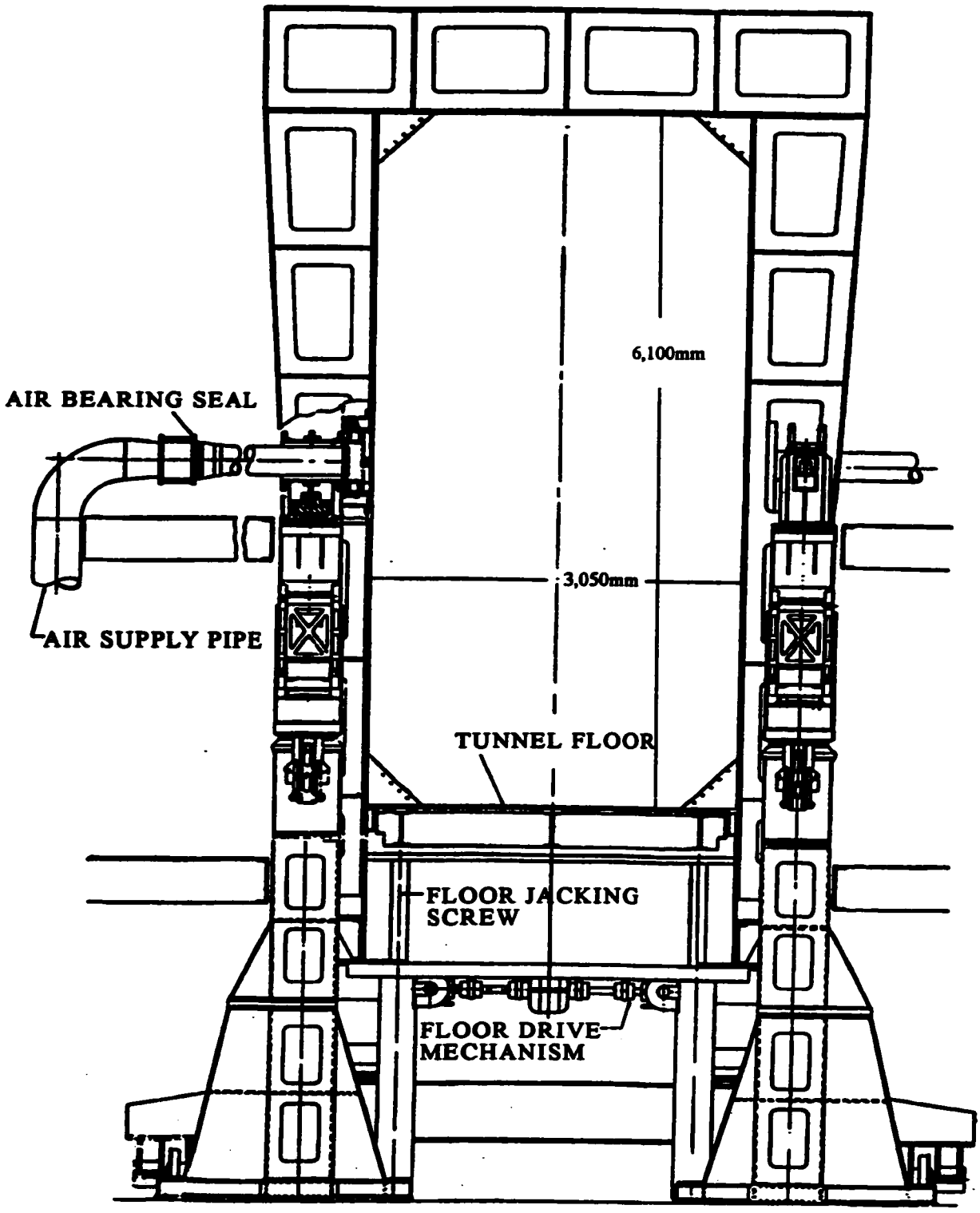

Figure 3-7. Wind tunnel working section (NRCC)

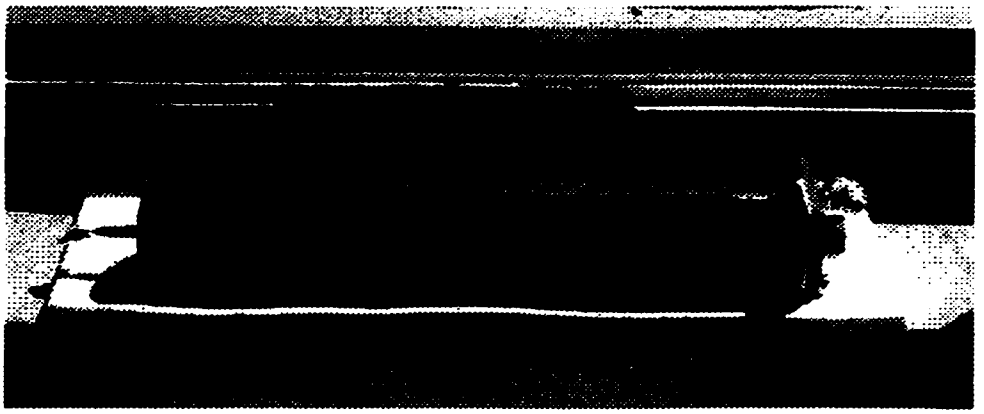

Figure 3-8. Airpot damper

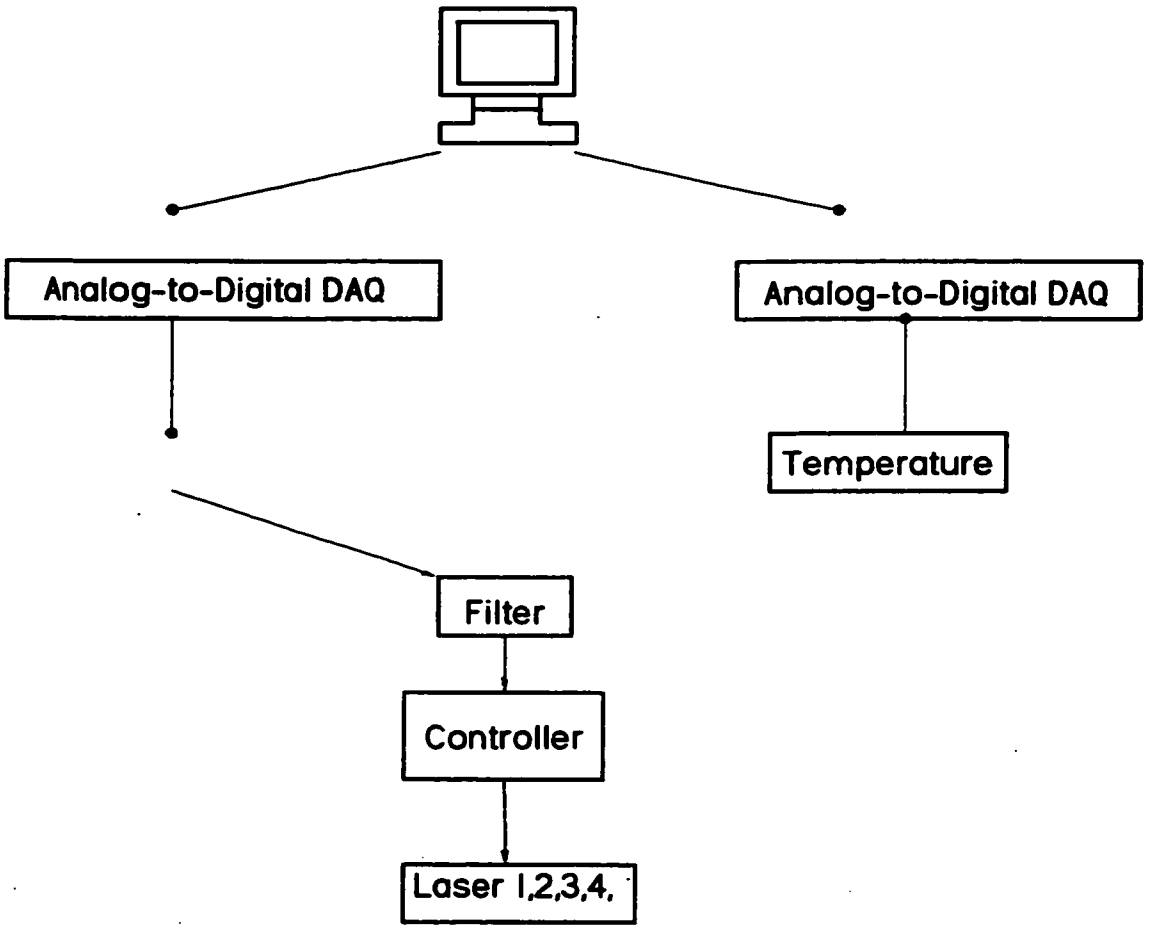

Figure 3-9. The flow chart of the outputs

CHAPTER 4

TEST RESULTS

4.1. Summary of the test results

Both divergent type of cable motion and the limited amplitude response of the cable were observed.

4.1.1 Divergent type response

Divergent type response of the cable was observed only in Setup 2C. This response has the characteristics of galloping instability. The galloping motion is characterized by a quick increase of amplitude with increasing wind speed at the natural frequency of structure as mentioned in Chapter 2. The amplitude response of the cable and the response trace at a mean wind speed of 32m/s are given in Figs. 4-1 and 4-2, respectively.

It is shown in the time trace that the amplitude was less than 20mm at the mean wind speed range of 10 ~ 30m/s but when the mean wind speed reached 32m/s, corresponding to the reduced wind speed $U/fD = 140$, the amplitude increased from ± 20 to ± 80mm. Moreover, the vertical amplitude also showed a tendency of increasing further. It had to be manually suppressed due to the clearance of the wind tunnel ceiling for the model setup. The maximum peak-to-peak response observed was about $1D$, where D is the cable diameter.

4.1.2 Limited amplitude vibration

Limited amplitude vibration was observed with four different setup cases and they are shown in Figs. 4-3 through 4-15. Test results indicate that all of these have the characteristics of a high-speed vortex excitation.

The characteristics of the motion are summarized as follows:

a) The amplitude of the motion is limited. The largest amplitude observed was with the setup 2A. When the wind speed is 19m/s, the amplitude of the cable motion reaches the maximum of 67mm. The amplitude response is shown in Figure 4-7 and time trace at the wind speed of 30m/s is given in Figure 4-8.

b) The unstable motion was observed only in a limited wind speed range.

c) The maximum magnitude of the unstable motion depends on the orientation angle of the cable. It was larger with greater vertical inclination angle, as given in Table 4-1.

Table 4-1. Wind speed range of instability

Model setup	Cable inclination angle (θ)	Wind attack angle (β)	Cable-wind relative angle (ϕ)	Angle of the spring system (α)	Wind speed range (U: m/s)	Maximum Amplitude (mm)	Reynolds number (UD/v): $*10^5$
Setup 2A	60°	0°	60°	0°	18~19	67	1.9
Setup 1B	45°	0°	45°	0°	24~26	31	2.6~2.8
Setup 1C	30°	35.27°	45°	54.74°	34~38	25	3.6
Setup 3A	35°	0°	35°	0°	22	20	2.4~4.1

In setup 3B, which is equivalent to the case of a cable with a very shallow vertical inclination angle of 20° and horizontal yaw angle of 29.35°, no unstable motion was found within the wind speed range of 8 ~ 34m/s. The response observed was less than 5mm. Its amplitude response is in Figure 4-13 and the time trace and PSD are given in Figure 4-14.

d) When the cable motion becomes unstable, there are two types of response: one is very organized harmonic motion and the other displays with the regular beating, which is similar to what Matsumoto described as the case of three-dimensional Karman vortex shedding. He explained that this regular beating is caused by the fluid interaction between the axial vortices along the inclined cable surface and the Karman vortices in the wake of the cable. The Karman vortex shedding is amplified intermittently as a result, according to his explanation [15,16,17,18], which induces the beating type motion of the inclined cable.

e) In some of the setups, such as the setup 2A and setup 3B, an elliptical motion of the cable was observed, which correlates well with the field observation [25]. Samples are given in Figs. 4-11 and 4-15.

f) It is interesting to observe that all of these phenomena occurred more or less at the wind speed corresponding to the critical Reynolds number.

4.2 Parametric study

For this study, the cable surface roughness and the structural damping effects were considered to be the parameters that might have significant impact on the vibration of inclined dry cables.

4.2.1 Surface roughness effect

For the present study, the model was originally wrapped with a polyethylene sheet to give the smooth surface. However, for the rough surface, the cable surface was sprayed with liquid glue to examine if it would produce any differences in the cable response. Experimental results are given in Figs. 4-16 through 4-19. The surface roughness is characterized by the roughness shape and the distribution of the roughness particles. This effect changes the flow separation points on the cable surface. In fact, the rougher surface is, the earlier the separation point occurs closer to the upstream of the cable surface, depending on the upstream flow speed. The major effect of separation is the large suction on the downstream of the cable, causing the wake to be much wider.

4.2.2 Damping effect

Four different levels of structural damping (i.e. low, intermediate, high, and very high damping) were applied to examine the effect of damping on the cable response. The relationship between the damping and the response amplitude are given in Figure 4-20.

Originally, it was intended to use a commercially available dashpot type damper called "Airpot" to provide the system with the additional damping. However, the Airpot damper was found to have a sharp non-linearity as shown in Figure 4-20. Extremely high damping with small amplitudes is due to the friction between its piston and the cylinder wall. Because of this non-linearity, it was decided to use the Airpot damper only for the

"very high" damping case, which is the order of 1% of critical. For the other levels, the additional damping was given to the system by adding several elastic rubber bands on the springs. These lower damping values were from 0.03% to 0.5% of critical, covering the data range of the previous researchers. Figure 4-21 gives the wind-induced response of the cable model with the setup 1B under all four levels of damping. As clearly shown in the figure, when the damping is increased, the response is significantly reduced, but the position of the wind speed range where the vibration occurred did not change. This set of results indicates that this limited amplitude motion can be suppressed by increasing the damping of the cable. Figure 4-22 shows the wind-induced response for setup 2C with high structural damping.

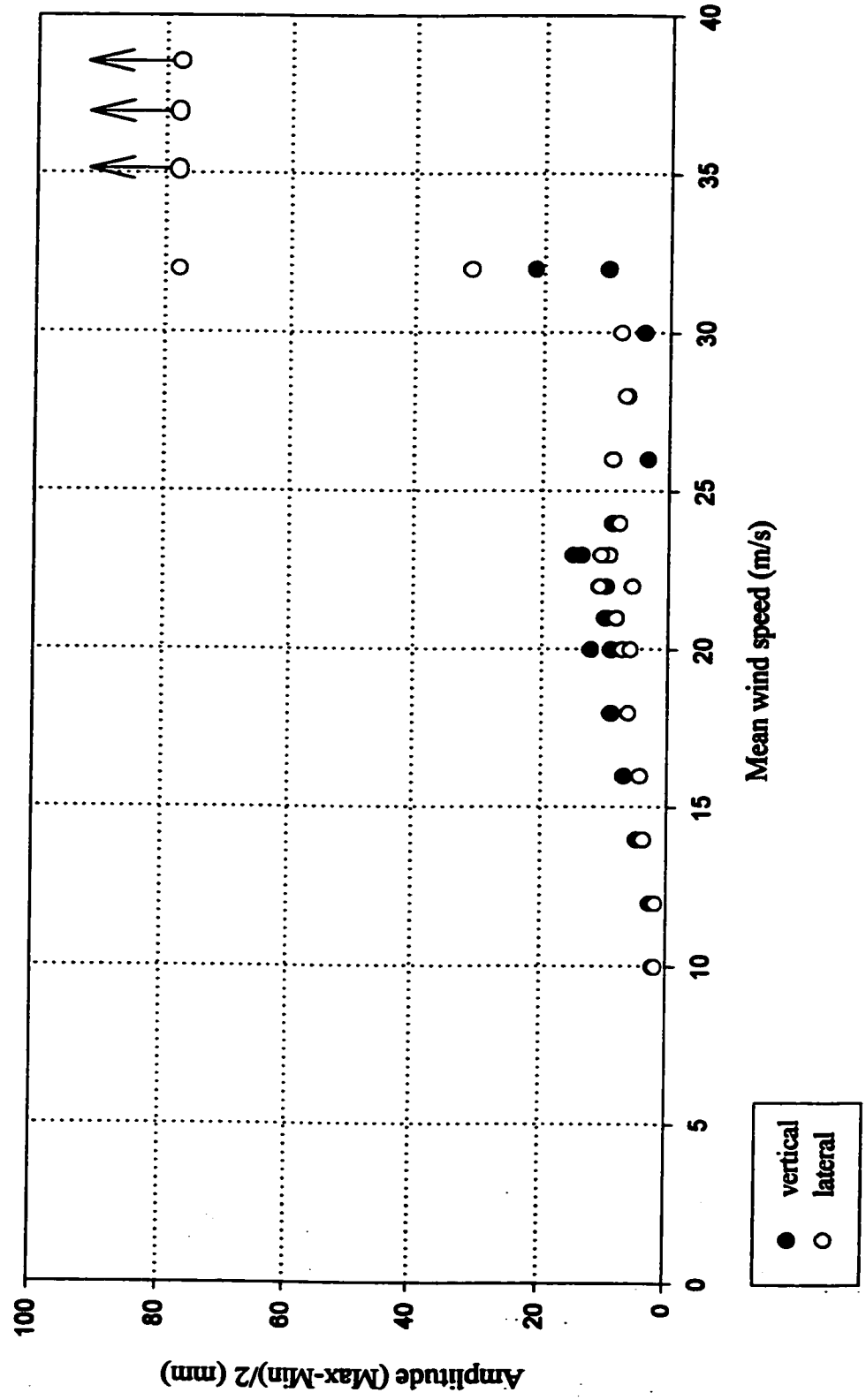

Figure 4-1. Wind-induced response of setup 2C with smooth surface and no additional damping

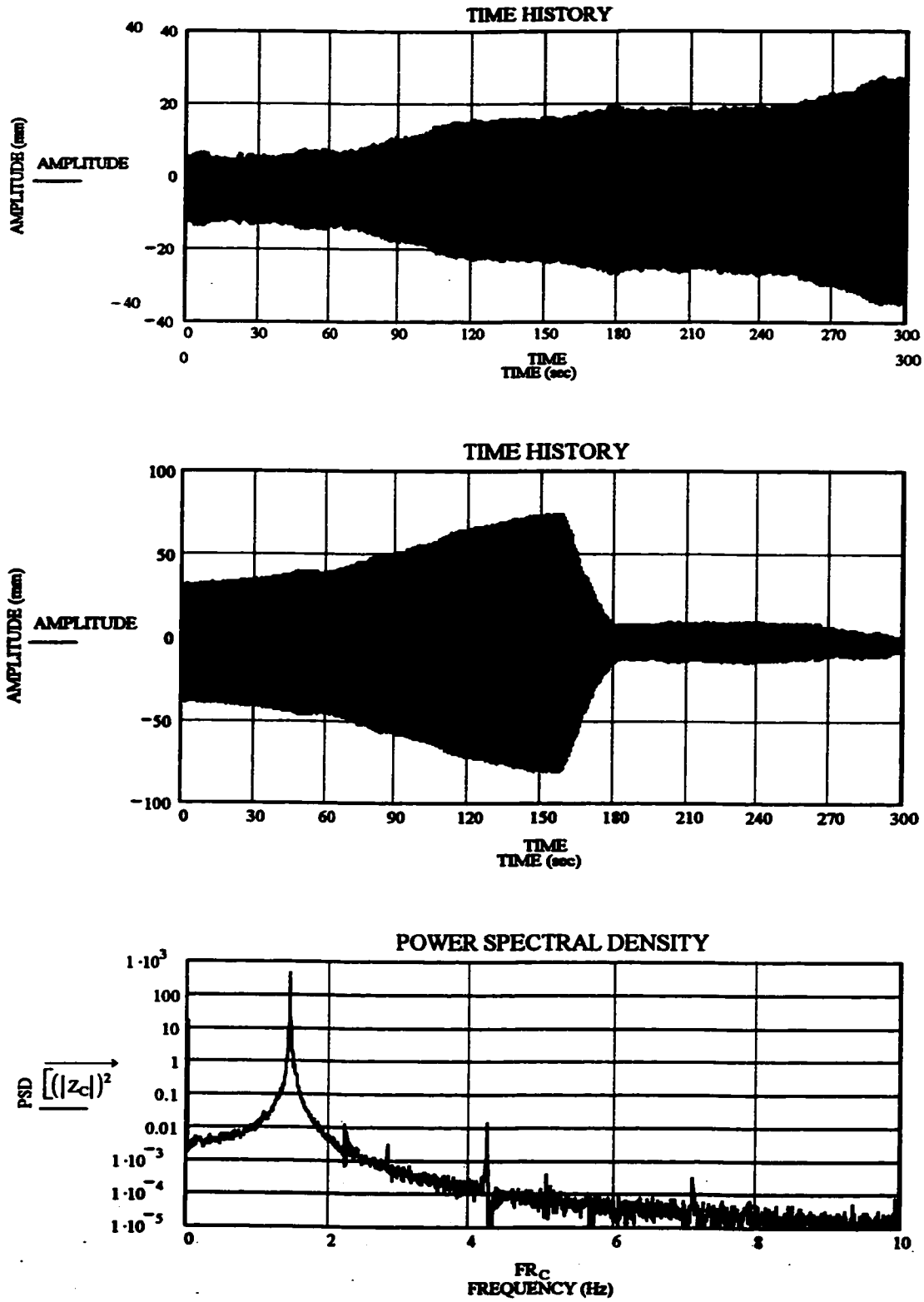

Frequency: 1.416Hz

Figure 4-2. Time trace and PSD of model setup 2C at the mean wind speed of 32m/s

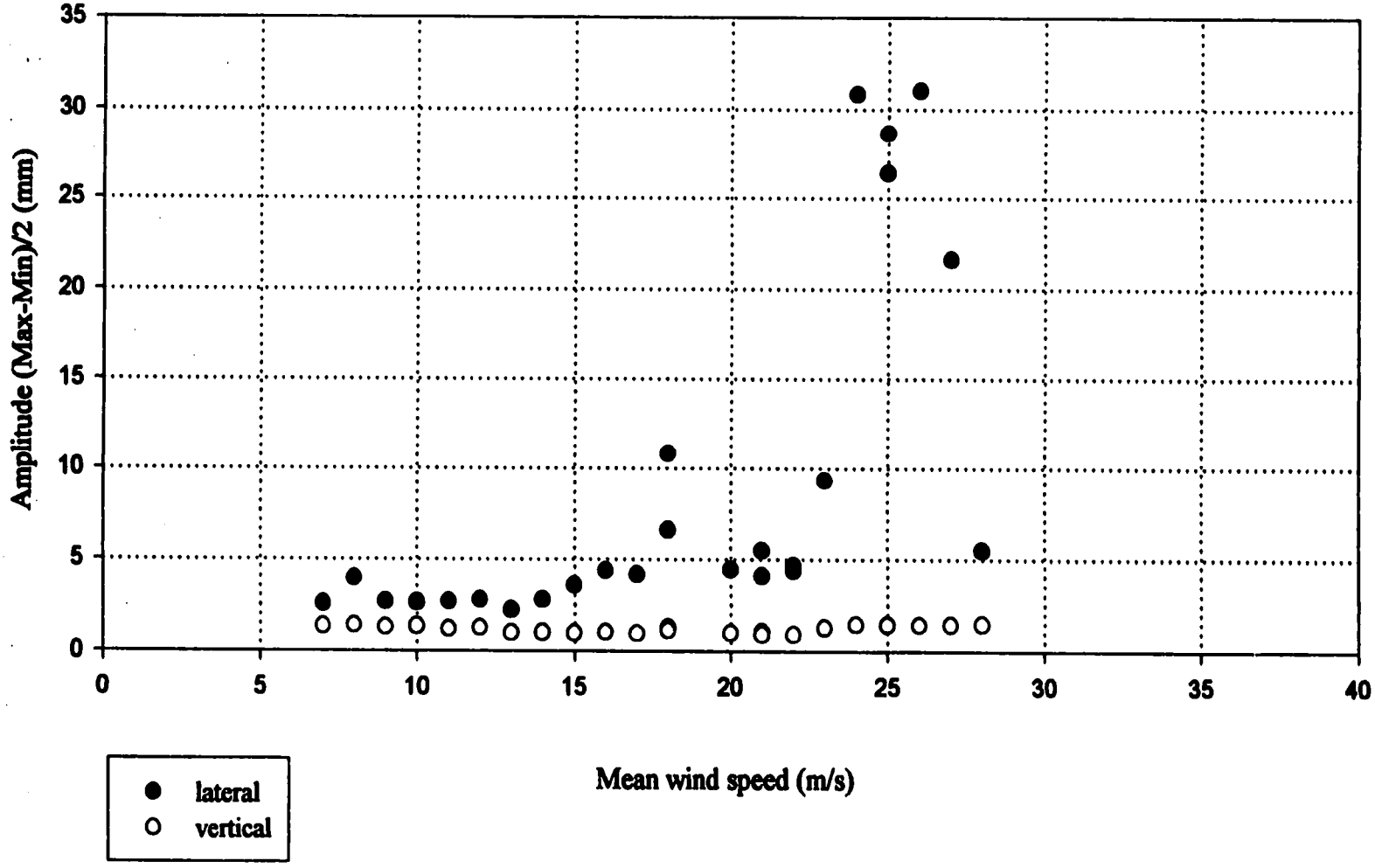

Figure 4-3. Wind-induced response of setup 1B with smooth surface and no additional damping

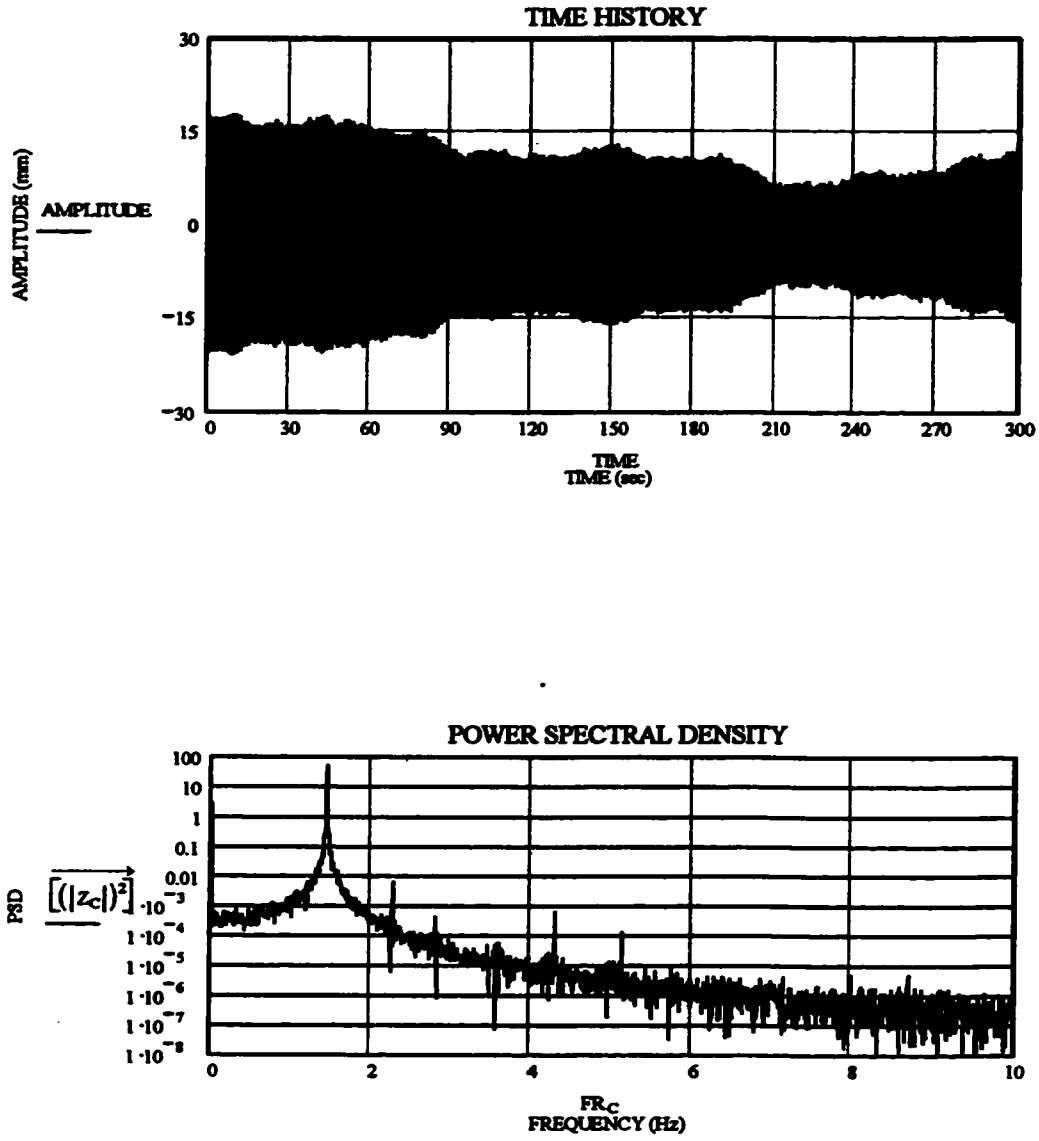

The corresponding frequency to the mean wind speed 26m/s is reached at 1.434Hz.

Figure 4-4. Time trace and PSD of model setup 1B at the mean wind speed of 26m/s

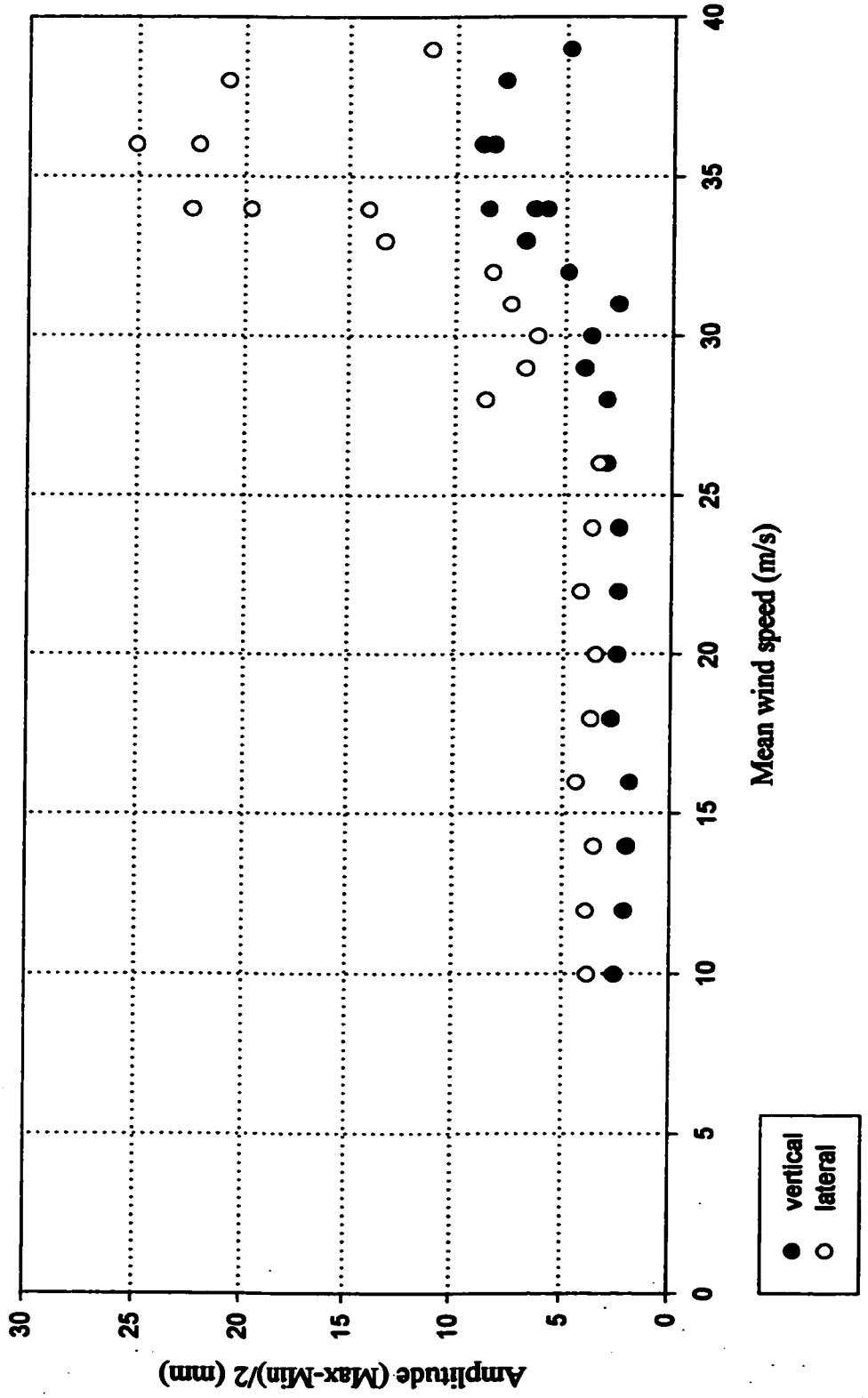

Figure 4-5. Wind-induced response of setup 1C with smooth surface and no additional damping

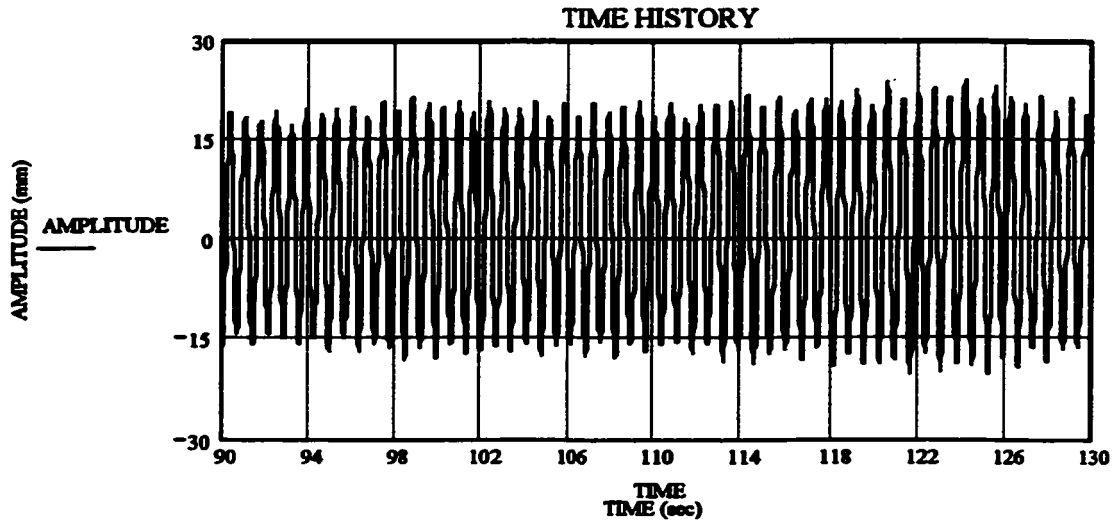

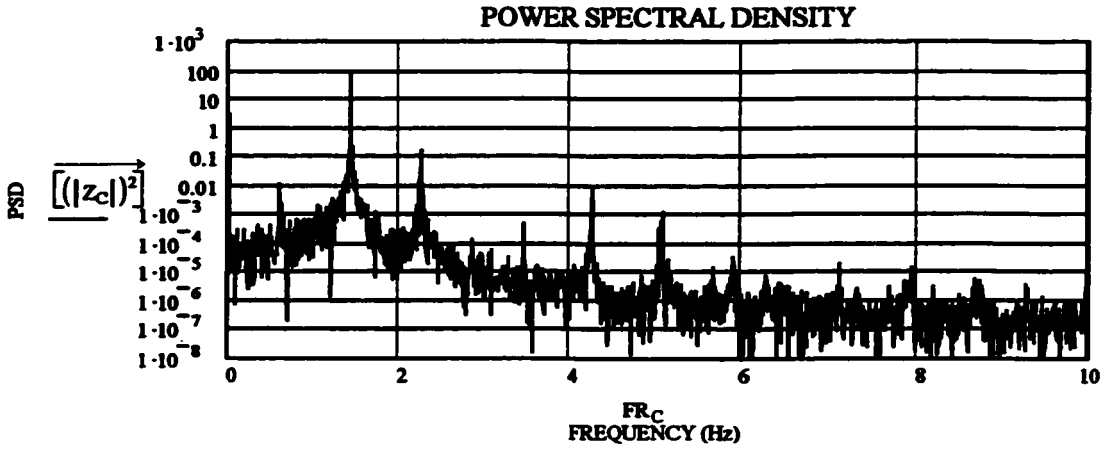

Frequency:

1. 1.422Hz
2. 2.246Hz
3. 4.266Hz
4. 5.090Hz

Figure 4-6. Time trace and PSD of model setup 1C at the mean wind speed of 36m/s

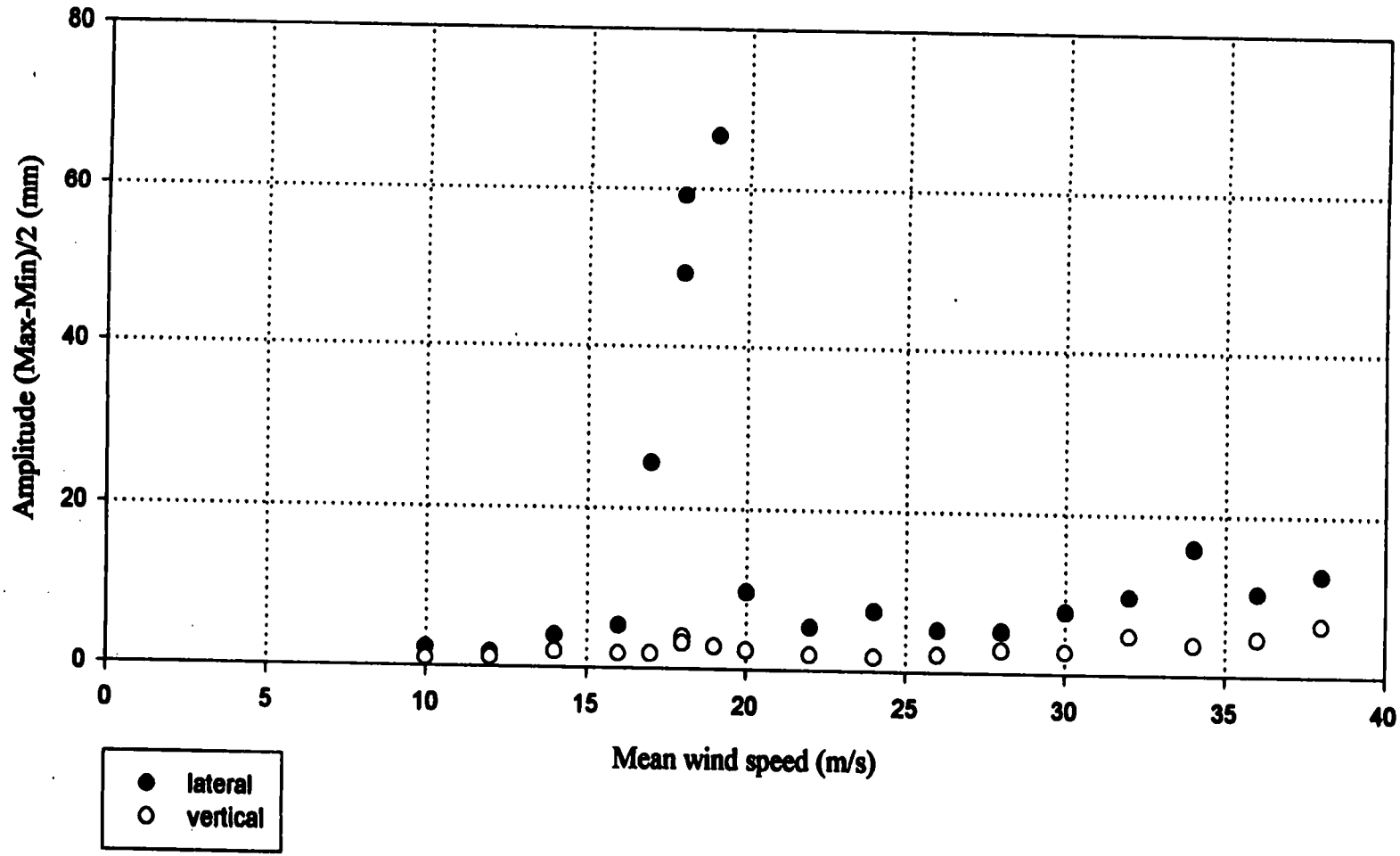

Figure 4-7. Wind-induced response of setup 2A with smooth surface and no additional damping

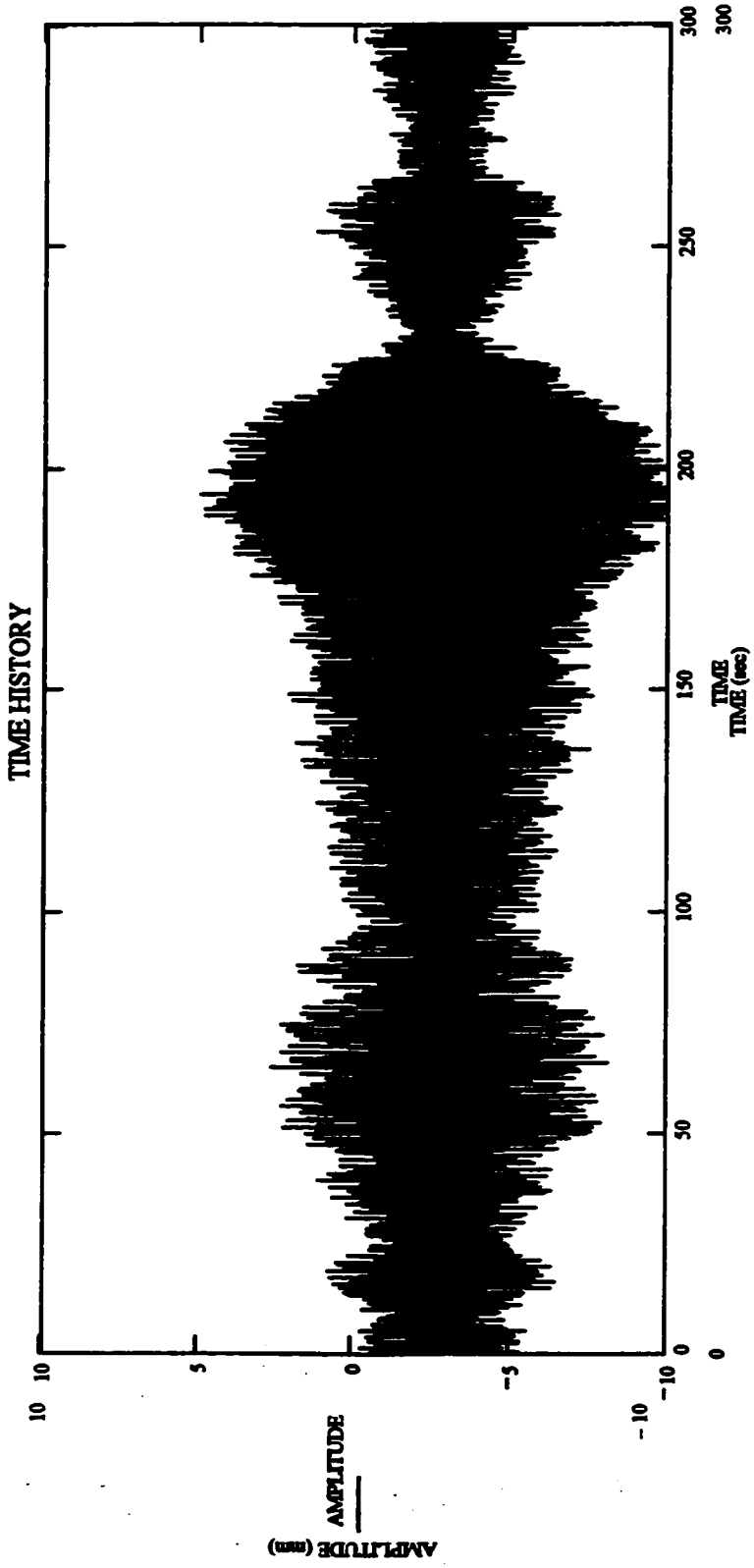

Figure 4-8. Time trace of setup 2A at the mean wind speed of 30m/s

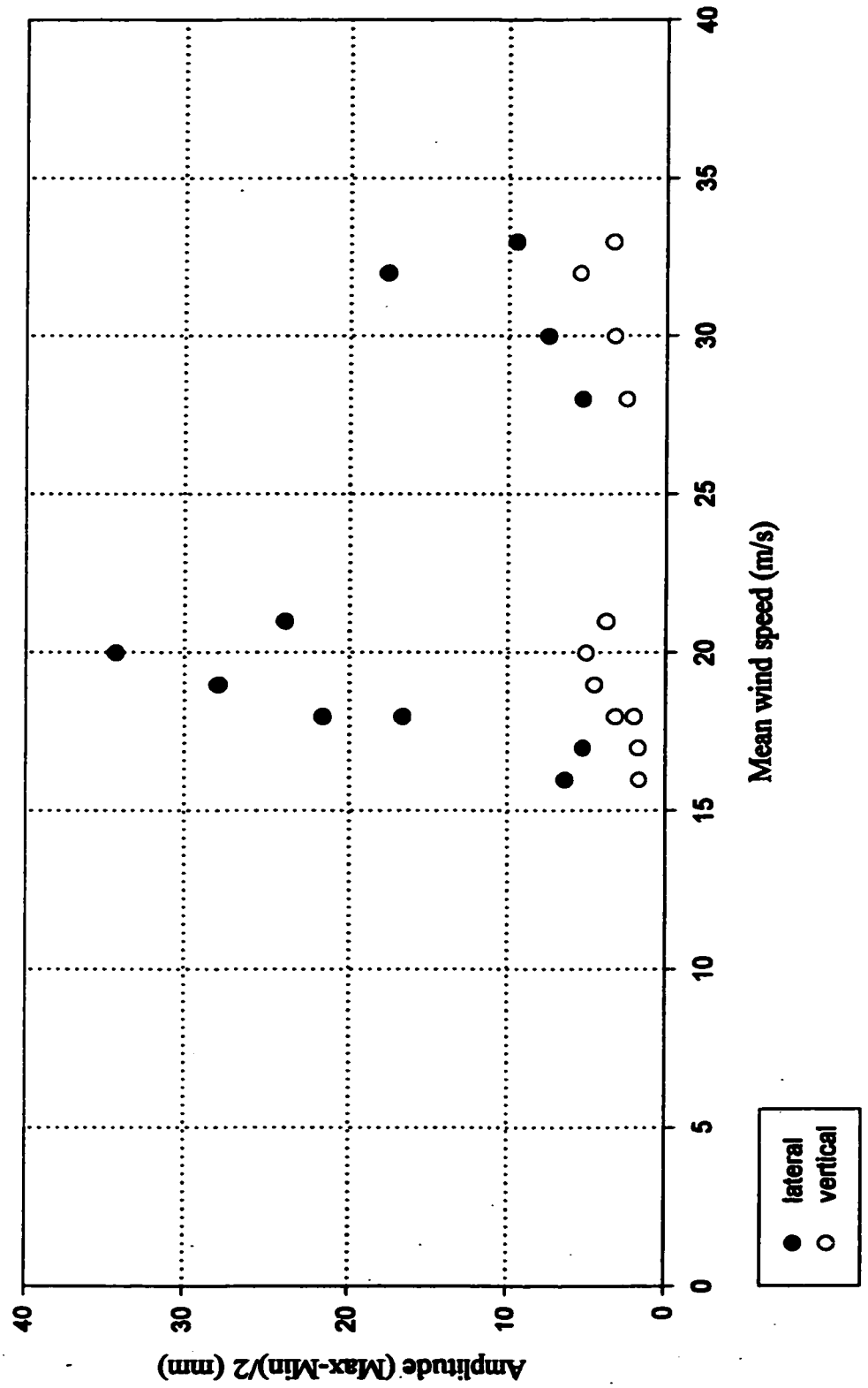

Figure 4-9. Wind-induced response of setup 2A with the same frequency between sway and vertical directions

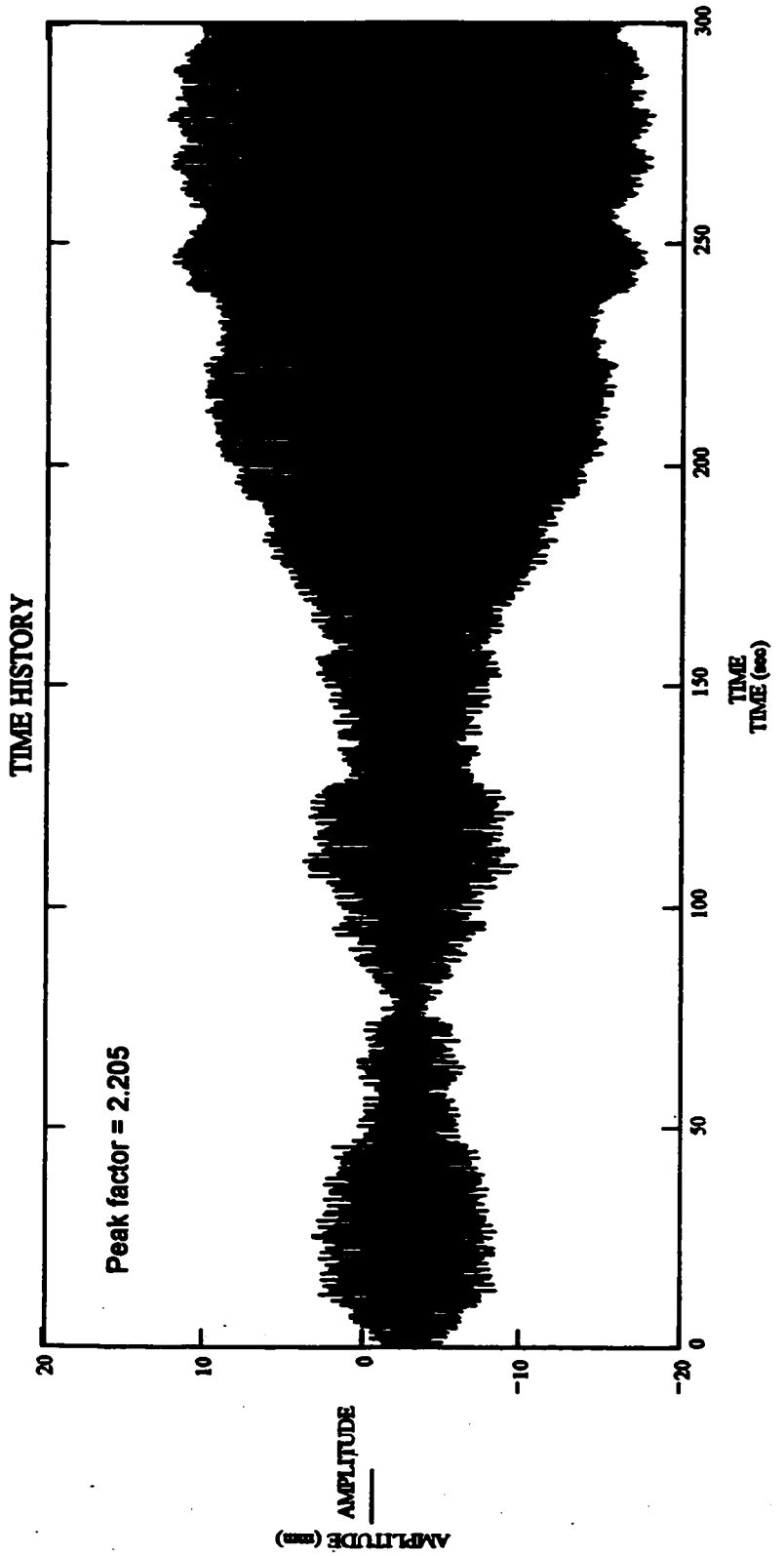

Figure 4-10. Time trace of the same frequency in setup 2A at the wind speed of 32m/s

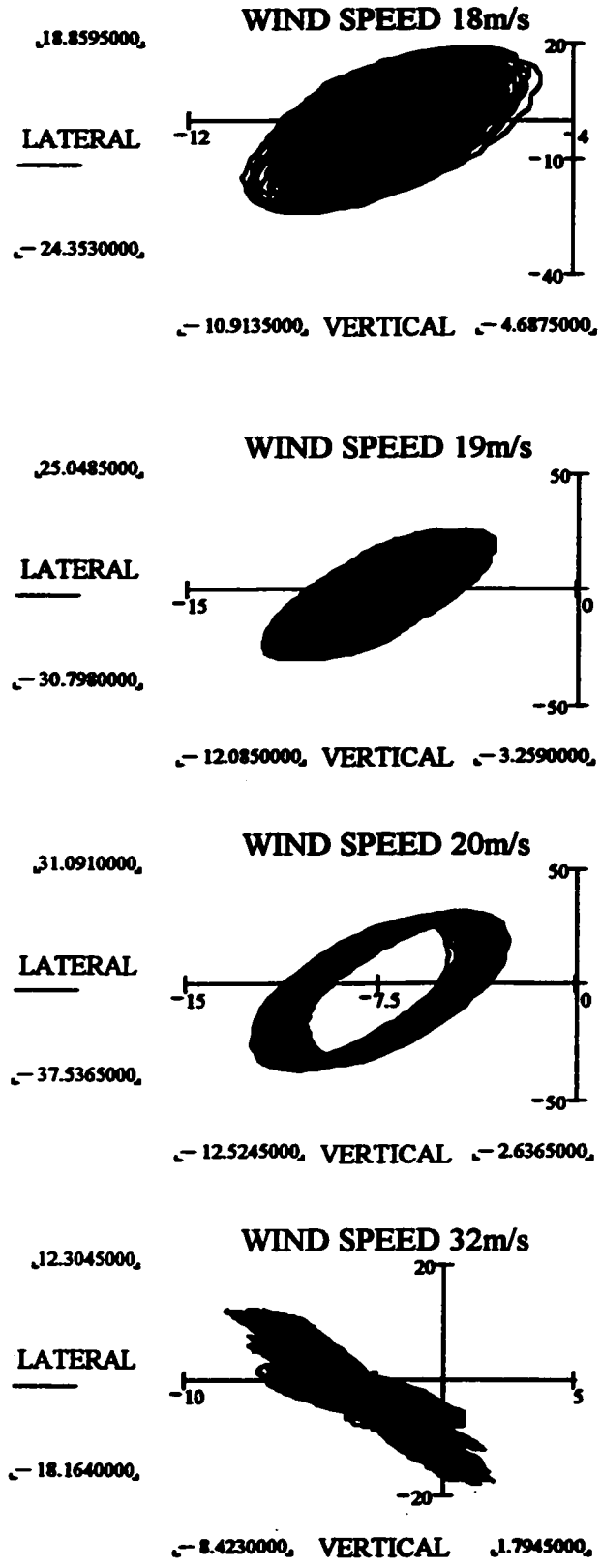

Figure 4-11. Lissajous diagrams

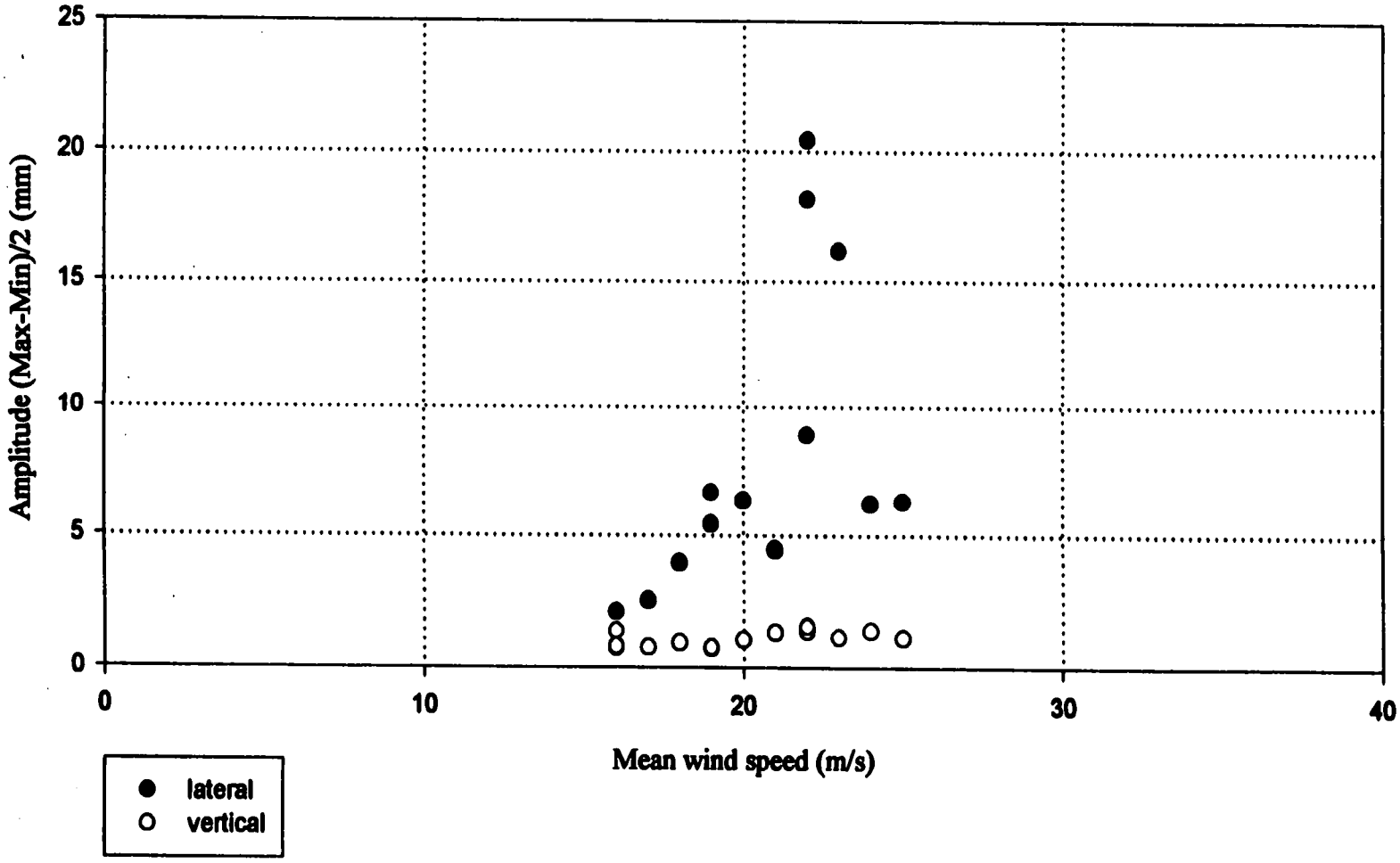

Figure 4-12. Wind-induced response of setup 3A with smooth surface and no additional damping

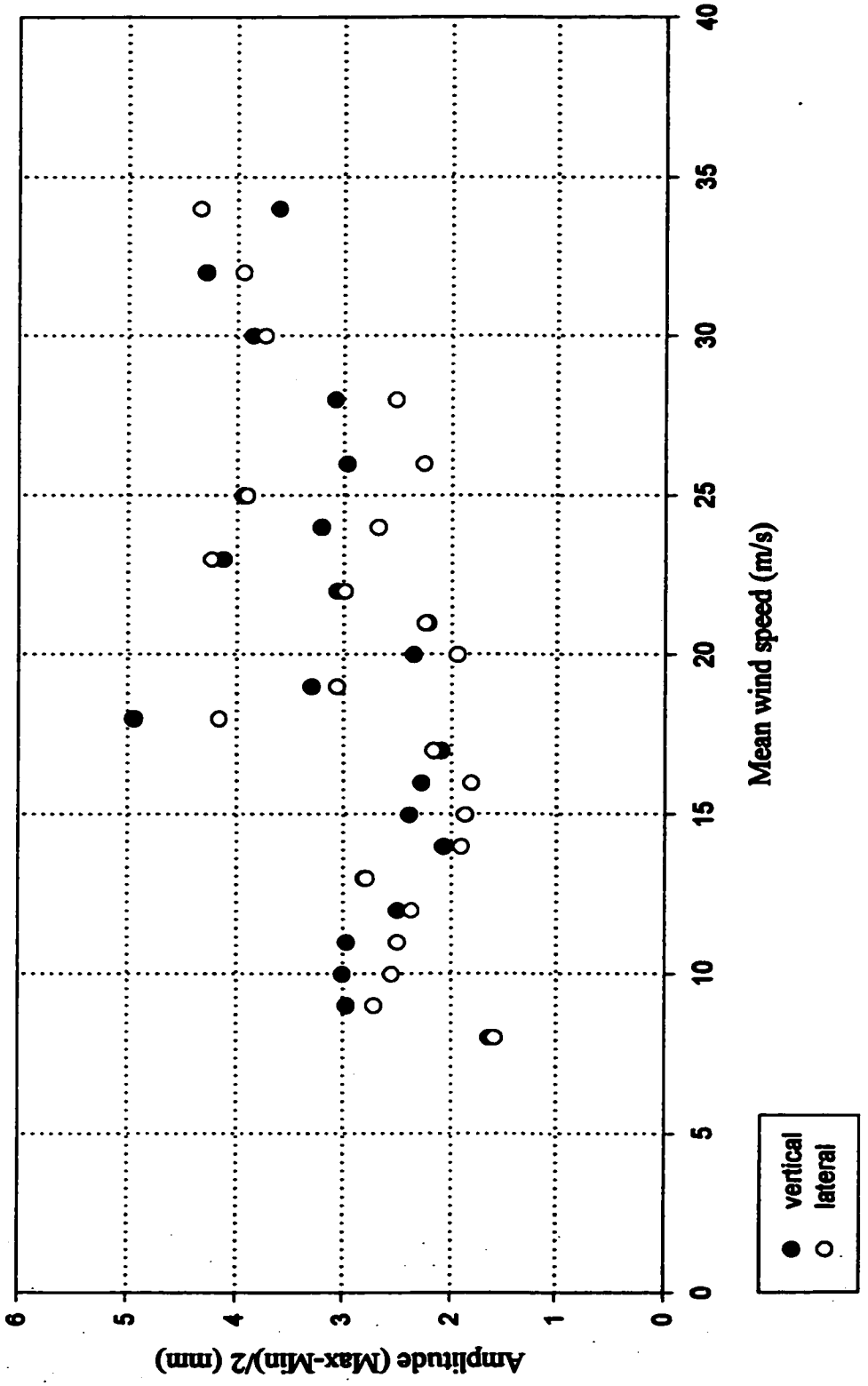

Figure 4-13. Wind-induced response of setup 3B with smooth surface and no additional damping

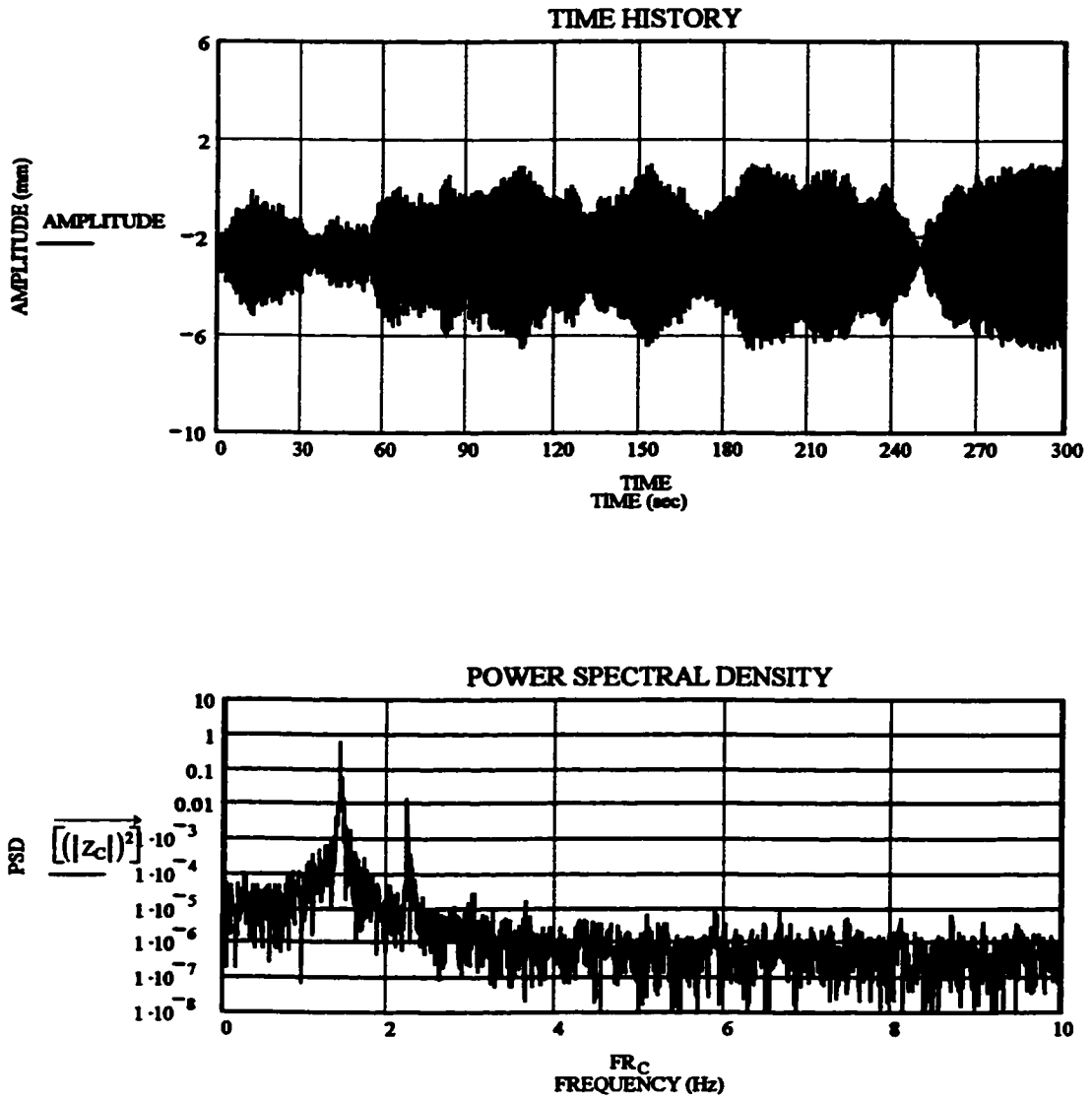

Frequency:

1. 1.422 Hz of first
2. 2.227 Hz of second

Figure 4-14. Time trace and PSD of model setup 3B at wind speed of 32m/s

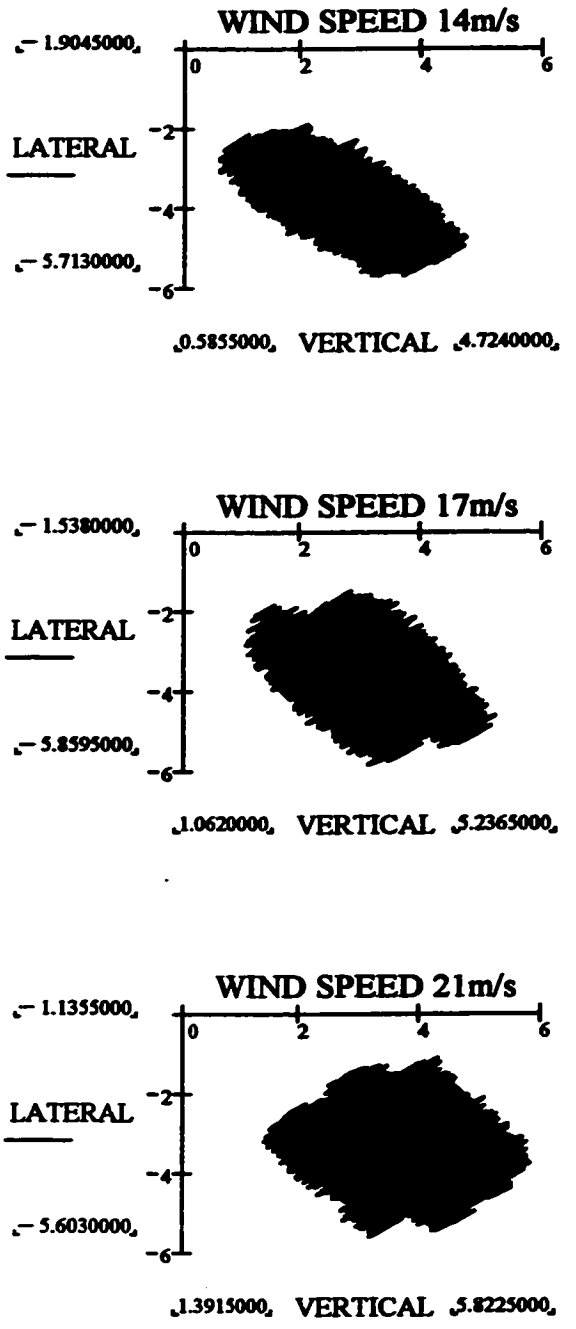

Figure 4-15. Lissajous diagrams

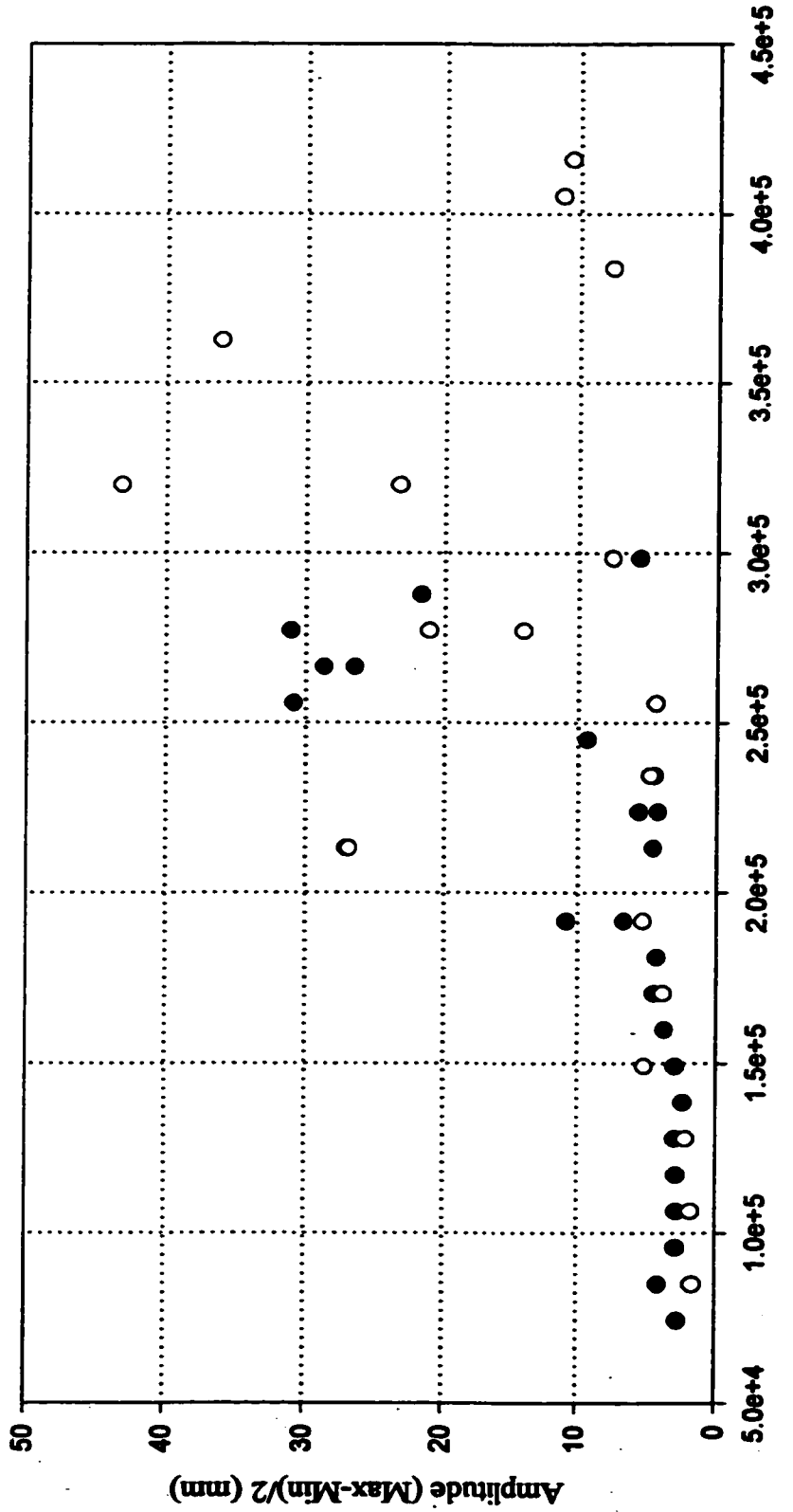

Figure 4-16. Surface effect with setup 1B

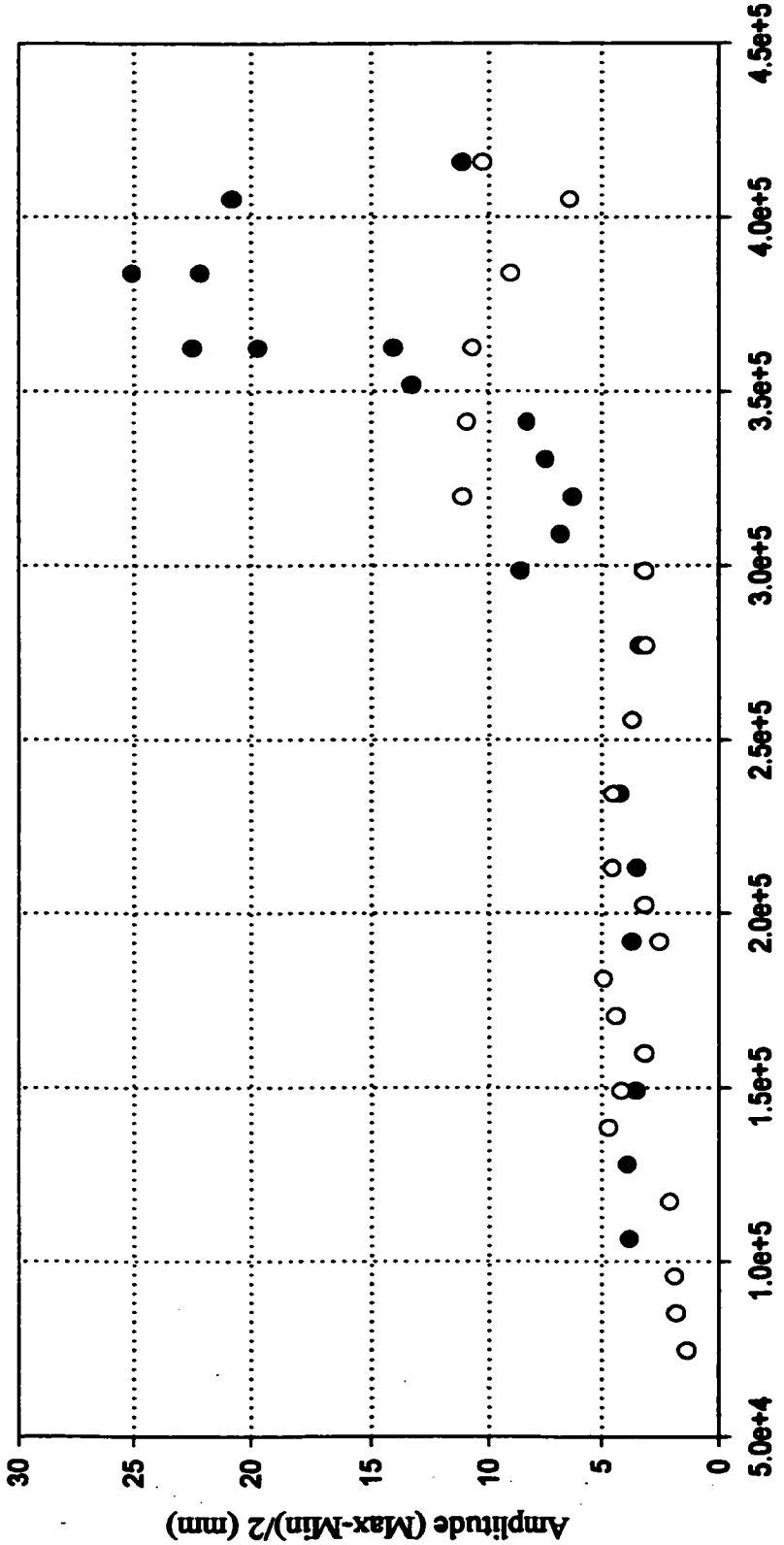

Figure 4-17. Surface effect with setup 1C

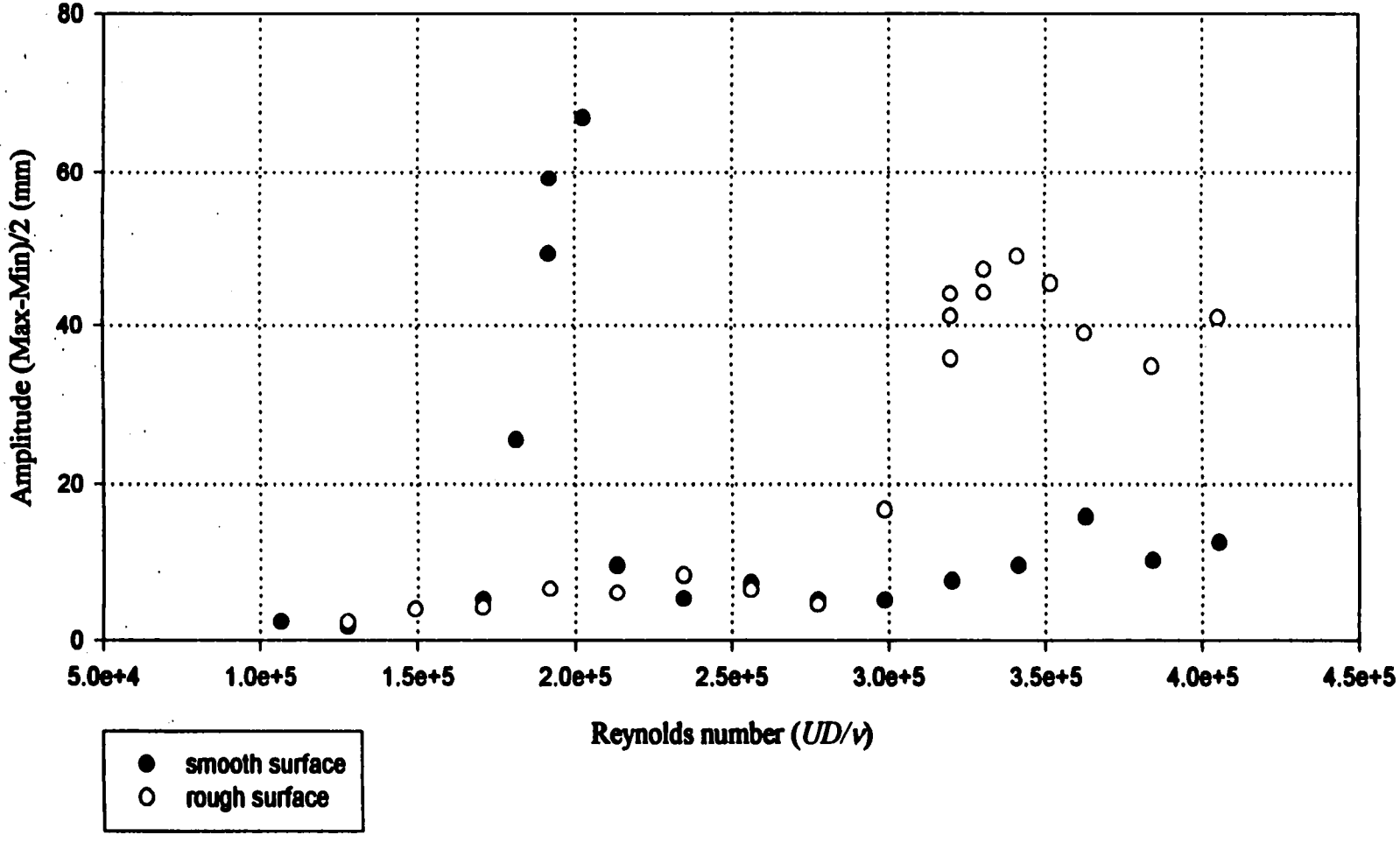

Figure 4-18. Surface effect with setup 2A

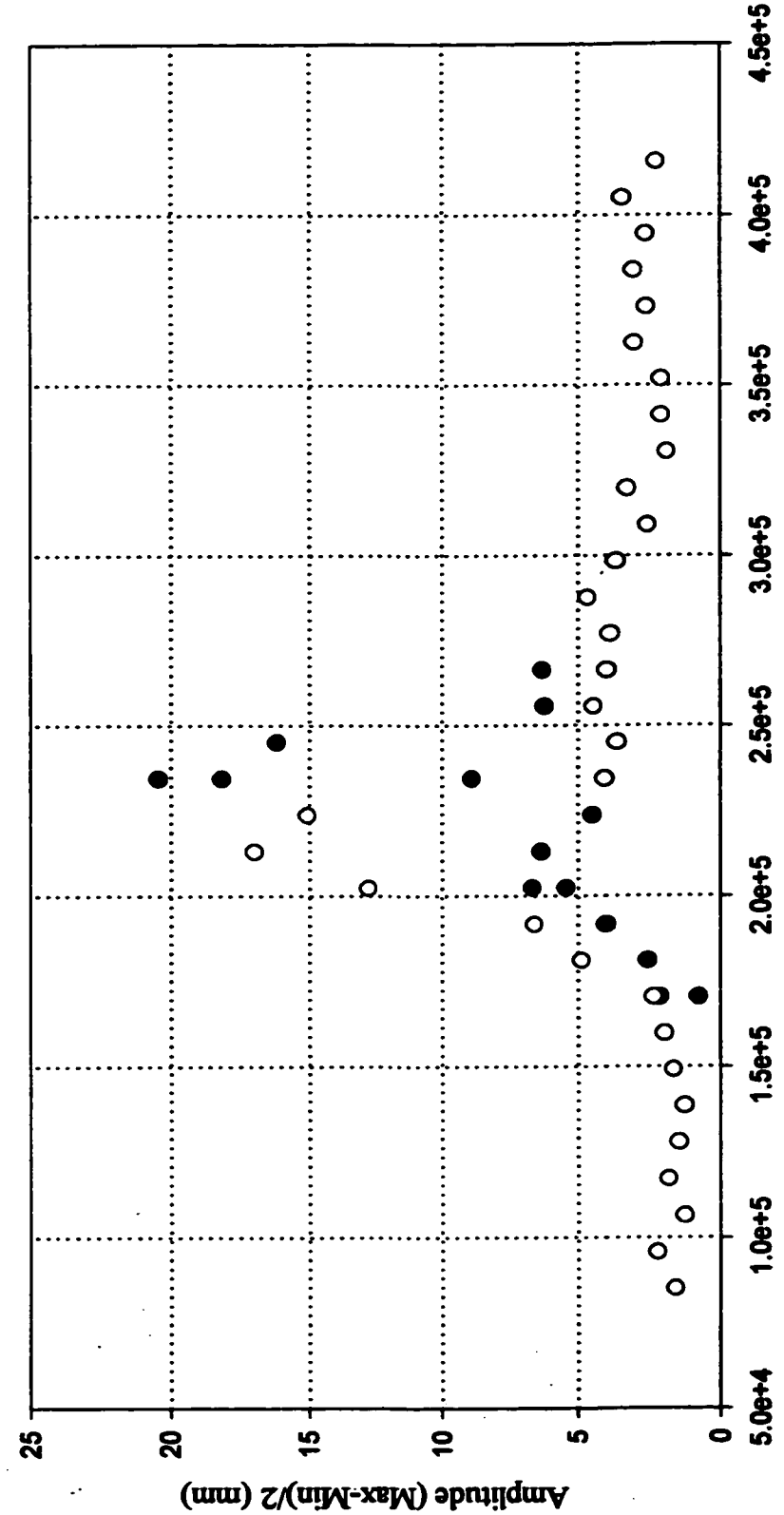

Figure 4-19. Surface effect with setup 3A

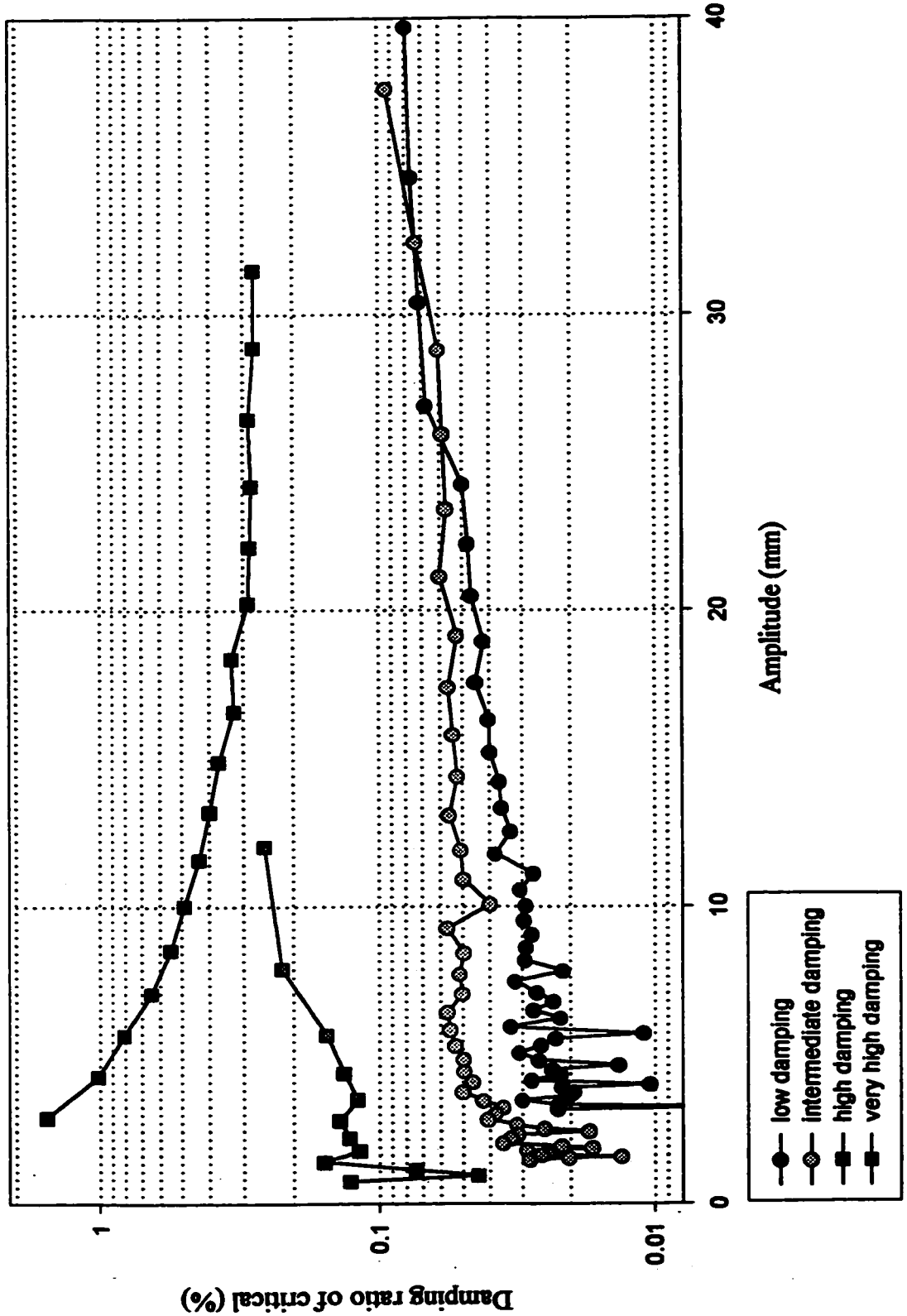

Figure 4- 20. Damping ratio versus amplitude at four different levels of damping

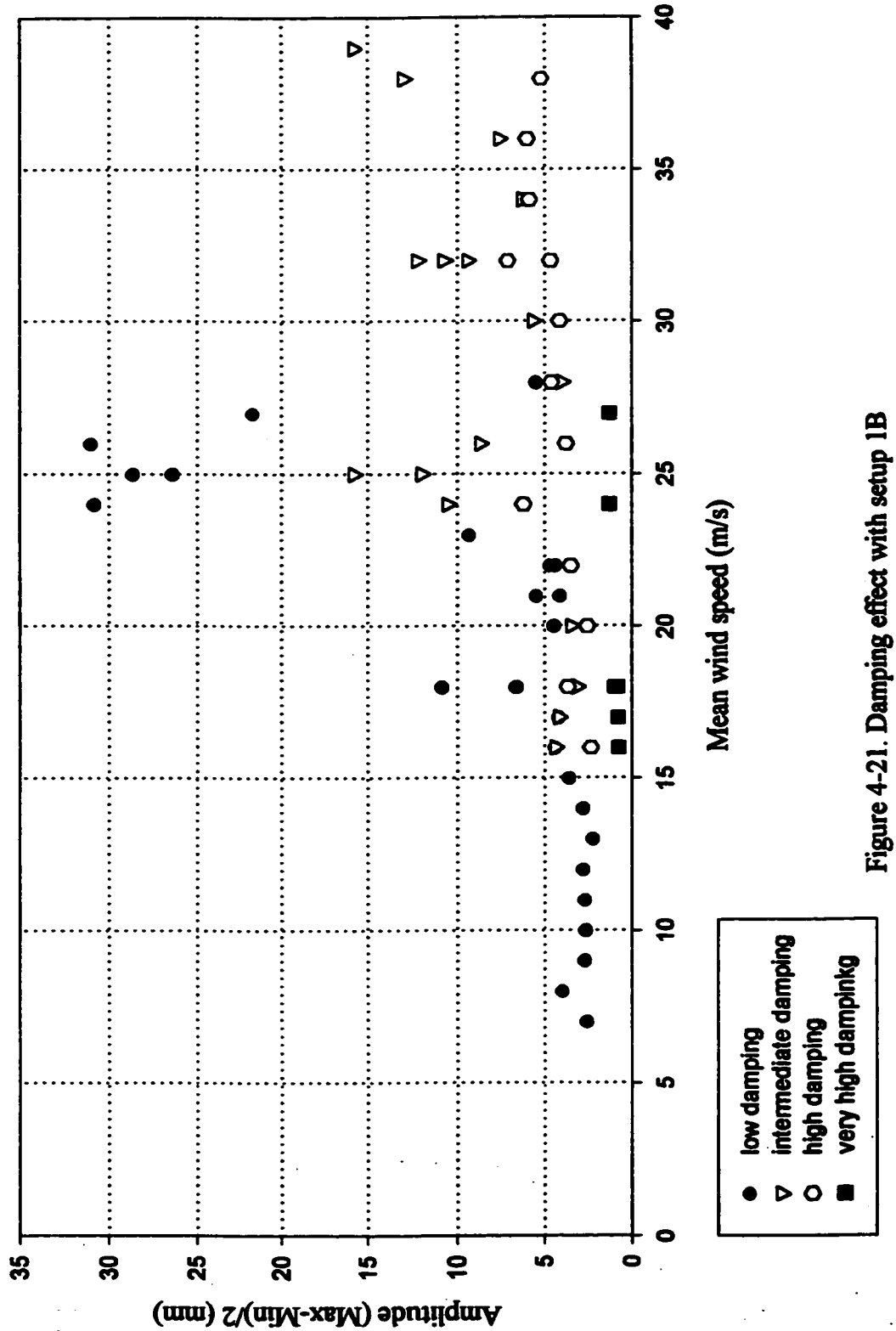

Figure 4-21. Damping effect with setup 1B

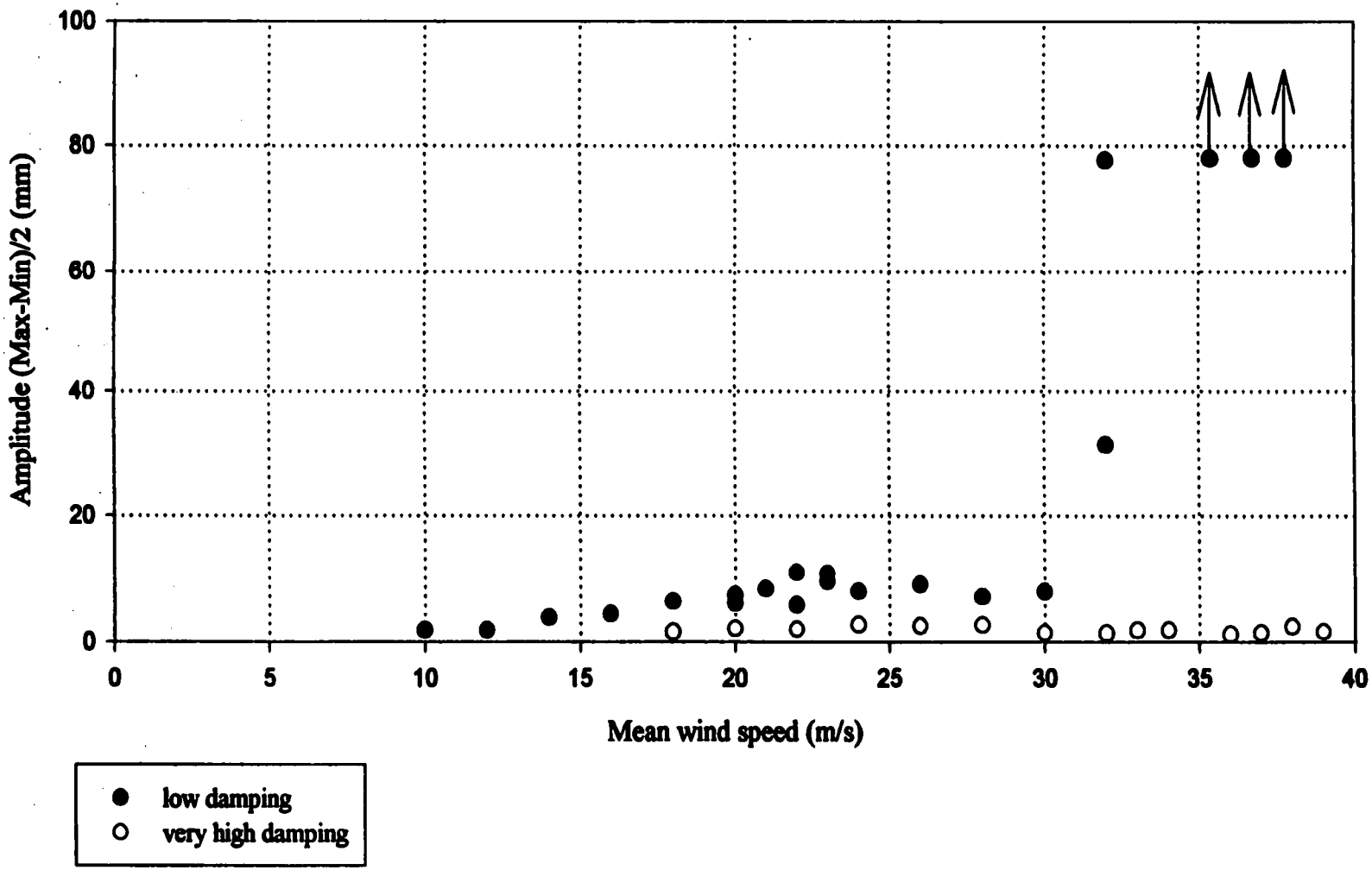

Figure 4-22. Damping effect with setup 2C

CHAPTER 5
DISCUSSIONS AND CONCLUSIONS

5.1 Main findings from the test results

A series of wind tunnel tests were conducted to investigate the aerodynamic behaviour of an inclined dry cable. Both the divergent type of galloping instability and the limited amplitude high-speed vortex shedding excitation were observed.

Main findings from the tests are as follows:

1. Galloping instability, which seems to grow into a large amplitude motion, was observed in only one case (Model setup 2C).
2. There are other vibrations observed in different setup cases and they seem to be categorized as " high-speed vortex excitation".
3. In the cases where the frequencies are very close to each other in two directions, elliptical motion of the cable was observed.
4. Parametric study shows that the vortex shedding oscillation can be easily suppressed with an increase of the structural damping. Increase of damping generally does not influence the range of wind speed where the motion was detected.

5.2 Comparison with the past research results

A limited number of experimental studies on inclined dry cables have been carried out particularly in Japan. Saito et al [12] defined an instability criterion for the inclined cable motion based on three different model setups. Miyata et al [26] investigated the inclined dry cable motion with one model setup. In order to make the comparison, these two sets of results, as well as the results obtained from this study are shown together in Figure 5-1. This figure shows the relationship between the critical

Reduced wind speed and Scruton number. This critical reduced wind speed is defined as the onset wind speed when galloping instability occurs. The Scruton number is the effect of structural damping in this study. As can be seen from this figure, the line given in the figure shows the lower limit of the scattered data of critical wind speeds found by Japanese researchers. Among the results from the present study, only the one corresponding to the setup 2C is the divergent galloping motion, whereas the others are high-speed vortex shedding excitations. The Scruton number in this figure is defined as $Sc = m\delta/(\rho D^2)$, where m = the cable mass per unit length, δ = the logarithmic decrement, ρ = the air density, and D = the cable diameter. As can be seen from the figure, the boundary for instability defined by Saito is much lower when compared with the results given by Miyata and this study. Further to this, a similar instability criterion that could be defined by this study's findings would have much higher than that given by Saito when the realistic range of the Scruton number is between 3 and 10.

5.3 Conclusions

Based on the experimental results obtained in this study, most of the cases showed the high-speed vortex excitation but the galloping was also observed in one setup case, which has the wind-relative angle (ϕ) 60 degrees and the rotation angle of the spring system (α) 54.7 degrees. As can be expected, the galloping type response at the available wind speed of wind tunnel facility, was suppressed by adding the structural damping value of as high as 0.5% of critical, which corresponds to the "very high" damping value in this study. Furthermore, it was found that the high speed vortex excitation was sensitive to the cable surface roughness. The results found by this study have much higher critical wind speed than the results identified by Japanese researchers.

In order to further clarify the problem of dry cable galloping, it is advisable to perform further study in future, particularly on the cause and mechanism of vibration and the Reynolds number effect on the inclined cable vibration.

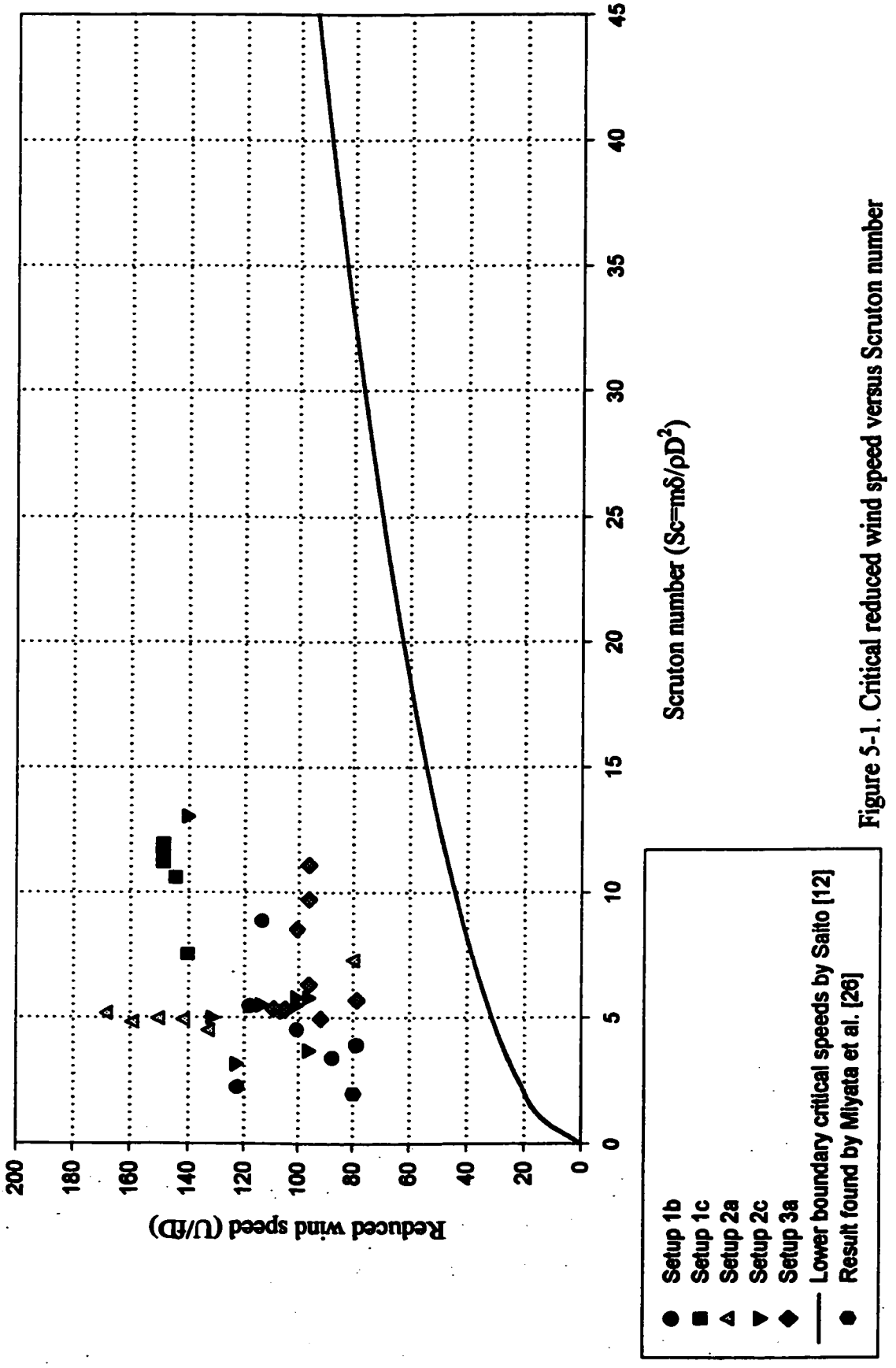

Figure 5-1. Critical reduced wind speed versus Scruton number

REFERENCES

1. A. G. Davenport, "Gust loading factors." *Journal of Structural Division, ASCE*, Vol. 93, June 1967, pp. 11-34.
2. J. P. Den Hortog, "Transmission line vibration due to the sleet." *Trans. AIEE*, Vol. 51, December 1932, pp. 1074-1076.
3. C. Scruton, "The use of wind tunnels in industrial aerodynamic research." *AGARD* Fluid Dynamics Panel held in Istanbul, Turkey, October 1960.
4. G. V. Parkinson and N. P. H. Brooks, "On the aerodynamic instability of bluff cylinders." *Trans. ASME*, Vol. 83, 1961, pp. 252-258.
5. M. Novak, "Aeroelastic galloping of the prismatic bodies." *Journal of the Engineering Mechanics, ASCE*, Vol. 95, February 1969, pp. 115-142.
6. P. A. Irwin, "Wind vibrations of cables on cable-stayed bridges." *Proceeding of the ASCE Structures Congress.*' 1997, pp. 383-387.
7. K. R. Cooper and R. L. Wardlaw, "Aeroelastic instabilities in wakes." *Proceeding of International Conference on Wind Effects on Buildings and Structures.*' Tokyo, 1971, pp. 647-655.
8. A. Simpson and J. W. Flowers, "An important mathematical model for the aerodynamic forces on tandem cylinders in motion with aeroelastic application." *Journal of Sound and Vibration*, Vol. 51, 1977.
9. H. P. Ruscheweyh, "The mechanism of rain-wind-induced vibration." *Wind Engineering into 21st Century*, 1999.
10. Y. Hikami and N. Shiraishi, "Rain-wind induced vibrations of cables in cable stayed briidges." *Journal of Wind Engineering and Industrial Aerodynamics*, Vol. 29, 1988, pp. 409-418.
11. H. Yamaguchi, "Analytical study on growth mechanism of rain vibration of cables." *Journal of Wind Engineering and Industrial Aerodynamics*, Vol. 33, 1990, pp. 73-80.

12. T. Saito, M. Matsumoto and M. Kitazawa, "Rain-wind excitation of cables on cable-stayed Higashi-Kobe bridge and cable vibration control." *Proceeding of the International Conference on Cable-Stayed and Suspension bridges (AFPC)*, Deauville, Vol. 2, 1994, pp. 507-513.
13. D. A. Davis and D. J. W. Richards, "Investigation of conductor oscillation on the 275kV crossing over the Rivers Severn and Wye." *Proceedings I. E. E.*, Vol. 110, January 1963, pp. 205-219.
14. D. J. W. Richards, "Aerodynamic properties of the Severn crossing conductor." *Proceeding of International Conference on Wind Effects on Buildings and Structures.*' Teddington, Vol. 2. June 1963, pp. 688-727.
15. M. Matsumoto, C. W. Kinsly, N. Shiraishi, M. Kitazawa and T. Saito. " Inclined-Cable aerodynamics." *Structural Design, Analysis and Testing: Proceedings of the Structures Congress, ASCE*, 1989, pp. 81-90.
16. M. Matsumoto, "Observed behaviour of prototype cable vibration and its generation Mechanism." *Bridge Aerodynamics edited by A. Larsen and S. Esdahl*, 1998, pp. 189-211.
17. M. Matsumoto, T. Yagi, D. Tsushima and Y. Shigemura, "Vortex-induced vibrations of inclined cables at high wind velocity." *Wind Engineering into 21st Century*, 1999, pp. 979-986.
18. M. Matsumoto, "Vortex shedding of bluff bodies: A review." *Journal of Fluids and Structures*, Vol. 13, 1999, pp. 791-811.
19. Electric Power Research Institute, "Transmission Line Reference Book: Wind-induced conductor motion." *EPRI*, Palo Alto, 1979.
20. P. Van Dyke, R. Paquette, and M. St-Louis, "Design and test of a new Aeolian vibration damper." *4th International Symposium on Cable Dynamics*, Montréal, Canada, May 28 – 30, 2001, pp. 301-308.
21. M. Ito, "Suppressing wind-induced vibrations of bridges."*Proceeding of Canada-Japan Workshop on Bridge Aerodynamics*, Ottawa, Canada, September 25-27 1989, pp. 63-72.

22. M. Matsumoto et al, "Wind-induced cable vibration of cable-stayed bridges in Japan." *Proceeding of Canada-Japan Workshop on Bridge Aerodynamics*, Ottawa, Canada, September 25-27 1989, pp. 101-110.

23. M. Virlogeux, "Cable vibration in cable-stayed bridges." *Bridge Aerodynamics edited by A. Larsen and S. Esdahl*, 1998, pp. 213-233.

24. H. Yamaguchi and Y. Fujino, "Stayed cable dynamics and its vibration control." *Bridge Aerodynamics edited by A. Larsen and S. Esdahl*, 1998, pp. 234-263.

25. M. Matsumoto et al, "Aerodynamic behaviour of inclined circular cylinders-cable aerodynamics." *Journal of Wind Engineering and Industrial Aerodynamics*, Vol. 33, 1990, pp. 63-72.

26. T. Miyata, H. Yamada, and T. Hojo, "Aerodynamic response of PE stay cables with pattern-indented surface." *Proc. of IABSE Conference, Cable-stayed and suspension bridges*, Deauville, France, Oct. 1994, Vol. 2, pp. 515-522. .

27. P. A. Irwin, "Private Communications." 2000.

28. Task committee on wind forces committee on loads and stresses structural division, "Wind forces on structures." *Trans. of ASCE*, November 1962, pp. 1124-1198.

29. C. Scruton, "An introduction to wind effects on structures Engineering Design Guide 40." *Oxford University Press*, 1981.

30. D. Ghiocel and D. Lungu, "Wind, Snow and Temperature effects on structures based on Probability." *Abacus Press*, 1975.

31. T. Sarpkaya, "Vortex-induced Oscillations." *Trans. of the ASME, Journal of Applied Mechanics*, Vol. 46, March 1979, pp. 241-258.

32. H. J. Niemann and N. Hölscher, "A review of recent experiment on the flow past circular cylinder." *International Colloquium on Bluff Body Aerodynamics and its Application*, Kyoto, Japan, 1988, pp. 381-393.

33. M. M. Zdravkovich, "Conceptual overview of laminar and turbulent flows past smooth and rough circular cylinders." *International Colloquium on Bluff Body Aerodynamics and its Application*, Kyoto, Japan, 1988, pp. 93-102.

34. M. M. Zdravkovich, "Flow around circular cylinders Vol. 1." *Oxford University Press*, 1997.

35. C. Farell and J. Blessmann, "On critical flow around smooth circular cylinders." *Journal of Fluid Mechanics*, Vol. 136, November 1983, pp. 375-391.

36. E. Achenbach and E. Heinecke, "On vortex shedding from smooth and rough cylinders in the range of Reynolds numbers $6x10^3$ to 5 $x10^6$." *Journal of Fluid Mechanics*, Vol. 109, August 1983, pp. 239-251.

37. E. Achenbach, "Influence of surface roughness on the cross-flow around a circular cylinder." *Journal of Fluid Mechanics*, Vol. 46, August 1971, pp.321-335.

38. O. Güven, C. Farell and V. C. Patel, "Surface-roughness effects on the mean flow past circular cylinders." *Journal of Fluid Mechanics*, Vol. 98, August 1980, pp. 673-701.

39. G. Buresti, "The effect of surface roughness on the flow regime around circular cylinders." *Journal of Wind Engineering and Industrial Aerodynamics*, Vol. 8, 1981, pp. 105-114.

40. *MathCad user's Guide 2000 Professional*, Mathsoft, November 1999.

41. G. L. Larose and S. J. Zan, "The aerodynamic forces on the stay cables of cable-stayed bridges in the critical Reynolds number range." *4th International Symposium on Cable Dynamics*, Montréal, Canada, 2001, pp. 77-84.

42. M. Matsumoto et al, "Field observation system of cable aerodynamics in natural wind." *4th International Symposium on Cable Dynamics*, Montréal, Canada, 2001, pp. 219-225.

43. J. H. G. Macdonald, "Susceptibility of inclined bridge cables to large amplitude vibrations considering aerodynamic and structural cable damping." *4th International Symposium on Cable Dynamics*, Montréal, Canada, 2001, pp. 243-250.

44. H. Tanaka, "Cable Dynamics", *IMAC Project Report prepared for VCE*, Vienna, October 2000.

45. S. H. Cheng and H. Tanaka, "Inclined Cable Aerodynamics", *Preliminary Report prepared for RWDI*, University of Ottawa, May 2001.

APPENDIX A

ANGLE RELATIONSHIP FOR CABLE AND WIND [27]

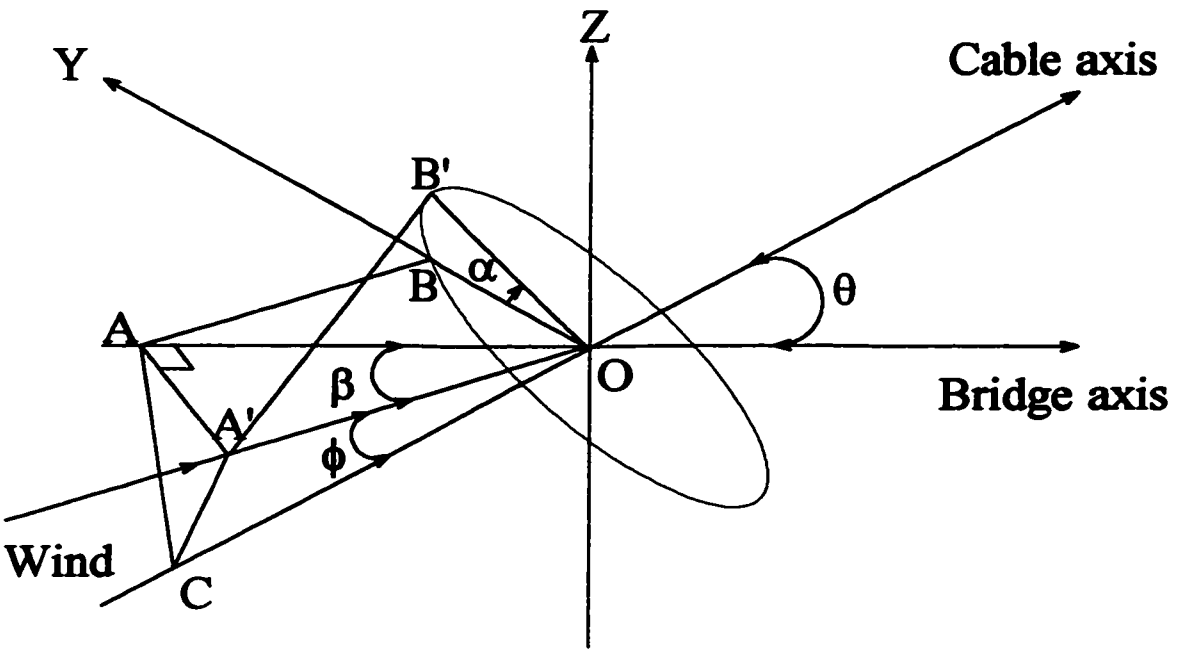

Figure A-1. Angle definition

The wind blows horizontally at an angle β to the bridge axis as shown in Figure A-1. The plane of $AA'O$ is horizontal in this diagram. The cable is assumed to be in a vertical plane parallel to the bridge axis and is at an angle θ to the horizontal.

In figure,

$$AO = A'O\cos\beta \qquad (1)$$

and also

$$AO = CO\cos\theta \qquad (2)$$

Therefore

$$A'O = CO\frac{\cos\theta}{\cos\beta} \tag{3}$$

Also $AA' = A'O(\sin\beta)$ and $AC = CO(\sin\theta)$.

$$AC = \sqrt{(A'O)^2\sin^2\beta + (CO)^2\sin^2\theta}$$

$$\cos\phi = \frac{(CO)^2 + (A'O)^2 - (A'C)^2}{2(CO)(A'O)}$$

Since the scale of length is arbitrary we can call CO=1. Thus

$$\cos\phi = \frac{1 + (A'O)^2 - (A'C)^2}{2(CO)(A'O)} \tag{4}$$

Therefore

$$\cos\phi = \frac{1 + \dfrac{\cos^2\theta}{\cos^2\beta} - \cos^2\theta\tan^2\beta - \sin^2\theta}{2\dfrac{\cos\theta}{\cos\beta}}$$

Multiply top and bottom by $\cos^2\beta$ to obtain

$$\cos\phi = \cos\beta\cos\theta \tag{5}$$

For the spring rotation angle, lateral direction is both normal to the wind vector and normal to the bridge axis. In the wind tunnel this would be the direction across the wind tunnel and if the cable in the wind tunnel is vertical then this vector would be vertical in the tunnel. In figure this is the vector OB'. The line OB is horizontal on the real bridge and normal to the cable axis. The length of OB' and of OB is the cable radius r. The coordinated of B' are $-r(\sin\alpha)(\sin\theta)$, $r(\cos\alpha)(\cos\theta)$, where is the angle between OB' and OB. The coordinates of A' are $-(A'O)(\cos\beta)$, $-(A'O)(\sin\beta)$, and zero. The distance

between A' and B' is the square root of $(A'O)^2+r^2$. However, the distance between A' and B' can be deduced from differences in their coordinates.

$$\begin{aligned}(A'O)^2+r^2 &= \left(-r\sin\alpha\sin\theta+(A'O)\cos\beta\right)^2+\left(r\cos\alpha+(A'O)\sin\beta\right)^2 \\ &\quad +r^2\sin^2\alpha\cos^2\theta \\ &= r^2+(A'O)^2+2r(A'O)(\cos\alpha\sin\beta-\sin\alpha\sin\theta\cos\beta)\end{aligned}$$

The left side of this equation cancels with the first two terms on the right and it then follows that

$$\tan\alpha=\frac{\tan\beta}{\sin\theta} \qquad (6)$$

APPENDIX B
FREE VIBRATION CHARACTERISTICS

The damping and natural frequency are obtained from the free vibration tests. The damping ratio (ζ) is defined as follows:

$$\delta = \frac{1}{n}\ln\left(\frac{x_i}{x_{i+1}}\right) \tag{B-1}$$

$$\zeta = \frac{\delta}{\sqrt{(2\pi)^2 + \delta^2}} \tag{B-2}$$

where δ = logarithmic decrement, ζ = damping ratio, and n = number of cycles between x_i and x_{i+1}.

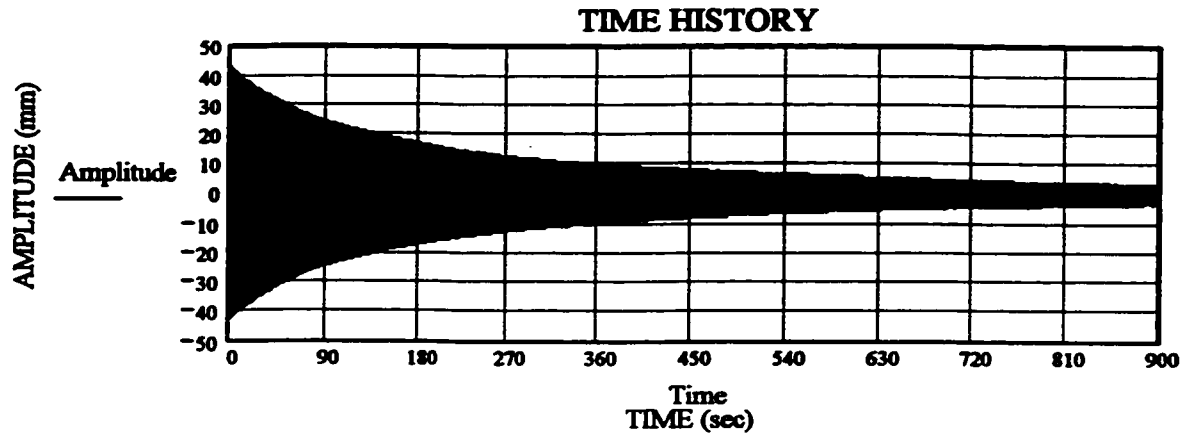

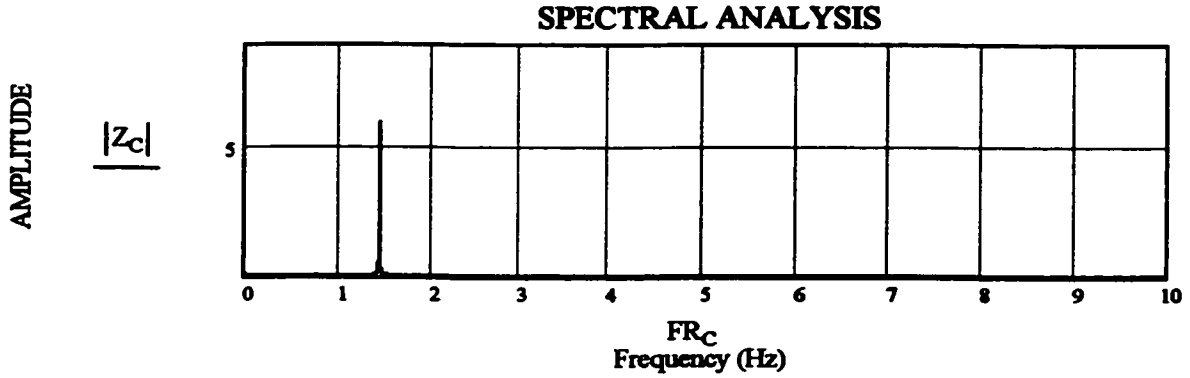

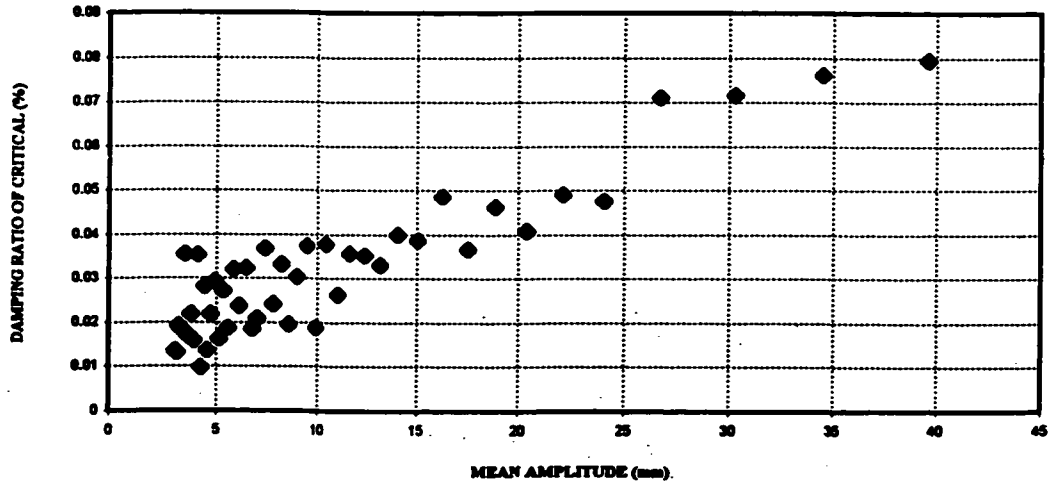

Figure B-1. Model setup 1B (lateral direction)

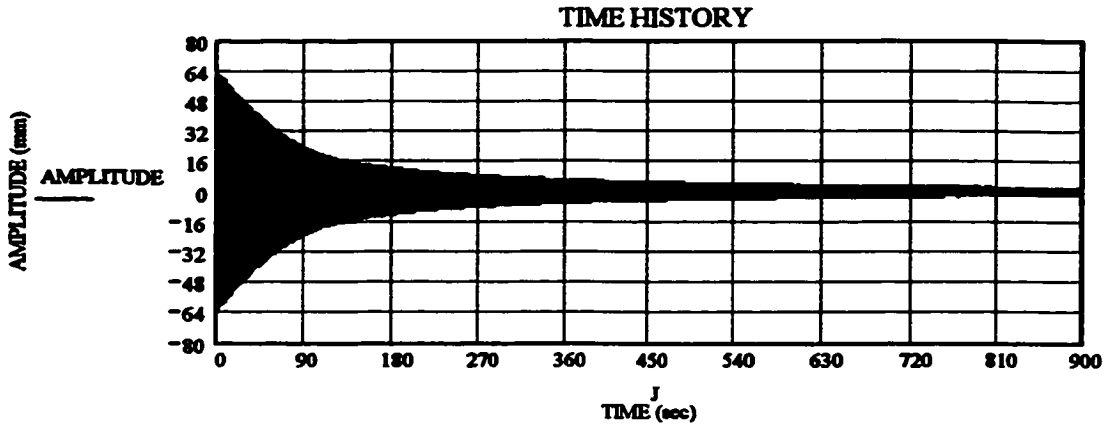

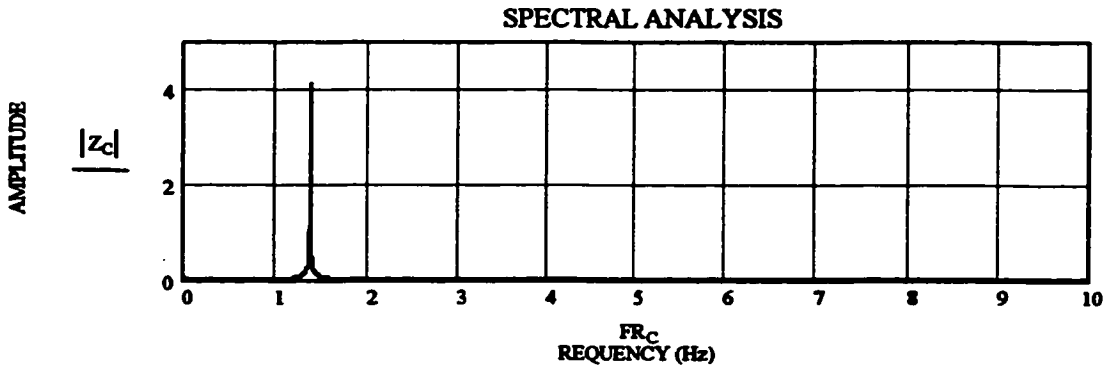

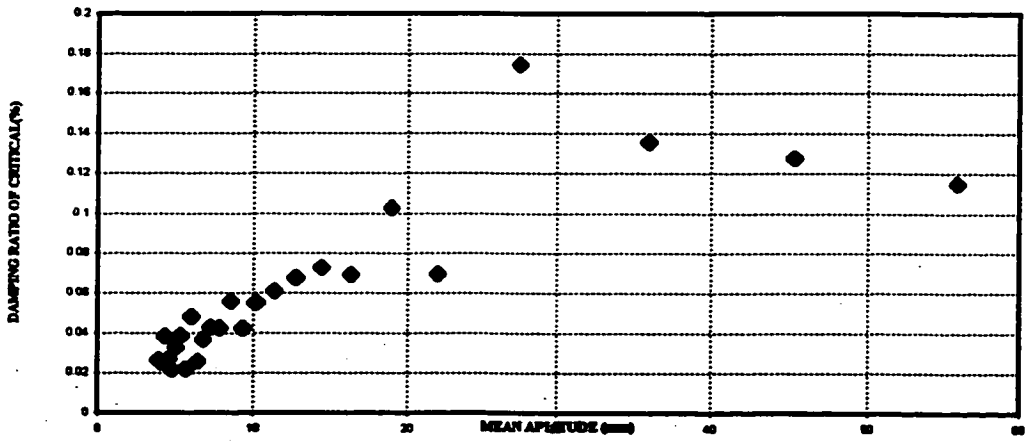

Figure B-2. Model setup 1B (vertical direction)

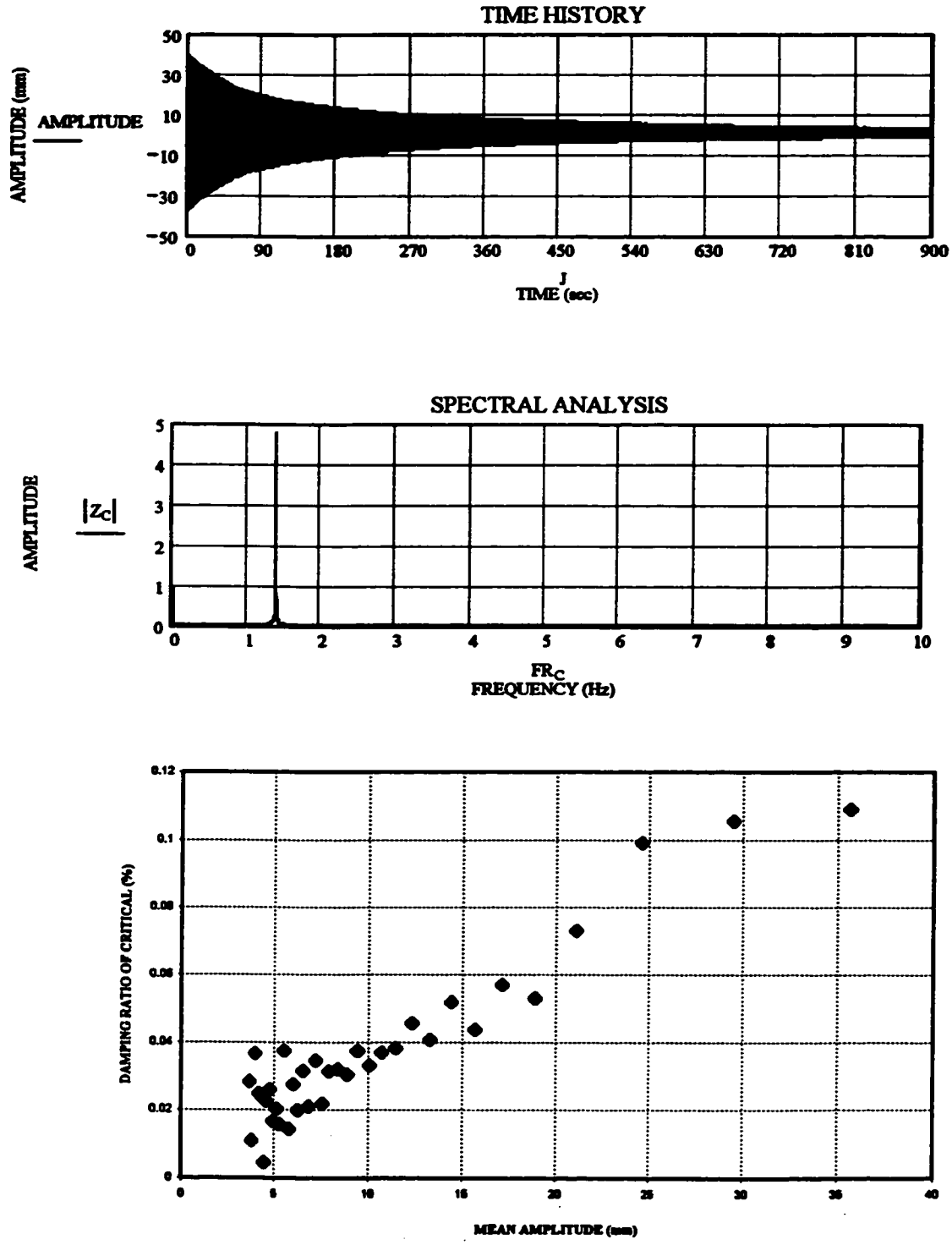

Figure B-3. Model setup 1C (vertical direction)

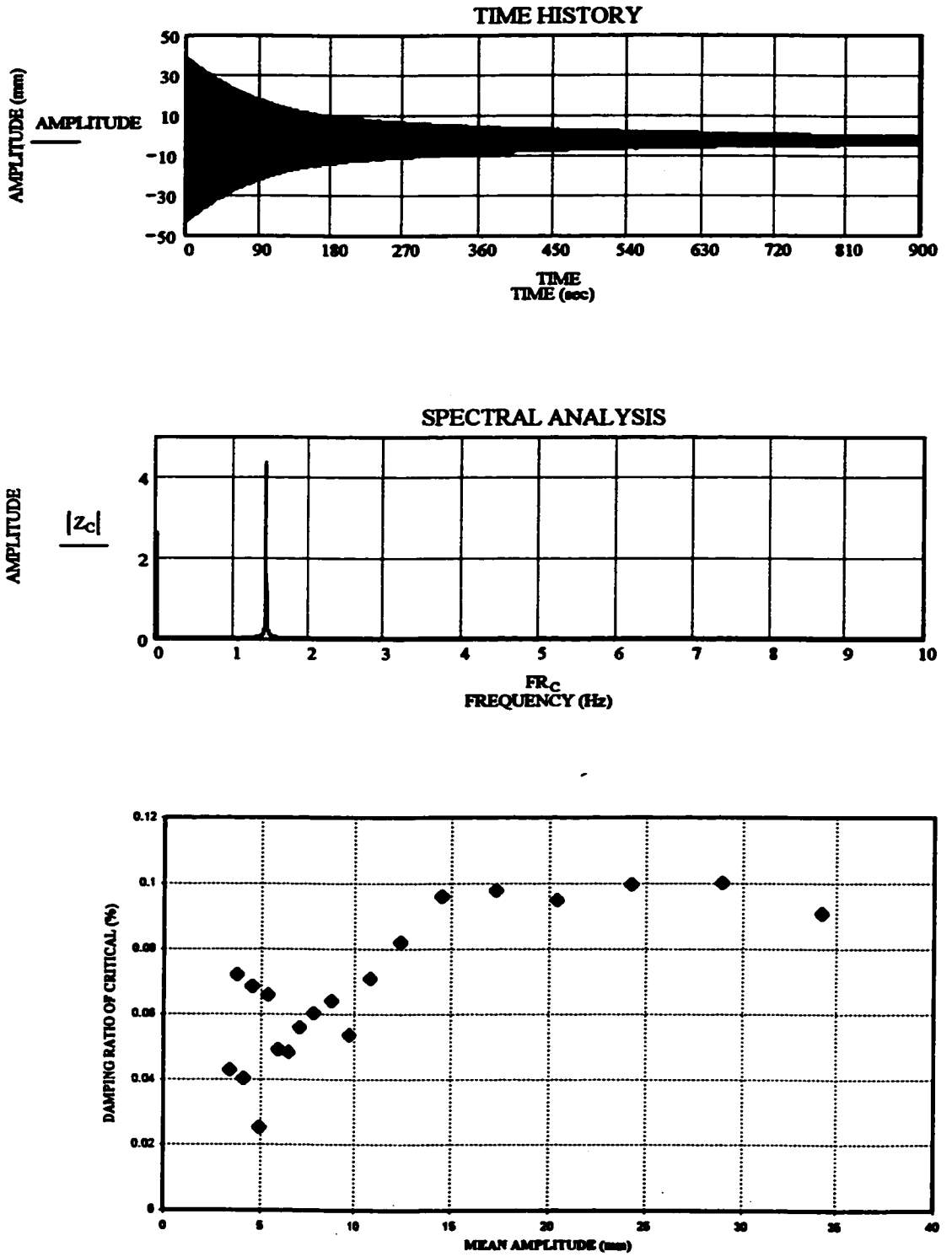

Figure B-4. Model setup 1C (lateral direction)

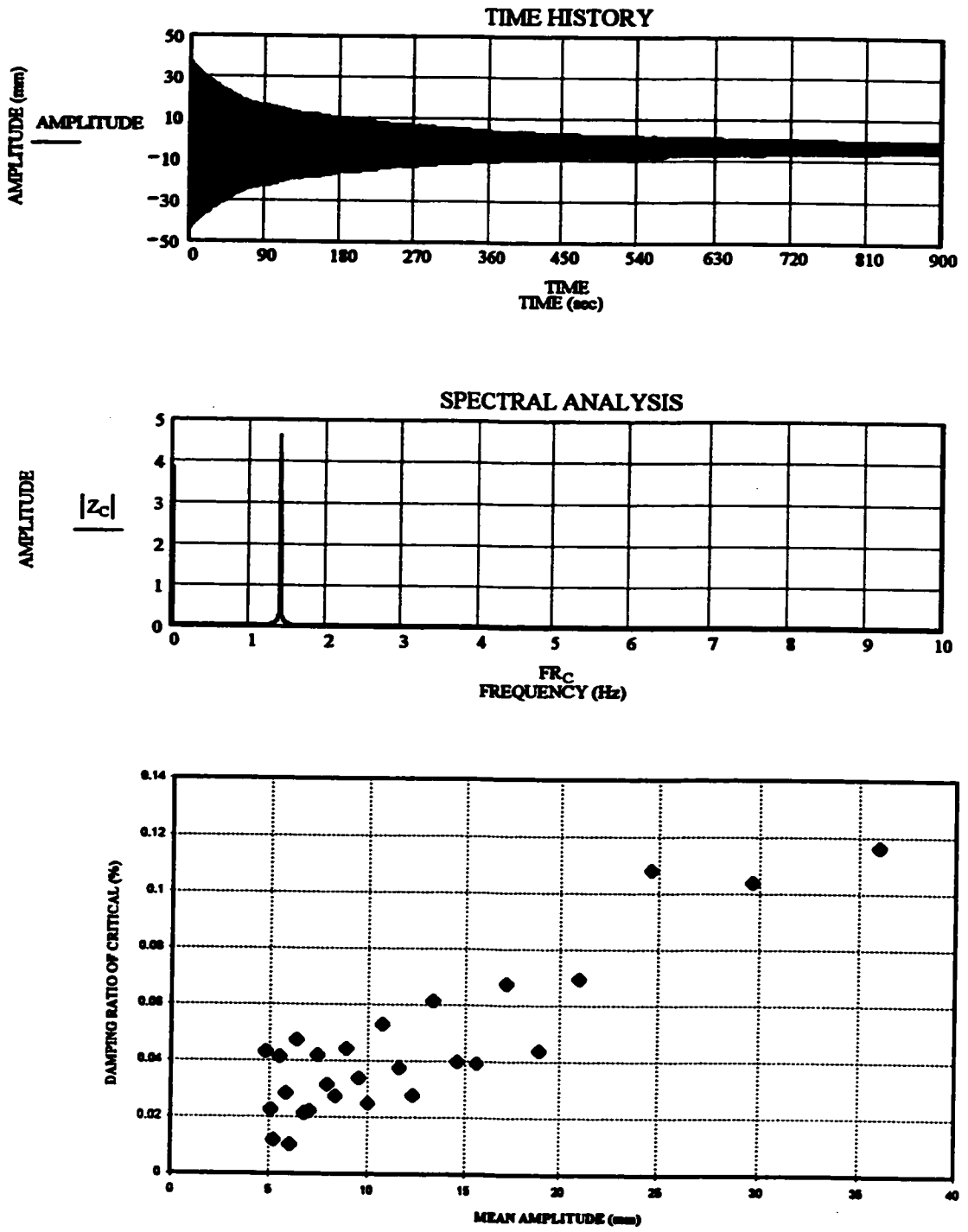

Figure B-5. Model setup 2C (vertical direction)

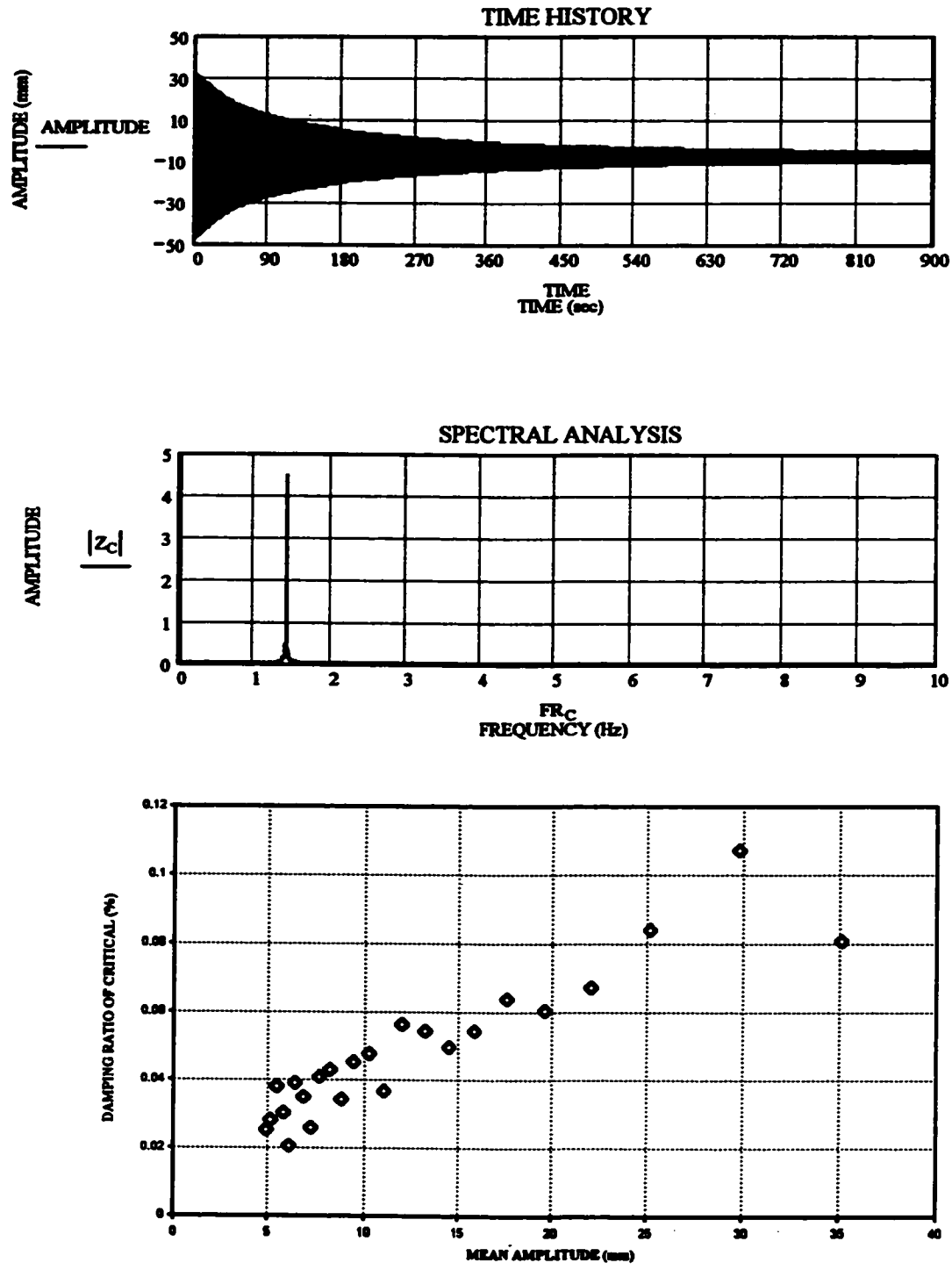

Figure B-6. Model setup 2C (lateral direction)

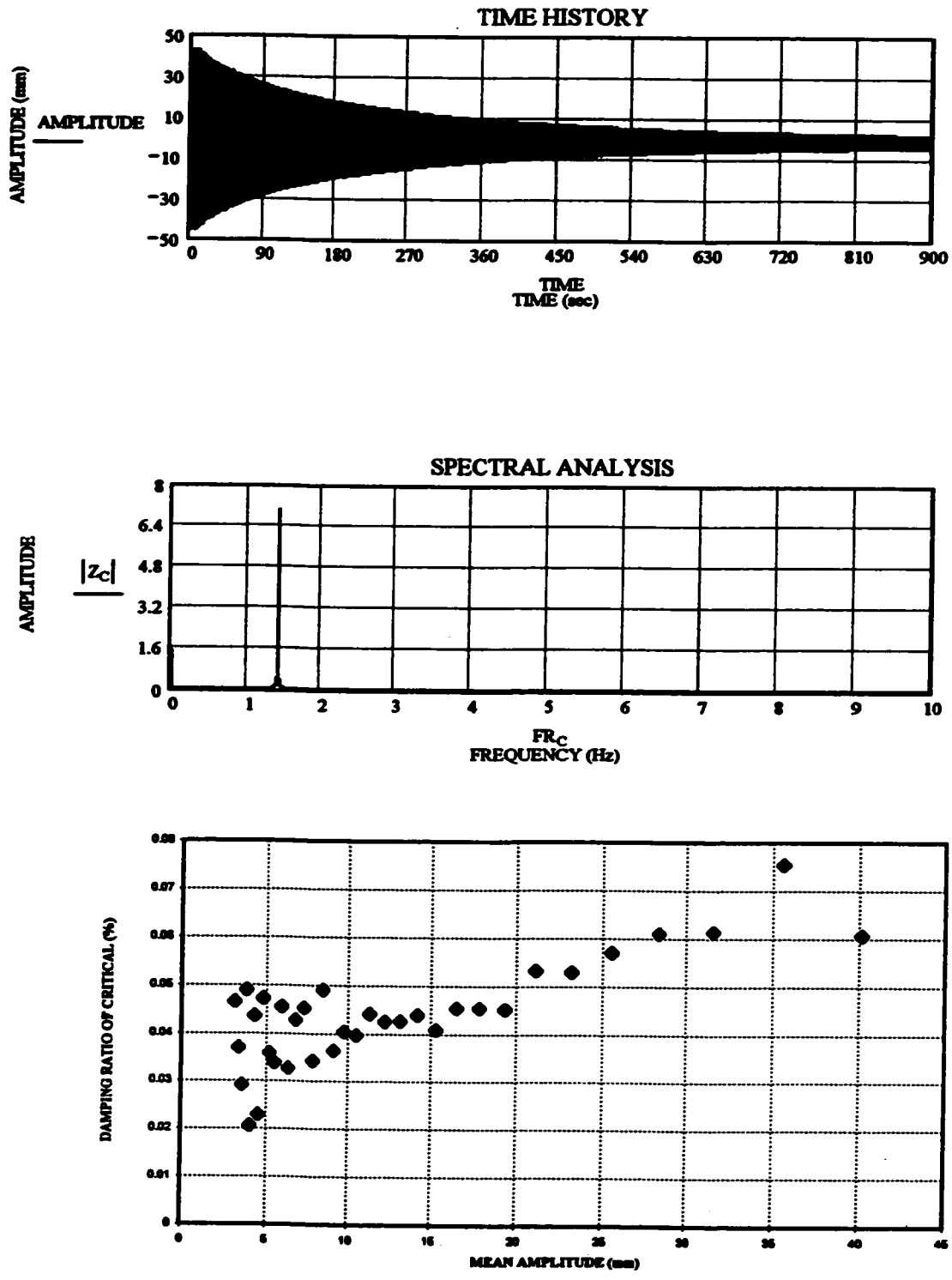

Figure B-7. Model setup 2A (lateral direction)

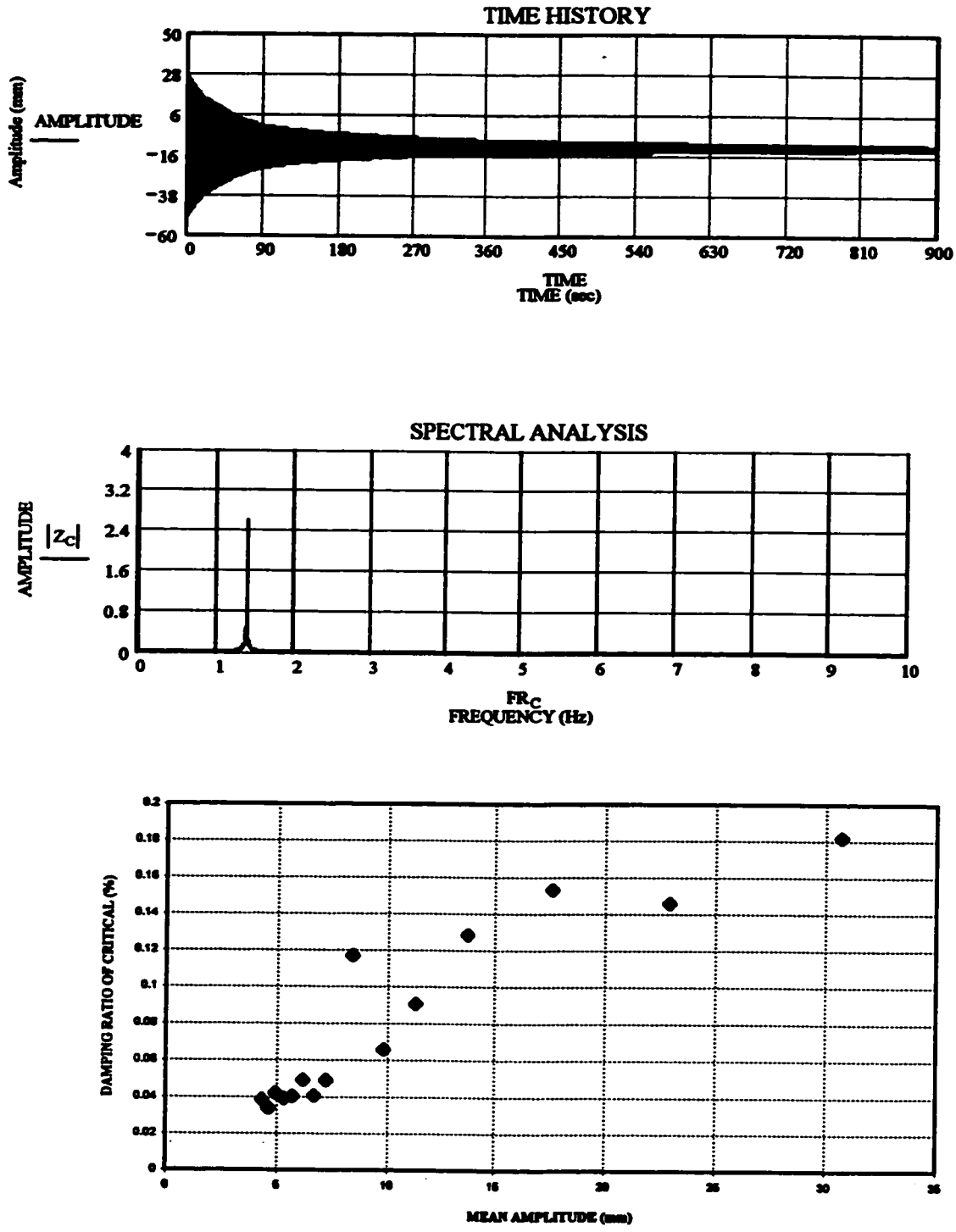

Figure B-8. Model setup 2A (vertical direction)

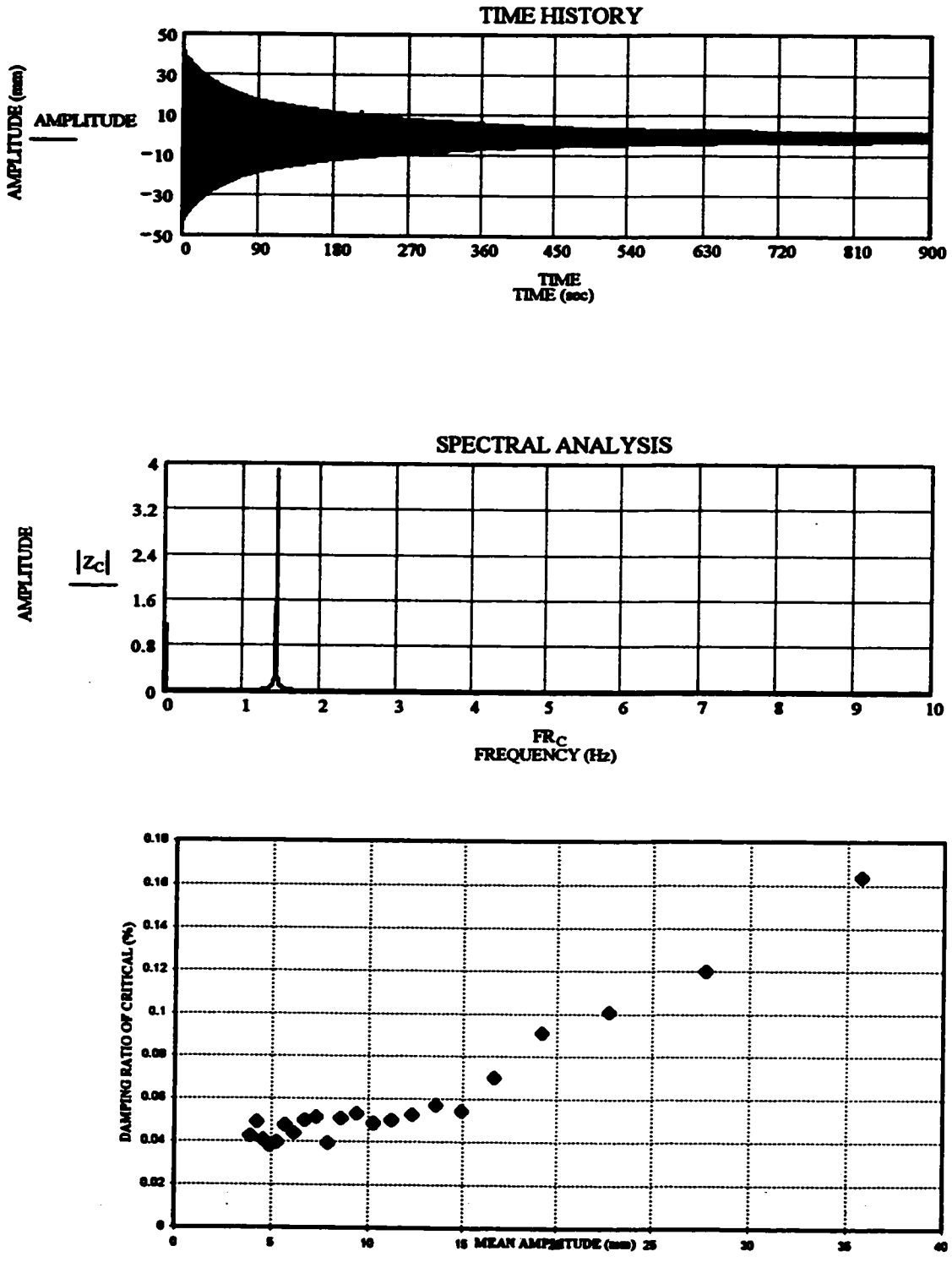

Figure B-9. Model setup 3A (lateral direction)

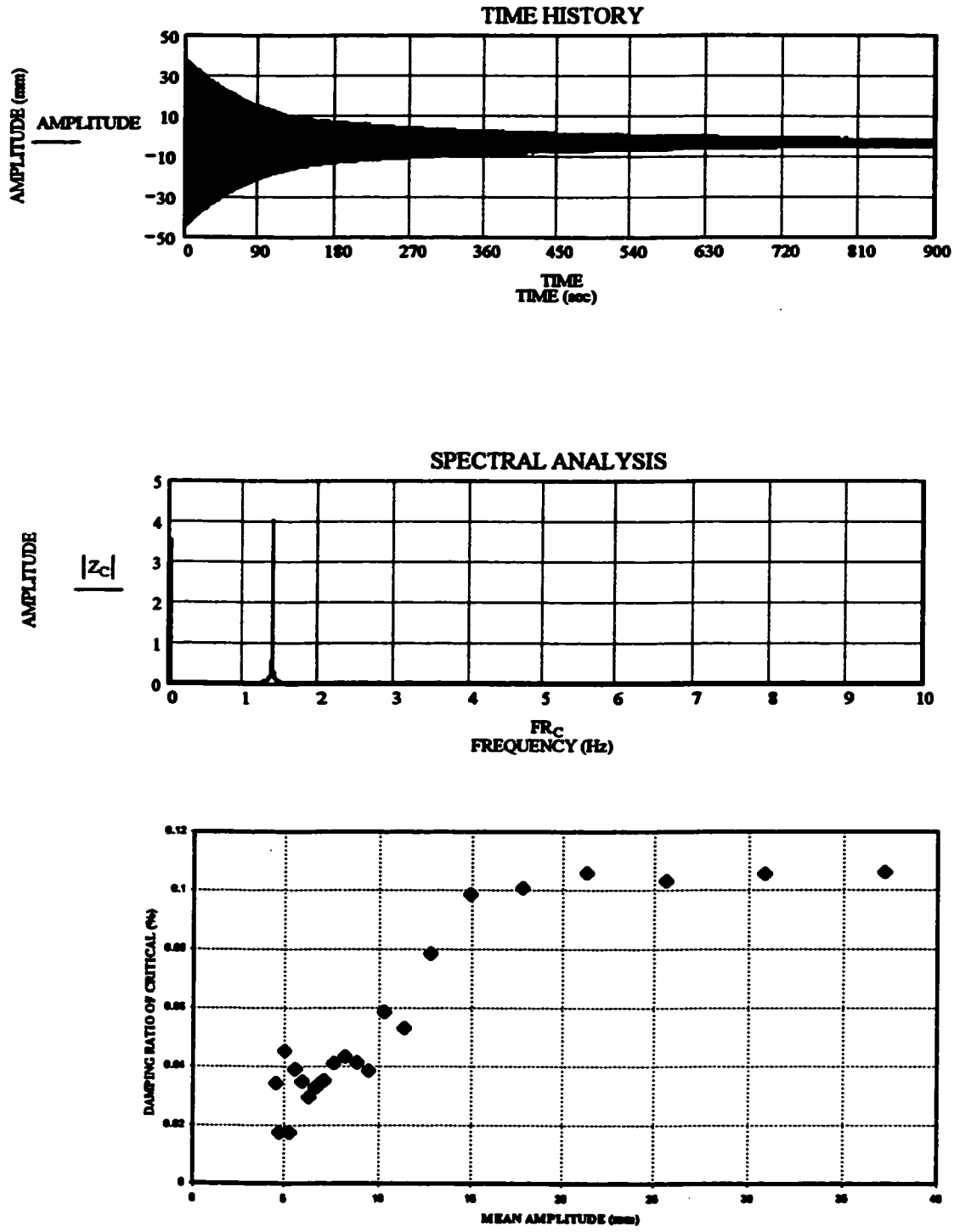

Figure B-10. Model setup 3A (vertical direction)

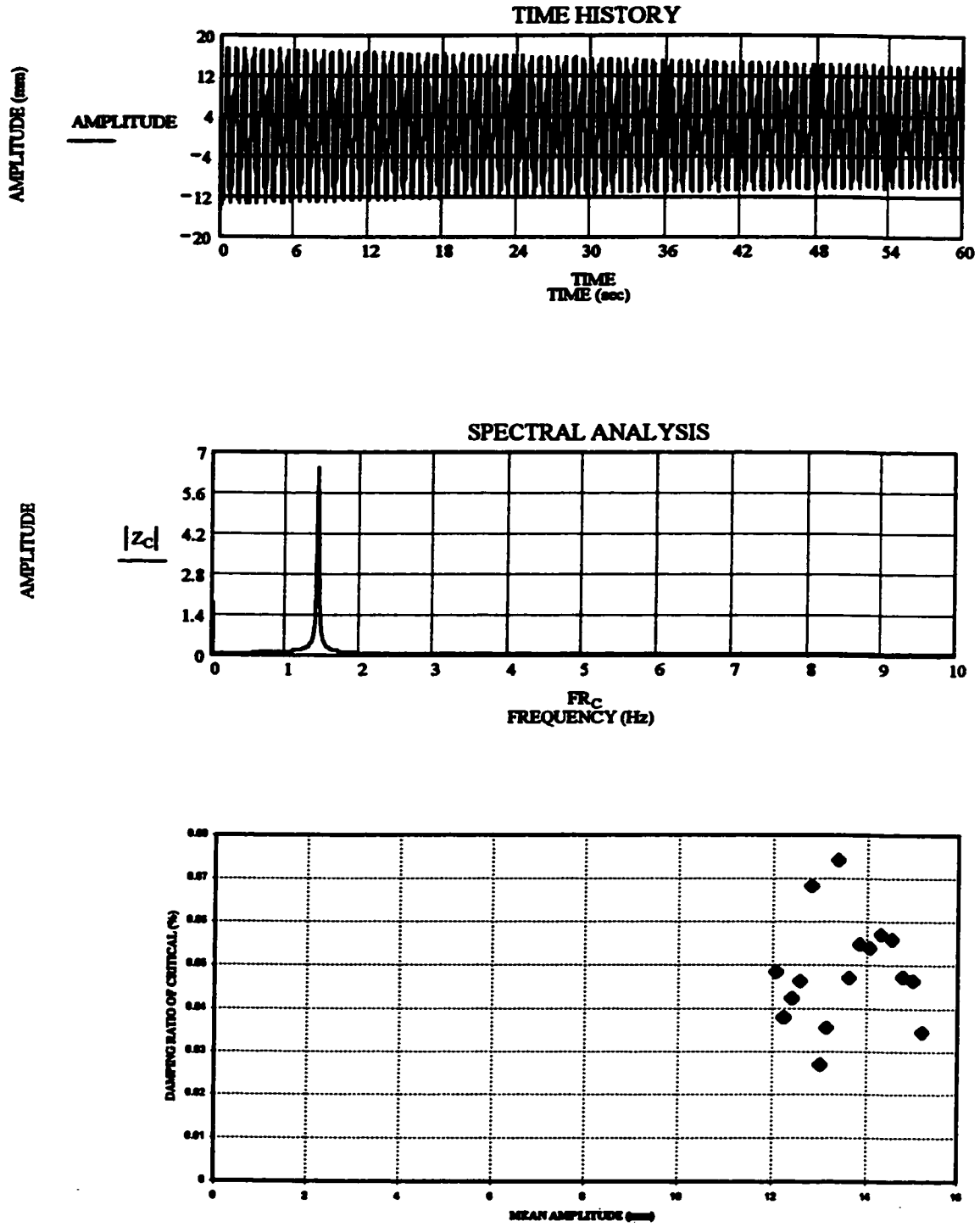

Figure B-11. Model setup 3B (vertical direction)

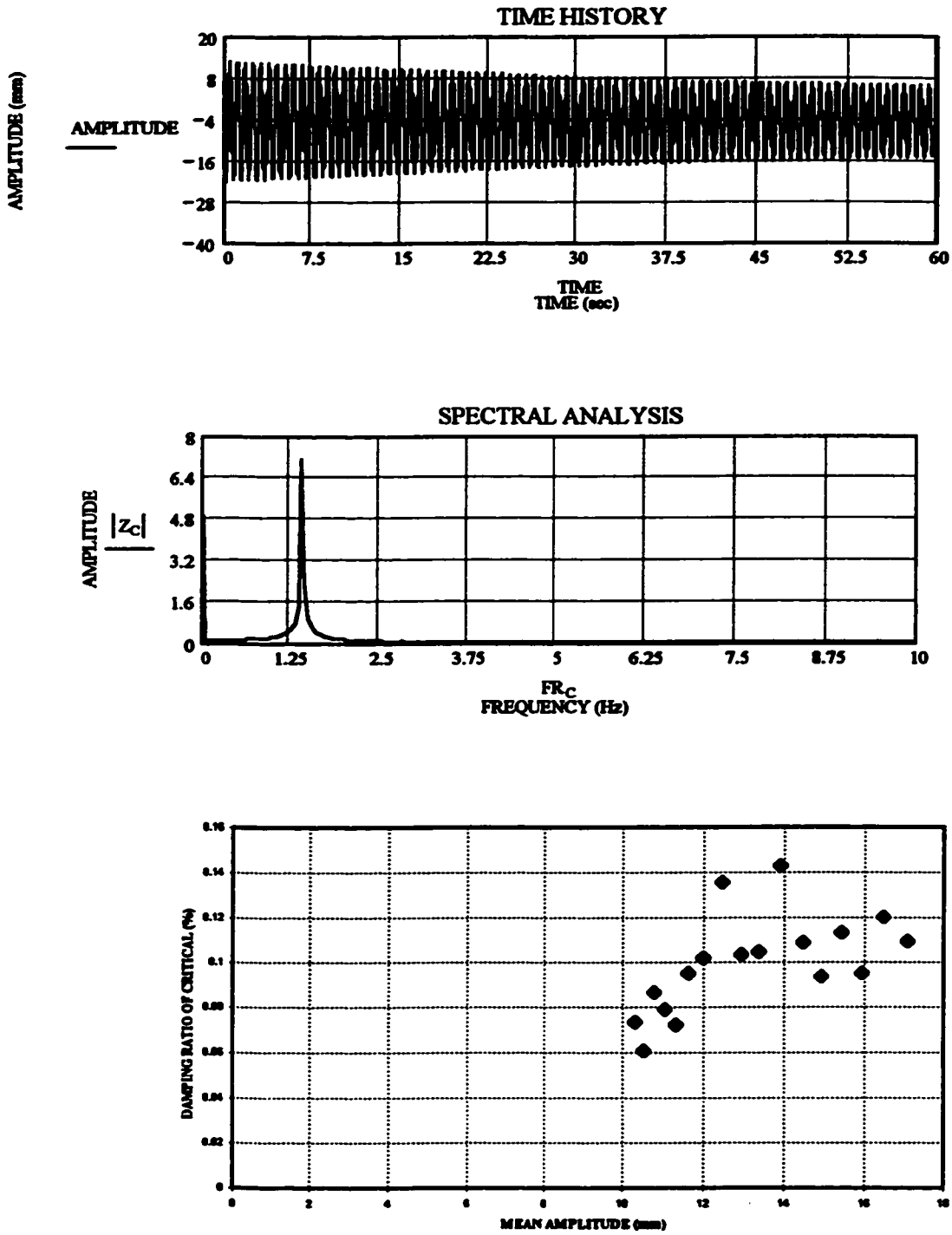

Figure B-12. Model setup 3B (lateral direction)